Electronic Supporting Information for

BN-Substituted Coronene Diimide–Triphenylamine Donor-Acceptor-Donor Triads: Photophysical and (Spectro)-Electrochemical Studies and Lewis Behavior

Jonas Hoffmann,[a,b,c] Denis Jaquemin,[d] Muriel Hissler,[c] and Anne Staubitz[a,b*]

*E-mail: muriel.hissler@univ-rennes1.fr, staubitz@uni-bremen.de

a. University of Bremen, Institute for Analytic and Organic Chemistry, Leobener Straße 7, D-28359 Bremen, Germany

b. University of Bremen, MAPEX Center for Materials and Processes, Bibliothekstraße 1, D-28359 Bremen, Germany

c. Université Rennes 1, CNRS, ISCR-UMR 6226, 263 Av. Général Leclerc, F-35042 Rennes, France

d. Université de Nantes, CNRS, CEISAM UMR 6230, F-44000 Nantes, France

Table of Content

List of Abbreviations

APCI	Atmospheric pressure chemical ionization
ATR	Attenuated total reflection
aq.	Aqueous
br (IR)	Broad signal
br (NMR)	Broad signal
BBO	Broadband Observe
CDI	Coronene diimide
COSY	Correlation spectroscopy
Cy	Cyclohexyl (moiety)
d (NMR)	Doublet
Dip	2,6-Diisopropylphenyl (moiety)
DBU	1,8-Diazabicyclo[5.4.0]undec-7-ene
DCM	Dichloromethane
dd (NMR)	Doublet of doublet
DFT	Density functional theory
DSS	4,4-Dimethyl-4-silapentane-1-sulfonic acid
EI	Electron ionization
HMBC	Heteronuclear multiple-bond correlation spectroscopy
HOMO	Highest occupied molecular orbital
HRMS	High resolution mass spectrometry
HSQS	Heteronuclear single-quantum correlation spectroscopy
IR	Infrared spectroscopy
LUMO	Lowest unoccupied molecular orbital
m (IR)	Medium intensity
m (NMR)	Multiplet
m$_c$ (NMR)	Multiplet (centered)
Mp.	Melting point
NMP	*N*-Methyl-2-pyrrolidone
NMR	Nuclear magnetic resonance
PDI	Perylene diimide
PeT	Photoinduced electron transfer
PTCDA	Perylene tetracarboxylic dianhydride
qd (NMR)	Quartet of doublets
quin. (NMR)	Quintet

R_f	Retention factor
s (IR)	Strong intensity
s (NMR)	Singlet
sat.	Saturated
SCE	Standard calomel electrode
Sept. (NMR)	Septet
SPS	Solvent purification system
t (NMR)	Triplet
TEA	Triethylamine
TICT	Twisted intramolecular charge transfer
TLC	Thin-layer chromatography
TMS	Trimethylsilyl
TPA	Triphenylamino
Tph	Thienyl
tt (NMR)	Triplet of triplets
w (IR)	Weak intensity

General Methods and Materials

All NMR tubes and glassware were dried in an oven at 200 °C overnight before use. If not stated otherwise, all reaction vessels were heated to minimum of 200 °C under a vacuum (1.3 x 10^{-2} mbar to 6.2 x 10^{-2} mbar) and purged with nitrogen or argon at least three times before adding the reagents. Syringes were purged with nitrogen or argon three times prior to use. Unless noted otherwise, a nitrogen filled glovebox from Inert, Innovative Technology, Inc. Company (< 0.1 ppm O_2 and < 0.1 ppm H_2O) was used for all reactions. All dry solvents were obtained from a solvent purification system (SPS, from Inert, Innovative Technology, Inc. Comp), degassed by three freeze-pump-thaw cycles and stored under a nitrogen atmosphere unless noted otherwise. In general, solvents were distilled prior to use except for HPLC grade solvents. For Kugelrohr distillation a Kugelrohr oven from Büchi was used.

Analyses

All NMR spectroscopic measurements were carried out at 300 K. ^{1}H NMR spectra were recorded on a Bruker DRX 500 (500 MHz), a Bruker Avance 600 (600 MHz), a Bruker Avance Neo (600 MHz) with a TXI probe head or a Bruker Avance Neo (600 MHz) with BBO probe head. ^{13}C{^{1}H} NMR spectra were recorded on a DRX 500 (125 MHz), a Bruker Avance 600 (150 MHz), a Bruker Avance Neo (150 MHz) with a TXI probe head or a Bruker Avance Neo (150 MHz) with BBO probe head. ^{1}H and ^{13}C{^{1}H} NMR spectra were referenced against the residual solvent signals. ^{1}H NMR spectra in D_2SO_4 were referenced against 20 µL of a solution containing 4,4-dimethyl-4-silapentane-1-sulfonic acid (DSS) in D_2O (1 mg/ µL).[1] ^{11}B{^{1}H} NMR spectra were recorded on a Bruker DRX 500 (180 MHz) spectrometer The reference of the ^{11}B{^{1}H} NMR spectra was $BF_3{\cdot}OEt_2$ in $CDCl_3$. The ^{11}B{^{1}H} NMR spectra of the **BNCDI**s were performed using a quartz tube and a blank spectrum of $CDCl_3$ was subtracted to ensure that weak/broad signals could be detected without interference of the glass peak from residual boron in the probe head. ^{29}Si{^{1}H} NMR spectra were recorded on a Bruker Avance Neo (119 MHz) spectrometer with BBO probe head. The reference for ^{29}Si{^{1}H} NMR spectra was tetramethylsilane in $CDCl_3$. Where possible, NMR signals were assigned using ^{1}H COSY, ^{1}H/^{1}H NOESY, ^{1}H/^{13}C{^{1}H} HSQC and ^{1}H/^{13}C{^{1}H} HMBC experiments.

Tab. S1: List of NMR solvents.

Solvent	Supplier	Purity	Comments
Benzene-d_6	Deutero	99%	Dried over CaH_2, degassed and stored in a glovebox
Chloroform-d_1	Deutero	99.9%	
Sulfuric acid-d_2 in D_2O	Deutero	96-98%	
D_2O	Deutero	99.9%	

IR spectra were recorded on a Perkin Elmer Paragon 1000 FT-IR spectrometer with a A531-G Golden-Gate ATR-unit or a Nicolet Thermo iS10 scientific spectrometer with a diamond ATR unit.

Melting points were measured with a BÜCHI Melting Point M-560 instrument. If no melting point is given for a solid, no melting behavior was observed up to 300 °C.

Electron impact (EI) mass spectrometric experiments were measured using the direct inlet or indirect inlet methods on a MAT95 XL double-focusing mass spectrometer from Finnigan or a JEOL JMS-100 GCV (AccuTOFGCV) mass spectrometer. The ionization energy of the electron impact ionization was 70 eV. Atmospheric pressure chemical ionization (APCI) and electron spray ionization (ESI) experiments were performed on a Bruker Impact II from Bruker Daltonics.

UV/Vis spectra were recorded on a Perkin Elmer Lambda 14 or a Jasco V-770 spectrometer at 20 °C using a quartz cuvette with a length of 1 cm.

The UV-Vis emission and excitation spectra measurements were recorded on a FL 920 Edinburgh Instrument and corrected for the response of the photomultiplier. Quantum yields were calculated relative to fluorescein ($\phi = 0.90$ in NaOH 0.1 N). Excitation was performed at 460 nm.

The NIR emission spectra were recorded on a C9920-03 Hamamatsu system equipped with a UV/Vis detector (350 - 950 nm) and a NIR detector (950 – 1700 nm) at the Capther facility (Scanmat, UMS 2001). Excitation was performed at 375 nm with a diode laser.

Chemicals and Solvents

Tab. S2: Overview of chemicals.

Chemical	Supplier	Purity	Comments
Acetic acid	Grüssing Inc.	99.5%	
Ammoniumchloride	Carl Roth	> 99.7%	
Boron tribromide solution	Sigma Aldrich		1 M in DCM
Boron trichloride solution	Sigma Aldrich		1 M in DCM
Bromine	Acros Organics	99%+	
1-Bromobutane	Merck	>98%	
2-Bromothiophene	TCI	> 98%	
4-Bromotriphenylamine	ChemPur	97%	
1-Butanol	Grüssing Inc.	99%	
n-Butyllithium	Sigma Aldrich		2.5 M in *n*-hexane
Calcium hydride	Acros Organics	90-95%	
Cyclohexylamine	Merck	> 99%	
1,2-Dibromoethane	TCI	> 99%	
2,6-Di*iso*propylaniline	Merck	> 99%	
DBU	Sigma Aldrich	98%	
DSS	Deutero	99%	
n-Hexylamine	Merck	99.9%	Distilled from CaH_2, degassed by the freeze-pump-thaw technique and stored in the glovebox.
Hydrochloric acid	Grüssing	37%	
Imidazole	Merck	99%	
Magnesium	Riedel-de Haen	> 99%	
Magnesium sulfate	Grüssing Inc.	99%	
Molecular sieves	Merck		3 Å
Perylene-3,4,10-11-tetracarboxylic acid dianhydride (PTCDA)	Merck	98%	
Potassium carbonate	Grüssing Inc.	85%	
Potassium hydroxide	Grüssing Inc.	85%	
Sodium bisulfite	Sigma Aldrich		40% *w/w*
Sodium hydroxide	Grüssing Inc.	99%	
Sulfuric acid	Grüssing Inc.	95-97%	
tetrabutylammonium hexafluorophosphate	Sigma Aldrich	> 99%	
p-Toluenesulfonic acid monohydrate	Riedel-de Haen	> 99%	

Trimethylsilylchloride	Sigma Aldrich	> 99%	
Tetra-*n*-butylammonium fluoride hydrate	Sigma Aldrich	98%	

Tab. S3: List of the utilized solvents.

Solvent	Supplier	Purity	Comments
Acetonitrile	Sigma Aldrich	≥ 99.5%	HPLC grade
Chloroform	Sigma Aldrich	≥ 99.0%	
Dichloromethane	Fisher Scientific	99.8%	
Dichloromethane (dry)	Fisher Scientific	99.8%	Dried via solvent purification system, degassed by freeze-pump-thaw technique and stored in the glovebox
Diethyl ether (for SPS)	Riedel-de Haen	> 99.5%	Distilled, dried via solvent purification system, degassed by freeze-pump-thaw technique and stored in the glovebox.
Ethanol	Th. Geyer	99%	
Methanol	Fisher Scientific	99.9	HPLC grade
N-Methyl-2-pyrrolidinone	Acros Organics	99%	anhydrous
Petrol ether	Grüssing Inc	techn.	Bp. 60 -90 °C
Toluene	Sigma Aldrich	> 99.7%	
Toluene (dry)	Acros	≥ 99.85%	Extra dry, stored over 3 Å molecular sieve, degassed by the freeze-pump-thaw technique and stored in the glovebox.
Triethylamine	ChemPur	99%	Dry, degassed by the freeze-pump-thaw technique and stored in the glovebox.

Chromatography

Unless stated otherwise chromatographic purifications were performed with silica gel (Merck, grain size 15-40 µm). Thin layer chromatography (TLC) was performed by using TLC Silicagel 60 F254 from MERCK on alumina plates. For the detection of the spots, a UV lamp (λ = 254/366 nm) was used.

Syntheses

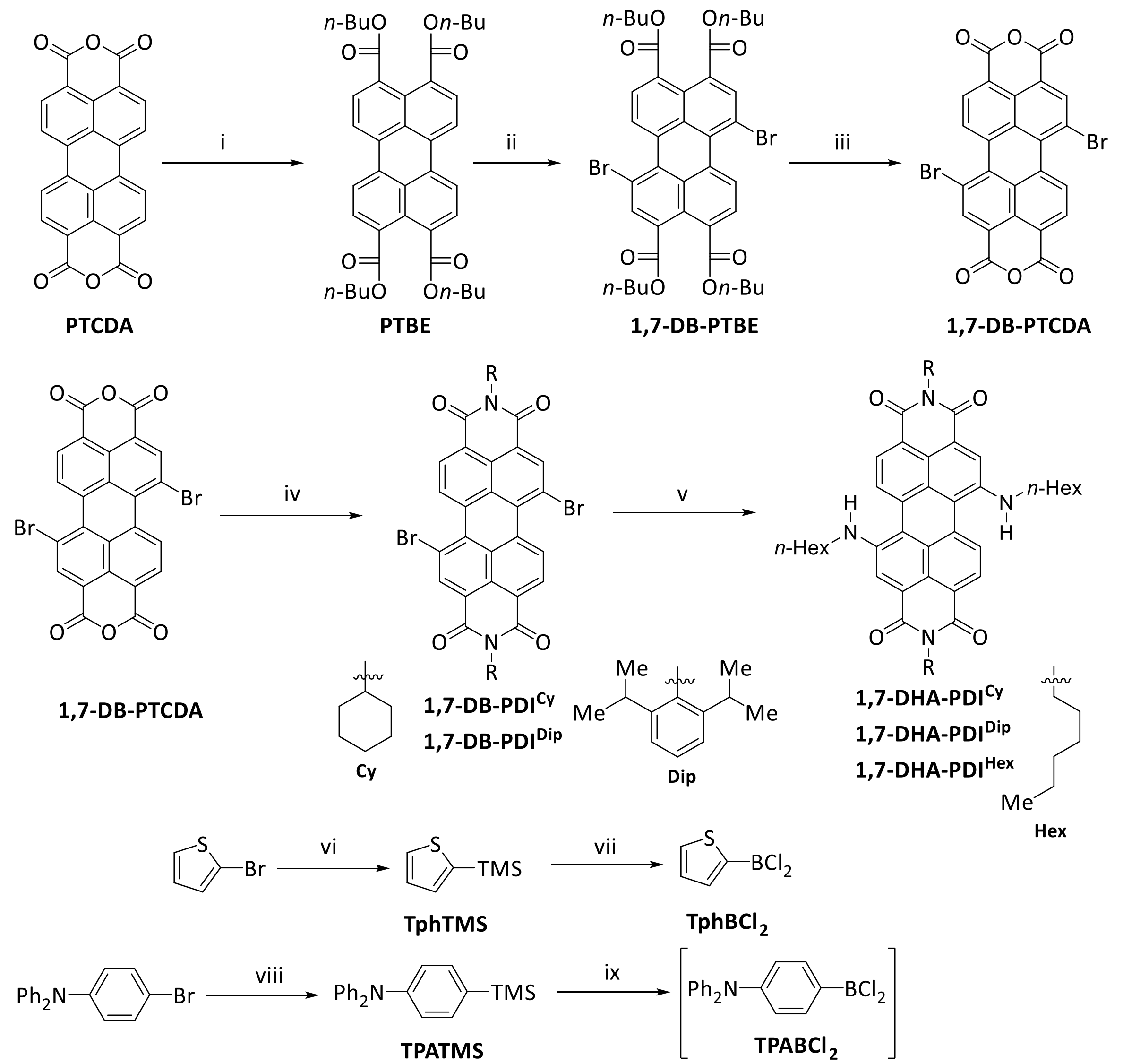

Scheme 1: Conditions: i) 1-butanol, 1-bromobutane, DBU, MeCN, 85 °C, 24 h, 92% ii) Br_2, K_2CO_3, DCM, 25 °C, 24 h, 45% isomerically pure product iii) *p*-TsOH H_2O, toluene, 100 °C, 30 h, 76% vi) NMP, AcOH a) cyclohexylamine 85 °C 4 h, 52% b) 2,6-di*iso*propylaniline, 120 °C, 24 h, 63% v) *n*-hexylamine, 60 °C, 6 h, 50-51%, on a larger scale 10% of **1,7-DHA-PDI^{Dip}** and 9% of **1,7-DHA-PDI^{Hex}** vi) *n*BuLi, -78 °C, Et_2O, 1 h then TMSCl, -78 °C to 25 °C, 78% vii) BCl_3, DCM, -50 C, 72% viii) 1,2-dibromoethane, magnesium, THF, 80 °C, 30 min, TMSCl, 50 °C, 2 h and 25 °C, 2 d, 71% ix) BCl_3, DCM, 25 C, 14 h, used *in situ*.

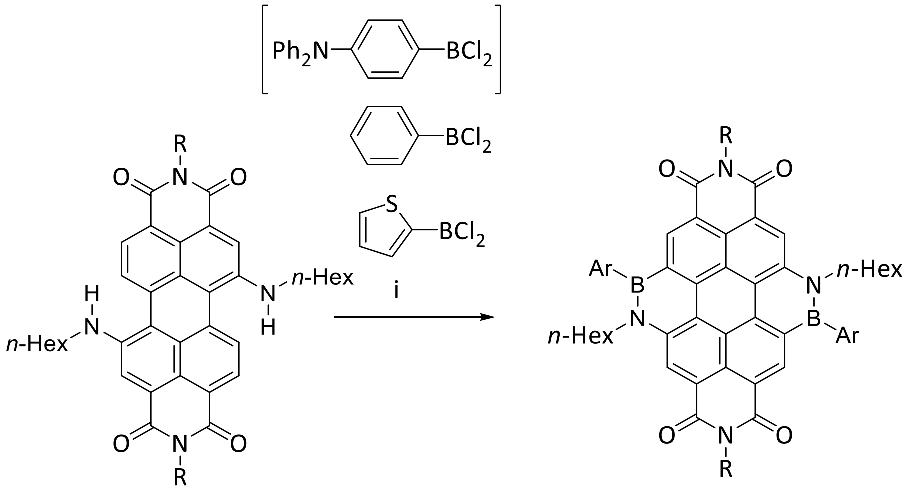

1,7-DHA-PDI^{Cy}
1,7-DHA-PDI^{Dip}
1,7-DHA-PDI^{Hex}

Ph-BNCDI^{Cy}, Ph-BNCDI^{Dip}, Ph-BNCDI^{Hex}
Tph-BNCDI^{Cy}, Tph-BNCDI^{Dip}
TPA-BNCDI^{Cy}, TPA-BNCDI^{Dip}

Scheme 2: Condition: i) TEA, toluene, 110 °C, 4-24 h, 50-98%.

Perylene-3,4,9,10-tetra-*n*-butylester (**PTBE**)

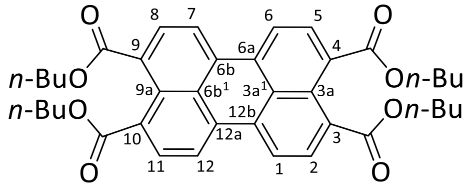

This synthetic procedure published for a similar compound and was adapted with changes from the literature[2] and was not performed under inert conditions.

A mixture of perylene-3,4,9,10-tetracarboxylic dianhydride (**PTCDA**, 4.00 g, 10.2 mmol), DBU (6.40 mL, 40.8 mmol), *n*-butanol (25.6 mL, 81.6 mmol) in MeCN (150 mL) was stirred at 25 °C for 0.5 h. To this slightly orange mixture, 1-bromobutane (8.73 mL, 81.6 mmol) was added, followed by MeCN (30 mL). The mixture was stirred for 24 h at 85 °C. After cooling to 25 °C and additional stirring for 21 h, the beginning precipitation was completed by adding methanol (250 mL). The mixture was filtered to give the product as an orange solid without further purification (**PTBE**, 6.10 g, 9.40 mmol, 92%).

^{1}H NMR (500 MHz, CDCl$_3$) δ = 8.22 (d, ^3J = 7.9 Hz, 4H, *H*-1,6,7,12), 8.00 (d, ^3J = 7.9 Hz, 4H, *H*-2,5,8,11), 4.34 (t, ^3J = 6.8 Hz, 8H, CH_2-C_3H_7), 1.84 -1.75 (m, 8H, CH_2-CH_2-C_2H_5), 1.53-1.44 (m, 8H, C_2H_4-CH_2-CH_3), 1.00 (t, ^3J = 7.4 Hz, 12H, CH_3) ppm. **^{13}C{^{1}H} NMR** (125 MHz, CDCl$_3$): δ = 168.67 (*C*OO-(C_4H_9)), 133.17 (*C*-3,4,9,10), 130.62 (*C*-6a,6b,12a,12b), 130.54 (*C*-2,5,8,11-), 129.13 (*C*-3a,9a), 128.95 (*C*-3a^1,6b^1), 121.51 (*C*-1,6,7,12), 65.49 (CH_2-C_3H_7), 30.80 (CH_2-CH_2-C_2H_5), 19.42 (C_2H_4-CH_2), 13.95 (CH_3) ppm. **HRMS** (EI): *m/z* calcd. for $C_{40}H_{44}O_8$ 652.30362 $[M]^{+\cdot}$; found 652.30296 $[M]^{+\cdot}$ (100%). **IR** (ATR): $\tilde{\nu}$ = 2958 (m), 2930 (w), 2870 (w), 1721 (s), 1705 (m), 1588 (m), 1472 (m), 1270 (s), 1267 (m), 1167 (s), 1131 (s), 1096 (m), 1004 (m, 939 (m), 842 (m), 805 (m), 746 (s) cm^{-1}. **Mp.**: 165 °C.

The analytical data were in agreement with previously published values.[3]

1,7-Dibromoperylene-3,4,9,10-tetra-*n*-butylester (1,7-DB-PTBE)

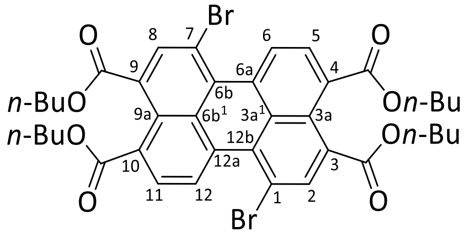

This synthetic procedure was adapted from the literature[4] and was not performed under inert conditions.

A mixture of perylene-3,4,9,10-tetra-*n*-butylester (**PTBE**, 5.00 g, 7.66 mmol) and K_2CO_3 (2.50 g, 18.1 mmol) in DCM (60 mL) was stirred at 25 °C. To this mixture, bromine (5.12 mL, 100 mmol) was added dropwise over a period of 2 h 5 min and the mixture was stirred for 24 h at 25 °C. Then a saturated aqueous solution of $NaHSO_3$ (35 mL, 40% *w/w*) was added dropwise over a period of 4 h. The organic layer was washed with water (100 mL), dried over $MgSO_4$, filtered, and after the removal of the solvent, the remaining orange material was dried (3.4×10^{-4} mbar, 60 °C, 24 h). An isomeric mixture of of 1,6- and 1,7-isomers in a ratio of 1:4 as determined by ^{1}H NMR spectroscopy was obtained (5.90 g, 7.28 mmol). The isomeric mixture (5.90 g) was dissolved in DCM (60 mL) and further MeCN (540 mL) was added to the solution. The flask was left open in the fume hood for 3 days and crystals were isolated (3.47 g). The second recrystallization using DCM (40 mL) and MeCN (370 mL) yielded the pure isomer (**1,7-DB-PTBE**, 2.81 g, 3.47 mmol, 45%, lit.[4]: 62%).

^{1}**H NMR** (500 MHz, $CDCl_3$): δ = 8.91 (d, ^3J = 7.9 Hz, 2H, *H*-6,12), 8.28 (s, 2H, *H*-2,8), 8.07 (d, ^3J = 7.9 Hz, 2H, *H*-5,11), 4.35 (td, ^3J = 6.8 Hz, ^4J = 1.7 Hz, 8H, CH_2-C_3H_7), 1.84-1.73 (m, 8H, CH_2-CH_2-C_2H_5), 1.54-1.44 (m, 8H, C_2H_4-CH_2), 1.01 (t, ^3J = 7.4 Hz, 12H, CH_3) ppm. ^{13}**C{^{1}H} NMR** (126 MHz, $CDCl_3$): δ = 168.13 (*C*OO-(C_4H_9)-4,10), 167.26 (*C*OO-(C_4H_9)-3,9), 136.80 (*C*H-2,8), 131.93 (*C*-6b,12b), 131.87 (*C*-6a,12a), 131.27 (*C*-3,9), 130.61 (*C*-(3a,9a or 3a^1,6b^1)), 130.60 (*C*-(3a,9a or 3a^1,6b^1)), 129.17 (*C*H-5,11), 127.77 (*C*H-6,12), 126.64 (*C*-4,10), 118.85 (*C*-1,7), 65.96 (CH_2-C_3H_7), 65.74 (CH_2-C_3H_7), 30.76 (CH_2-CH_2-C_2H_5), 30.73 (CH_2-CH_2-C_2H_5), 19.40 (C_2H_4-CH_2), 19.37 (C_2H_4-CH_2-CH_3), 13.93 (CH_3) ppm. **HRMS** (EI)**:** *m/z* calcd. for $C_{40}H_{42}{}^{81}Br_2O_8$ 810.10490 $[M]^{+\cdot}$, found 810.10195 $[M]^{+\cdot}$ (100). **IR** (ATR): $\tilde{\upsilon}$ = 2958 (m), 2932 (w), 2872 (w), 1717 (s), 1475 (m), 1397 (m), 1299 (s), 1267 (m), 1223 (m), 1194 (m), 1172 (s), 1058 (m), 1030 (m), 980 (m), 938 (m), 887 (m), 864 (m), 840 (m), 755 (m) cm^{-1}. **Mp**.: 125 °C.

The analytical data were in agreement with reported values.[4]

1,7-Dibromoperylene-3,4,9,10-tetracaboxylic dianhydride (1,7-DB-PTCDA)

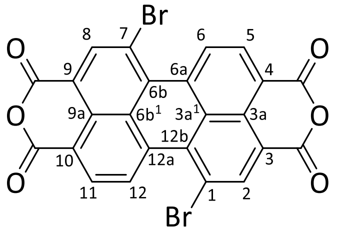

This synthetic procedure was adapted from the literature[4] and was not performed under inert conditions.

A mixture of 1,7-dibromoperylene-3,4,9,10-tetra-*n*-butylester (**1,7-DB-PTBE**, 2.50 g, 3.08 mmol) and *p*-TsOH·H_2O (2.50 g, 15.4 mmol) in toluene (90 mL) was stirred at 100 °C for 30 h. Subsequently, the reaction mixture was filtered and washed with methanol (250 mL) and water (150 mL). Then the precipitate was stirred with chloroform (200 mL) at 71 °C for 2 h. After having cooled to 23 °C, the precipitate was filtered and washed again with chloroform (400 mL). Drying (60 °C, 10 h, 1.6 x 10^{-3} mbar) afforded the product as a red solid (**1,7-DB-PTCDA**, 1.29 g, 2.34 mmol, 76%, lit.[4]: 95%).

^{1}**H NMR** (500 MHz, D$_2$SO$_4$): δ = 9.02 (d, ^3J = 7.9 Hz, 2H, *H*-6,12), 8.35 (s, 2H, *H*-2,8), 8.13 ppm (d, ^3J = 7.9 Hz, 2H, *H*-5,11) ppm. ^{1}**H-**^{13}**C{**^{1}**H} HSQC/HMBC NMR** (126 MHz, D$_2$SO$_4$): δ = 158.2 (*C*OO-3,9), 157.3 (*C*OO-4,10), 136.4 (*C*-2,8), 130.2 (*C*-6b,12b), 130.1 (*C*-6a,12a), 128.8 (*C*-5,11), 124.1 (*C*-6,12), 123.3 (*C*-(3a^1,6b^1)), 123.0 (*C*-(3a,9a)), , 119.0 (*C*-1,7), 110.7 (*C*-4,10), 110.4 (*C*-3,9) ppm.[1] **HRMS** (EI): *m/z* [M]$^{+\cdot}$ calcd. for C$_{24}$H$_6$O$_6$^{79}Br$_2$ 547.85256; found 547.85214 (100%). **IR** (ATR): $\tilde{\nu}$ = 1773 (s), 1724 (s), 1593 (s), 1593 (s), 1376 (w), 1297 (m), 1285 (m), 1230 (m), 1213 (m), 1138 (m), 1057 (m), 1037 (m), 956 (w), 859 (w), 804 (w), 733(w), 693 (m) cm^{-1}.

The analytical data were in agreement with reported values.[4]

1,7-Dibromo-*N*,*N'*-di(cyclohexyl)perylene-3,4,9,10-tetracaboxylic acid diimide (1,7-DB-PDI^{Cy})

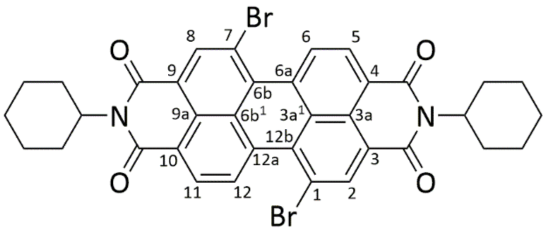

This synthetic procedure was adapted from the literature,[5] where a similar molecule was described.

A mixture of 1,7-dibromoperylene-3,4,9,10-tetracaboxylic acid dianhydride (**1,7-DB-PTCDA**, 1.00 g, 1.82 mmol) and NMP (30 mL) was placed in an ultrasonic bath for 1 h. Then cyclohexylamine (0.630 mL, 5.45 mmol) and acetic acid (0.676 mL, 11.8 mmol) were added and the reaction mixture was heated to 85 °C under a nitrogen atmosphere for 7 h. After cooling to 25 °C, the reaction mixture was poured into methanol (150 mL) and cooled to -10 °C for 12 h. The solid was separated by filtration, washed with methanol (250 mL), dried (6.2 x 10^{-2} mbar, 22 °C, 2 h) and was purified by column chromatography (silica, eluent: chloroform:petrol ether (3:1), R$_f$(CHCl$_3$) = 0.75). The product was obtained as a dark red solid (**1,7-DB-PDI^{Cy}**, 670 mg, 52%).

^{1}**H NMR** (500 MHz, CDCl$_3$) δ = 9.48 (d, ^3J = 8.2 Hz, 2H, *H*-6,12), 8.89 (s, 2H, *H*-2,8), 8.68 (d, ^3J = 8.2 Hz, 2H, *H*-5,11), 5.03 (tt, ^3J = 12.4, 3.6 Hz, 2H, C*H*), 2.55 (qd, ^3J = 12.4, 9.0 Hz, 4H, CH-C*H*$_{ax}$), 1.92 (d, ^3J = 12.4 Hz, 4H, CH-CH$_2$-CH$_{ax}$), 1.81-1.76 (m, 6H, CH-C*H*$_{eq}$ and CH-(CH$_2$)$_2$-C*H*$_{ax}$), 1.51-1.31 (m, 6H, C*H*$_2$, CH-CH$_2$-C*H*$_{eq}$ and CH-(CH$_2$)$_2$-C*H*$_{eq}$) ppm. ^{13}**C{**^{1}**H} NMR** (125 MHz, CDCl$_3$): δ = 163.49 (*C*OO-4,10), 162.94 (*C*OO-3,9), 138.11 (*C*H-2,8), 132.99 (*C*-6b,12b), 132.83 (*C*-6a,12a), 130.13 (*C*H-5,11), 129.41 (*C*-3,9), 128.62 (*C*H-6,12), 127.19 (*C*-3a,9a), 123.87 (*C*-4,10), 123.46 (*C*-3a^1,6b^1), 120.86 (*C*-1,7), 54.41 (*C*H), 29.26 (CH-*C*H$_2$), 26.66 (CH-CH$_2$-*C*H$_2$), 25.55 (CH-(CH$_2$)$_2$-*C*H$_2$) ppm. **HRMS** (EI): *m/z* [M]$^{+\cdot}$ calcd. for C$_{36}$H$_{26}$^{79}Br^{81}BrN$_2$O$_4$ 710.02389; found 710.02443. calcd. for C$_{36}$H$_{26}$^{81}Br$_2$N$_2$O$_4$ 712.02184; found 712.02315; 547.84 (100%). **IR** (ATR): $\tilde{\nu}$ = 2926 (w), 2852 (w), 1697 (m), 1655 (s), 1587 (m), 1575 (m), 1382 (m), 1326 (m), 1302 (w), 1257 (w), 1237 (s), 1187 (m), 1156 (m), 1143 (m), 979 (w), 859 (w), 824 (m), 808 (m), 745 (m), 690 (m), 683 (m), 657 (m) cm^{-1}.

The analytical data were in agreement with previously reported values.[5]

---

[1] Due to the low solubility only ^{1}H, ^{1}H -^{13}C{^{1}H}-HSQC and ^{1}H,^{13}C{^{1}H}-HMBC NMR signals were used to identify and assign the signals.

1,7-Dibromo-*N*,*N'*-bis(di*iso*propylphenyl)-perylene-3,4,9,10-tetracaboxylic acid diimide (1,7-DB-PDI^{Dip})

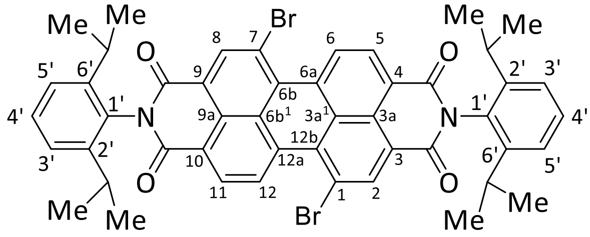

This synthetic procedure was adapted from the literature.[5]

This synthetic procedure was adapted from the literature.[4]: Under nitrogen atmosphere, a mixture of 1,7-dibromoperylene-3,4,9,10-tetracaboxylic acid dianhydride (**1,7-DB-PTCDA**, 3.79 g, 6.89 mmol) and NMP (40 mL) was placed in an ultrasonic bath for 1 h. Then 2,6-di*iso*propylaniline (7.36 g, 41.5 mmol) and acetic acid (2.25 mL, 39.5 mmol) were added, and the reaction was heated to 120 °C for 4 d. After cooling to 25 °C water (100 mL) was added. The precipitate was collected by vacuum filtration and washed with water (600 mL) and methanol (150 mL) and cooled to -10 °C for 12 h. The solid was collected by filtration and washed with cold methanol (50 mL). The resulting powder was dried (2.0 x 10^{-2} mbar, 200 °C, 14 h) and was purified by column chromatography (silica, eluent: DCM, R_f(DCM) = 0.75). The product was obtained as a dark red solid (**1,7-DB-PDI^{Dip}**, 3.80 g, 4.37 mmol, 63%, lit.[4]: 66%).

^{1}H NMR (601 MHz, $CDCl_3$) δ = 9.57 (d, ^3J = 8.2 Hz, 2H, *H*-6,12), 9.02 (s, 2H, *H*-2,8), 8.81 (d, ^3J = 8.2 Hz, 2H, *H*-5,11), 7.52 (t, ^3J = 7.8 Hz, 2H, Ph-*H*-4'), 7.37 (d, ^3J = 7.8 Hz, 2H, Ph-*H*-3',5'), 2.74 (sept., ^3J = 6.7 Hz, 4H, C*H*), 1.19 (dd, ^3J = 6.7 Hz, ^4J = 1.8 Hz, 24H, C*H*$_3$) ppm. **^{13}C{^{1}H} NMR** (151 MHz, $CDCl_3$): δ = 163.15 ((*C*(O)N)-4,10), 162.65 ((*C*(O)N)-3,9), 145.75 (Ph-*C*-2',6'), 138.63 (*C*-2,8), 133.59 (*C*-6b,12b), 133.43 (*C*-6a,12a), 130.80 (*C*-5,11), 130.27 (Ph-*C*-1'), 130.05 (Ph-*C*-4'), 129.79 (*C*-3,9), 128.87 (*C*-6,12), 127.85 (*C*-3a,9a), 124.36 (Ph-*C*-3',5'), 123.35 (*C*-4,10), 123.02 (*C*-$3a^1$,$6b^1$), 121.22 (*C*-1,7), 29.45 (*C*H(CH_3)), 24.19 and 24.16 (*C*H$_3$) ppm. **HRMS** (EI): *m/z* $[M]^{+\cdot}$ calcd. for $C_{48}H_{40}N_2O_4{}^{79}Br_2$ 866.13493; found 866.13370; 549.70 (100%). **IR** (ATR): υ = 2959 (m), 2925 (m), 1707 (s), 1668 (s), 1589 (s), 1383 (m), 1336 (s), 1248 (m), 1178 (m), 834 (m), 809 (m), 746 (m), 692 (w) cm^{-1}.

The analytical data were in agreement with previously reported values.[4]

1,7-Di(*n*-hexylamino)-*N*,*N'*-di(cyclohexyl)perylene-3,4,9,10-tetracaboxylic acid diimide (1,7-DHA-PDI^{Cy})

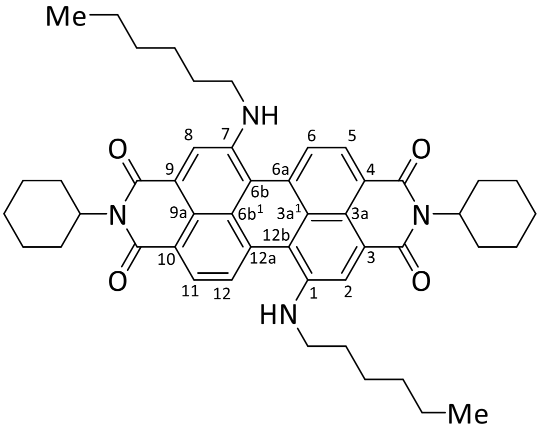

Under an argon atmosphere, 1,7-dibromo-*N*,*N'*-di(cyclohexyl)perylene-3,4,9,10-tetracarboxylic acid diimide (**1,7-DB-PDI^{Cy}**, 100 mg, 140 µmol) and *n*-hexylamine (10.0 mL, 76.0 mmol) were mixed. The mixture was stirred at 60 C for 3 d. Subsequently, the excess of *n*-hexylamine was removed with a rotary evaporator (80 °C, 10 mbar). The crude product was purified by column chromatography (silica, eluent: DCM, R_f(DCM) = 0.68) to yield the product as a green solid (**1,7-DHA-PDI^{Cy}**, 53 mg, 70.4 µmol, 50%).

^{1}H NMR (600 MHz, $CDCl_3$): δ = 8.60 (d, ^3J = 8.1 Hz, 2H, *H*-6,12), 8.16 (d, ^3J = 8.1 Hz, 2H, *H*-5,11), 7.96 (s, 2H, *H*-2,8), 5.59 (t, ^3J = 4.6 Hz, 2H, N*H*), 5.01 (tt, ^3J = 12.1, 3.6 Hz, 2H, C*H*), 3.19 (q, ^3J = 6.8 Hz , 4H, NH-CH_2), 2.57 (qd, ^3J = 12.1, 3.0 Hz, 4H, CH-CH_{ax}), 1.93 (d, ^3J = 12.6 Hz, 4H, CH-CH_2-CH_{ax}), 1.83 - 1.71 (m, 6H, CH-CH_{eq} and CH-$(CH_2)_2$-CH_{ax}), 1.66 (quin., ^3J = 7.1 Hz, 4H, NH-(CH_2)-CH_2), 1.51 - 1.21 (m, 18H, CH-CH_2-CH_{eq}, CH-$(CH_2)_2$-CH_{eq} and NH-$(CH_2)_2$-(CH_2)$_3$), 0.93 (t, ^3J = 7.1 Hz, 6H, CH_3) ppm. **^{13}C{^{1}H} NMR** (150 MHz, $CDCl_3$): δ = 164.36 ((*C*(O)N)-3,9), 163.91 ((*C*(O)N)-4,10), 145.89 (*C*-1,7), 133.86 (*C*-6a,12a), 129.89 (*C*-4,10), 126.97 (*C*-5,11), 123.17 (*C*-3,9), 122.45 (*C*-3a,9a), 121.46 (*C*-6,12), 120.66 (*C*-3a^1,6b^1), 117.94 (*C*-2,8), 116.73 (*C*-6b,12b), 54.00 (*C*H), 44.75 (NH-*C*H_2), 31.64 (NH-CH_2-*C*H_2), 29.44 (CH-*C*H_2), 29.27 (NH-$(CH_2)_2$-*C*H_2), 27.09 (NH-$(CH_2)_3$-*C*H_2), 26.76 (CH-CH_2-*C*H_2), 25.68 (CH-$(CH_2)_2$-*C*H_2), 22.74 (NH-$(CH_2)_4$-*C*H_2), 14.15 (*C*H_3) ppm. **HRMS** (APCI): *m/z* $[M+H]^+$ calcd. for $C_{48}H_{57}N_4O_4$ 753.43743; found 753.43686. **IR** (ATR): υ = 3314 (w), 2924 (m), 2851 (m), 1687 (s), 1641 (s), 1584 (s), 1568 (s), 1512 (w), 1452 (w), 1421 (m), 1330 (s), 1280 (m), 1257 (m), 1190 (m), 1124 (w), 1102 (w), 984 (m), 895 (w), 866 (w), 805 (m), 750 (m), 653 (m), 643 (m) cm^{-1}.

1,7-Di(*n*-hexylamino)-*N*,*N'*-bis(2,6-di(*iso*proypyl)phenyl)perylene-3,4,9,10-tetracaboxylic acid diimide (1,7-DHA-PDI$^{\mathrm{Dip}}$)

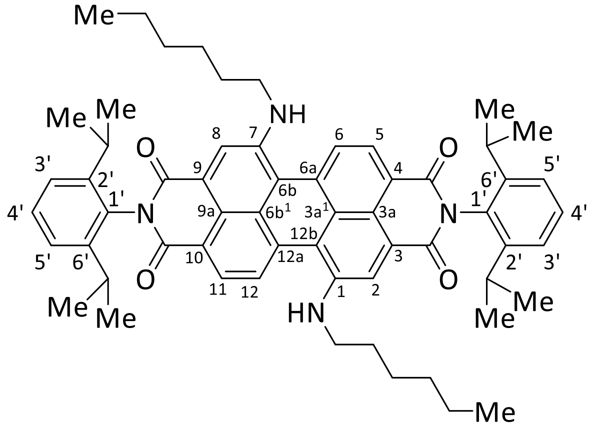

Under an argon atmosphere, 1,7-dibromo-*N*,*N'*-*bis*(di*iso*proypylphenyl)perylene-3,4,9,10-tetracarboxylic acid diimide (**1,7-DB-PDI$^{\mathrm{Dip}}$**, 100 mg, 117 µmol) and *n*-hexylamine (10.0 mL, 76.0 mmol) were mixed. The mixture was stirred at 60 °C for 3 d. Subsequently, the excess of *n*-hexylamine was removed at a rotary evaporator (80 °C, 10 mbar). The crude product was purified by column chromatography (silica, eluent: DCM, R$_f$(DCM) = 0.74) to yield the product as a green solid (**1,7-DHA-PDI$^{\mathrm{Dip}}$**, 54 mg, 59.3 µmol, 51%).

The reaction was also performed on a 2.34 mmol scale where the product was isolated in lower yield (**1,7-DHA-PDI$^{\mathrm{Dip}}$**, 204 mg, 0.22 mmol, 10%). As a side-product (R$_\mathrm{f}$(DCM) = 0.55), the product of a transamination of **1,7-DHA-PDI$^{\mathrm{Dip}}$** was isolated as a green solid (**1,7-DHA-PDI$^{\mathrm{Hex}}$**, 187 mg, 0.20 mmol, 9%).

^{1}H NMR (600 MHz, CDCl$_3$): δ = 8.91 (d, ^3J = 8.1 Hz, 2H, *H*-6,12), 8.46 (d, ^3J = 8.1 Hz, 2H, *H*-5,11), 8.30 (s, 2H, *H*-2,8), 7.49 (t, ^3J = 7.8 Hz, 2H, Ph-*H*-4'), 7.35 (d, ^3J = 7.8 Hz, 4H, Ph-*H*-3',5'), 5.81 (t, ^3J = 7.8 Hz, 2H, N*H*), 3.48 (q, ^3J = 7.1 Hz, 4H, NH-C*H*$_2$), 3.33-3.27 (m, 4H, NH-C*H*$_2$), 2.77 (sept., ^3J = 6.6 Hz, 4H, Ph-(C*H*)-(CH$_3$)$_2$), 1.79 (quin., ^3J = 7.1 Hz, 4H, NH-(CH$_2$)-C*H*$_2$), 1.43 - 1.32 (m, 8H, NH-(CH$_2$)$_2$-(C*H*$_2$)$_3$), 1.22 - 1.16 (m, 24H, Ph-(CH)-(C*H*$_3$)$_2$), 0.91 (t, ^3J = 7.0 Hz, 6H, C*H*$_3$) ppm. **^{13}C{^{1}H} NMR** (150 MHz, CDCl$_3$): δ = 163.84 ((*C*(O)N)-3,9), 163.75 ((*C*(O)N)-4,10), 146.19 (*C*-1,7), 145.67 (Ph-*C*-2',6'), 134.40 (*C*-6a,12a), 130.94 (Ph-*C*-1'), 130.54 (*C*-4,10), 129.51 (Ph-*C*-4'), 127.54 (*C*-5,11), 124.03 (Ph-*C*-3',5'), 123.24 (*C*-3,9), 123.00 (*C*-3a^1,6b^1), 121.78 (*C*-6,12), 120.42 (*C*-3a,9a), 118.85 (*C*-2,8), 117.21 (*C*-6b,12b), 44.90 (NH-*C*H$_2$), 31.46 (NH-CH$_2$-*C*H$_2$), 29.71 (NH-(CH$_2$)$_2$-*C*H$_2$), 29.51 (Ph-(*C*H)-(CH$_3$)$_2$), 26.90 (NH-(CH$_2$)$_3$-*C*H$_2$), 24.05 and 24.03 (Ph-(CH)-(*C*H$_3$)$_2$), 22.56 (NH-(CH$_2$)$_4$-*C*H$_2$), 14.00 (*C*H$_3$) ppm. **HRMS** (ESI): *m/z* [M+H]$^+$ calcd. for C$_{60}$H$_{69}$N$_4$O$_4$ 909.53152; found 909.53133. **IR** (ATR): υ = 3338 (w), 2956 (m), 2925 (m), 2855 (m), 1690 (s), 1653 (m), 1583 (m), 1568 (m), 1507 (m), 1456 (m), 1421 (m), 1338 (s), 1276 (s), 1197 (m), 1125 (m), 866 (m), 840 (m), 805 (m), 764 (m), 750 (s), 737 (m), 691 (m) cm^{-1}.

1,7-Di(*n*-hexylamino)-*N*,*N'*-di(*n*-hexyl)perylene-3,4,9,10-tetracaboxylic acid diimide (1,7-DHA-PDI$^{\mathrm{Hex}}$)

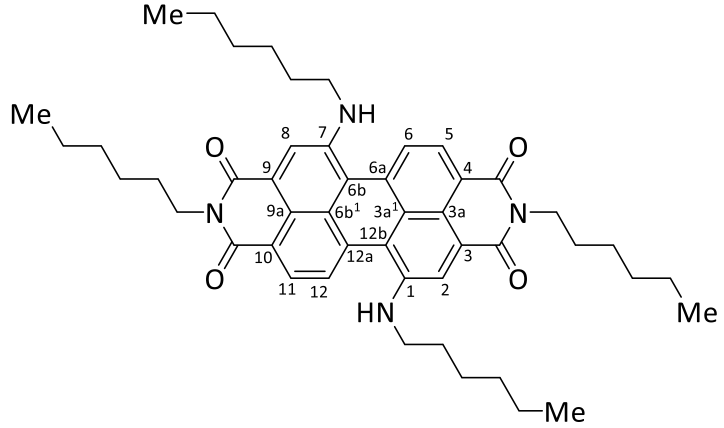

This product was isolated as side-product (see above).

^{1}H NMR (500 MHz, CDCl$_3$): δ = 8.48 (d, ^3J = 8.1 Hz, 2H, *H*-6,12), 8.09 (d, ^3J = 8.1 Hz, 2H, *H*-5,11), 7.80 (s, 2H, *H*-2,8), 5.49 (t, ^3J = 4.8 Hz, 2H, N*H*-CH$_2$), 4.08 (t, ^3J = 7.8 Hz, 4H, (CO)$_2$N-C*H*$_2$), 3.08 (dd, ^3J = 12.1, 6.9 Hz, 4H, NH-C*H*$_2$), 1.71 (quin, ^3J = 7.5 Hz, 4H, (CO)$_2$N-CH$_2$-C*H*$_2$), 1.58 (quin, ^3J = 7.3 Hz, 4H, NH-CH$_2$-C*H*$_2$), 1.47 - 1.28 (m, 24H, NH-(CH$_2$)$_2$-(C*H*$_2$)$_3$ and (CO)$_2$N-(CH$_2$)$_2$-(C*H*$_2$)$_3$) and (CO)$_2$N-(CH$_2$)$_2$-(C*H*$_2$)$_3$), 0.96 - 0.86 (m, 12H, C*H*$_3$) ppm. **^{13}C{^{1}H} NMR** (126 MHz, CDCl$_3$): δ = 163.67 ((*C*(O)N)-3,9), 163.19 ((*C*(O)N)-4,10), 145.77 (*C*-1,7), 133.80 (*C*-6a, 12a), 129.68 (*C*-4,10), 126.60 (*C*-5,11), 122.39 (*C*-3,9), 122.08 (*C*-3a,9a), 121.31 (*C*-6,12), 120.03 (*C*-3a^1,6b^1), 117.71 (*C*-2,8), 116.56 (*C*-6b,12b), 44.67 (NH-*C*H$_2$), 40.69 ((CO)$_2$N-*C*H$_2$), 31.71 ((NH-(CH$_2$)$_4$-*C*H$_2$) or ((CO)$_2$N-(CH$_2$)$_4$-*C*H$_2$)), 31.66 ((NH-(CH$_2$)$_4$-*C*H$_2$) or ((CO)$_2$N-(CH$_2$)$_4$-*C*H$_2$)), 29.37 (NH-CH$_2$-*C*H$_2$), 28.13 ((CO)$_2$N-CH$_2$-*C*H$_2$), 27.11 (NH-(CH$_2$)$_2$-*C*H$_2$), 27.01 ((CO)$_2$N-(CH$_2$)$_2$-*C*H$_2$), 22.75 (NH-(CH$_2$)$_4$-*C*H$_2$) and ((CO)$_2$N-(CH$_2$)$_4$-*C*H$_2$), (NH-(CH$_2$)$_4$-*C*H$_2$) 14.14 (*C*H$_3$) ppm. **HRMS** (ESI): *m/z* calcd. for $C_{48}H_{60}N_4O_4$ 756.46091 [M+H]$^+$, found 756.46031 [M+H]$^+$. **IR** (ATR): υ = 3318 (w), 2954 (m), 2920 (m), 2852 (m), 1734 (m), 1717 (s), 1685 (m), 1653 (m), 1590 (m), 1569 (m), 1560 (m), 1507 (m), 1489 (m), 1472 (m), 1420 (m), 1338 (s), 1276 (s), 1260 (m), 1181 (m), 1122 (m), 1091 (m), 1022 (m) 866 (m), 804 (m), 720 (m),682 (m) cm^{-1}.

2-(Trimethylsilyl)thiophene (TphTMS)

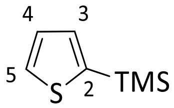

In a Schlenk tube, 2-bromothiophene (10.0 g,61.3 mmol) was dissolved in diethyl ether (100 mL) and cooled to -78 °C. To this solution, *n*-butyllithium (27.0 mL, 67.5 mmol, 2.5 M in *n*-hexane) was added over a period of 5 min and the reaction mixture was stirred for 1 h. Subsequently, trimethylsilyl chloride (8.10 mL, 67.4 mmol) was added in one portion and the reaction mixture was stirred for 18 h. The reaction mixture was added to a sat. aq. ammonium chloride solution (150 mL). The organic phase was separated, washed with water (2 x 150 mL), dried over magnesium sulfate, filtered, and after careful removal of the solvent using a rotary evaporator (b.p. (**TphTMS**) = 70 °C (20 mbar)), the product was obtained as a colorless oil (7.52 g, 48.1 mmol, 78%).

^{1}H NMR (600 MHz, $CDCl_3$) δ = 7.61 (dd, ^3J = 4.6 Hz, ^4J = 0.9 Hz, 1H, *H*-5), 7.28 (dd, ^3J = 3.3 Hz, ^4J = 0.9 Hz, 1H, *H*-3), 6.60 (dd, ^3J = 4.6 Hz, ^3J = 3.3 Hz, 1H, *H*-4), 0.34 (s, 9H, CH_3) ppm. **^{13}C{^{1}H} NMR** (151 MHz, $CDCl_3$) δ = 140.21 (*C*-2), 134.08 (*C*-3), 130.51 (*C*-5), 128.22 (*C*-4), 0.16 (CH_3) ppm. **^{29}Si{^{1}H} NMR** (119 MHz, $CDCl_3$) δ = -6.54 (s) ppm. **HRMS** (EI): *m/z* $[M]^{+\cdot}$ calcd. for $C_7H_{12}SSi$ 156.04235; found 156.04191; 141.10 (100%). **IR** (ATR): υ = 2956 (w), 1406 (m), 1325 (w), 1248 (s), 1213 (m), 1082 (m), 991 (m), 857 (m), 825 (s), 754 (s), 701 (s) cm^{-1}.

The analytical data were in accordance to previously reported values.[6]

Dichloro-2-thienyl borane (TphBCl$_2$)

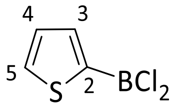

Under a argon atmosphere, 2-(trimethylsilyl)thiophene (**TphTMS**, 5.96 g, 38.1 mmol) was added to a solution of boron trichloride (60.0 mL, 60.0 mmol, 1 M in DCM) within 10 min at -50 °C. The reaction mixture was slowly warmed to 22 °C over the course of 14 h. After the solvent was removed *in vacuo*, the crude product was purified by inert Kugelrohr distillation (70 °C, 17 mbar) to give the product as a colorless oil (**TphBCl$_2$**, 4.66 g, 27.6 mmol, 72%). This very corrosive product was stored in the glovebox freezer (-25 °C).

^{1}H NMR (500 MHz, C_6D_6) δ = 7.64 (dd, ^3J = 3.7 Hz, ^4J = 1.0 Hz, 1H, *H*-5), 7.10 (dd, ^3J = 4.6 Hz, ^4J = 1.0 Hz, 1H, *H*-3), 6.60 (dd, ^3J = 4.6 Hz, ^3J = 3.7 Hz, 1H, *H*-4) ppm. **^{13}C{^{1}H} NMR** (126 MHz, C_6D_6) δ = 143.46 (*C*-3), 140.48 (*C*-5), 139.0 (*C*-2, only HMBC), 129.75 (*C*-4) ppm. **^{11}B{^{1}H} NMR** (160 MHz, C_6D_6) δ = 48.88 (s) ppm. Due to the corrosive nature of this molecule mass spectrometry data were not obtained.

The analytical data are in accordance with literature.[7]

4-(Trimethylsilyl)triphenylamine (TPATMS)

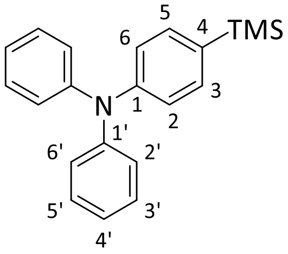

This synthetic procedure was adapted from the literature[8]: In a Schlenk flask, THF (2 mL) and 1,2-dibromoethane (200 µL, 2.32 mmol) were added to magnesium turnings (4.49 g, 184.8 mmol) at 25 °C, and the resulting mixture was stirred for 5 min. To this mixture, a part (4 mL) of a 4-bromotriphenylamine (**TPABr**, 10.0 g, 30.8 mmol) solution in THF (20 mL) was added and the mixture was heated to 55 °C. After 5 min stirring at this temperature the rest of the solution (16 mL) was added dropwise over the course of 20 min. After the addition was complete, the reaction mixture was stirred at 80 °C for a further 30 min. The still warm solution (≈40 °C) was transferred into another flask via a stainless steel cannula and chlorotrimethylsilane (3.36 g, 30.8 mmol) was added dropwise to this solution over the course of 10 min. After the addition was complete, the mixture was heated to 50 °C for 2 h, and then stirred at 25 C for 2 d. To this mixture, water (100 mL) was added, and the mixture was extracted with *n*-hexane (3 x 100 mL). All organic extracts were combined, dried over magnesium sulfate, filtrated and concentrated *in vacuo* to give an yellow oil (6.95 g, 21.9 mmol, 71%, lit.[8]: 84%).

^{1}H NMR (600 MHz, CDCl$_3$): δ = 7.39 (d, ^3J = 7.9 Hz, 2H, *H*-3,5), 7.08 -7.03 (m, 4H, *H*-3',5'), 7.13 (d, ^3J = 7.5 Hz, 4H, *H*-2',6'), 7.08 -7.03 (m, 4H, *H*-4' and *H*-2,6), 0.27 (s, 9H, C*H*$_3$) ppm. **^{13}C{^{1}H} NMR** (151 MHz, CDCl$_3$): δ = 148.46 (*C*-1), 147.77 (*C*-1'), 134.37 (*C*-3,5), 133.43 (*C*-4), 129.36 (*C*-3',5'), 124.73 (*C*-2',6'), 123.07 (*C*-4'), 122.86 (*C*-2,6), 14.14 (*C*H$_3$) ppm. **^{29}Si{^{1}H} NMR** (119 MHz, CDCl$_3$): δ = -4.67 (s) ppm. **HRMS** (EI): *m/z* calcd. for $C_{21}H_{23}NSi$ 317.15943 [M]$^{+\cdot}$, found 317.15971; 302.30 (100%). **IR** (ATR): υ = 3019 (w), 2951 (m), 1583 (s), 1485 (s), 1325 (m), 1314 (m), 1271 (s), 1247 (m), 1109 (m), 1075 (w), 1027 (w), 833 (s), 815 (m), 749 (m), 717 (m), 692 (s) cm^{-1}.

The analytical data were in agreement with reported values.[8]

1,7-Di(*n*-hexyl)-6,12-di(phenyl)-1,12,6,7-di([1,2]azaborinine)-*N*,*N'*-di(cyclohexyl)perylene-3,4,9,10-tetracarboxylic acid diimide (Ph-BNCDI^{Cy})

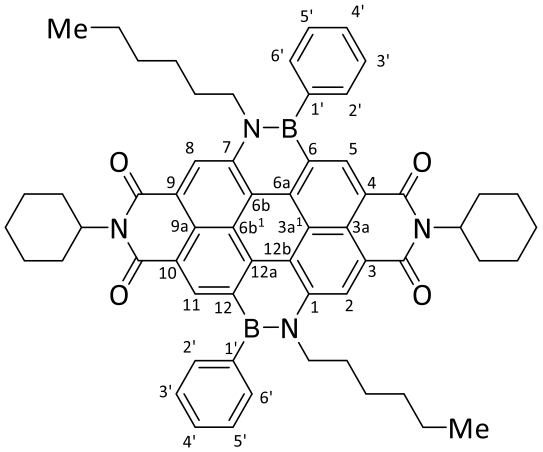

In a nitrogen filled glovebox, a Schlenk tube was charged with 1,7-di(*n*-hexylamino)-*N*,*N'*-di(cyclohexyl)perylene-3,4,9,10-tetracaboxylic acid diimide (**1,7-DHA-PDI^{Cy}**, 20.0 mg, 26.7 µmol), toluene (5.0 mL), triethylamine (0.5 mL) and dichlorophenyl borane (16.0 mg, 106 µmol). The reaction mixture was stirred for 14 h at 110 °C. After allowing the reaction to cool, all volatiles were removed and the residue was dissolved in DCM (30 mL), washed with brine (3 x 50 mL), NaOH (1 M, 3 x 50 mL) and water (3 x 50 mL). After drying over magnesium sulfate, filtration and removal of the solvent under reduced pressure, the crude product was subjected to column chromatography (silica, eluent: DCM, R_f = 0.80) to give the product (**Ph-BNCDI^{Cy}**, 18 mg, 19.4 µmol, 98%) as a red-violet solid.

^{1}H NMR (500 MHz, CDCl$_3$): δ = 9.53 (s, 2H, *H*-2,8), 9.34 (s, 2H, *H*-5,11), 7.73 (dd, ^3J = 7.7 Hz, ^4J = 1.4 Hz, 4H, Ph-*H*-2',6'), 7.69 - 7.55 (m, 6H, Ph-*H*-3',4',5'), 5.22 (tt, ^3J = 12.1 Hz , ^4J = 3.7 Hz, 2H, C*H*), 4.70 (t, ^3J = 12.1 Hz, 4H, N-C*H*$_2$), 2.69 (qd, ^3J = 12.5 Hz , ^4J = 3.3 Hz, 4H, CH-C*H*$_{ax}$), 2.09 - 1.93 (m, 8H, N-(CH$_2$)-C*H*$_2$ and CH-(CH$_2$)C*H*$_{ax}$) , 1.90 (d, ^3J = 10.9 Hz, 4H, CH-C*H*$_{eq}$), 1.75 (d, ^3J = 14.2 Hz, 2H, CH-(CH$_2$)$_2$-C*H*$_{ax}$), 1.59 - 1.45 (m, 4H, N-(CH$_2$)-C*H*$_2$), 1.46 - 1.33 (m, 6H, N-(CH$_2$)-C*H*$_2$ and CH-(CH$_2$)$_2$-C*H*$_{eq}$), 1.32 - 1.18 (m, 8H, (C*H*$_2$)$_2$-CH$_3$ and CH-(CH$_2$)C*H*$_{eq}$), 0.86 (t, ^3J = 7.0 Hz, 6H, C*H*$_3$) ppm. **^{13}C{^{1}H} NMR** (126 MHz, CDCl$_3$): δ = 165.12/165.09 ((*C*(O)N)-3,9/4,10), 138.88 (Ph-*C*-1', only HMBC), 138.69 (*C*-1,7), 137.34 (*C*-5,11), 134.01 (*C*-6a,12a), 132.68 (Ph-*C*-2',6'), 132.21 (*C*-6,12), 128.50 (Ph-*C*-4'), 128.37 (Ph-*C*-2',5'), 123.54/123.39 (*C*-3,9 or *C*-4,10), 123.26 (*C*-3a,9a), 120.77 (*C*-3a$_1$,6b$_1$), 120.71 (*C*-2,8), 120.39 (*C*-6b,12b), 54.48 (*C*H), 50.37 (N-*C*H$_2$), 31.33 (N-(CH$_2$)$_3$-*C*H$_2$), 31.24 (CH-CH$_2$-*C*H$_2$), 29.52 (CH-*C*H$_2$), 26.83 (N-CH$_2$-(CH$_2$)$_2$-*C*H$_2$), 25.68 (CH-(CH$_2$)$_2$-*C*H$_2$), 22.63 (N-(CH$_2$)$_4$-*C*H$_2$), 14.08 (*C*H$_3$) ppm. **^{11}B{^{1}H} NMR** (160 MHz, CDCl$_3$): δ = 39.63 (br) ppm. **HRMS** (EI): *m/z* $[M]^{+\cdot}$ Calcd. $C_{84}H_{80}{}^{11}B_2N_4O_4$ 924.49517; found 924.49473 (100%); $[M]^{+\cdot}$ Calcd. $C_{84}H_{80}{}^{10}B_2N_4O_4$ 922.50243; found 922.48756. **IR** (ATR): υ = 2922 (m), 2851 (m), 1697 (s), 1654 (s), 1596 (s), 1565 (m), 1449 (m), 1437 (s), 1413 (m), 1338 (m), 1299 (s), 1244 (s), 1197 (m), 1102 (m), 1058 (m), 958 (m), 895 (m), 812 (m), 758 (m), 738 (m), 703 (s), 656 (s) cm^{-1}.

1,7-Di(*n*-hexyl)-6,12-di(phenyl)-1,12,6,7-di([1,2]azaborinine)-*N*,*N'*-bis(2,6-di(*iso*proypyl)phenyl)perylene-3,4,9,10-tetracarboxylic acid diimide (Ph-BNCDI^{Dip})

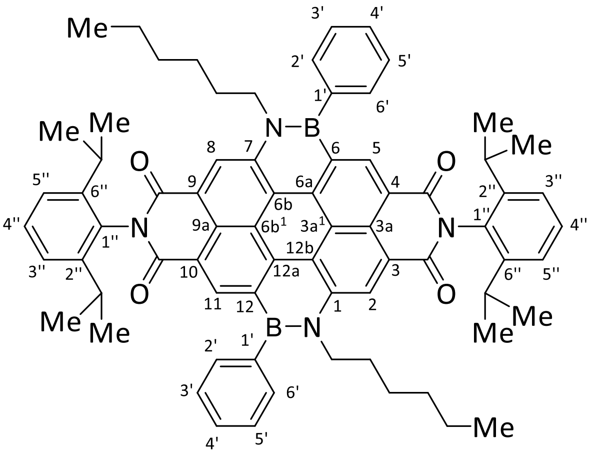

In a nitrogen filled glovebox, a Schlenk tube was charged with 1,7-di(*n*-hexylamino)-*N*,*N'*-*bis*(2,6-di(*iso*propyl)phenyl)perylene-3,4,9,10-tetracaboxylic acid diimide (**1,7-DHA-PDI^{Dip}**, 18.0 mg, 19.8 µmol), toluene (5.0 mL), triethylamine (0.5 mL) and dichlorophenyl borane (**PhBCl$_2$**, 16 mg, 106 µmol). The reaction mixture was stirred for 14 h at 110 °C. After allowing the reaction mixture to cool, all volatiles were removed *in vacuo.* The residue was dissolved in DCM (30 mL), washed with brine (3 x 50 mL), NaOH (1 M, 3 x 50 mL) and water (3 x 50 mL). After drying over magnesium sulfate, filtration and removal of the solvent, the crude product was subjected to column chromatography (silica, eluent: DCM, R$_f$ = 0.81) to give the product (**Ph-BNCDI^{Dip}**, 18 mg, 16.7 µmol, 84%) as a red-violet solid.

^{1}H NMR (500 MHz, $CDCl_3$): δ = 9.73 (s, 2H, *H*-2,8), 9.52 (s, 2H, *H*-5,11), 7.84 - 7.77 (dd, ^3J = 7.3 Hz, ^4J = 1.2 Hz 4H, Ph-*H*-2',6'), 7.64 (t, ^3J = 7.3 Hz, 4H, Ph-*H*-3',5'), 7.60 - 7.54 (m, 2H, Ph-*H*-4'), 7.51 (t, ^3J = 7.3 Hz, 2H, N-(Ph-*H*-4'')), 7.38 (d, ^3J = 7.9 Hz, 4H, N-(Ph-*H*-3,5'')), 4.79 (t, ^3J = 7.7 Hz, 4H, N-C*H*$_2$), 2.89 (sept. ^3J = 6.8 Hz, 4H, Ph-(C*H*)-(CH_3)$_2$), 2.13 - 2.04 (m, 4H, N-CH_2-C*H*$_2$), 1.47 - 1.38 (m, 4H, N-(CH_2)$_2$-C*H*$_2$), 1.30 - 1.15 (m, 32 H, N-(CH_2)$_2$-(C*H*$_2$)$_2$ and Ph-(CH)-(C*H*$_3$)$_2$), 0.82 (t, ^3J = 7.0 Hz, 6H, C*H*$_3$) ppm. **^{13}C{^{1}H} NMR** (126 MHz, $CDCl_3$): δ = 164.78 ((*C*(O)N)-4,10), 164.50 ((*C*(O)N)-3,9), 145.87 (N-(Ph-*C*-2'',6'')), 139.11 (*C*-1,7),138.94 (Ph-*C*-1', only HMBC) 138.04 (*C*-5,11), 134.77 (*C*-6a,12a), 132.69 (Ph-*C*-2',6'), 131.15 (N-(Ph-*C*-1'')), 129.68 (N-(Ph-*C*-4'')), 128.63 (Ph-*C*-3',5'), 128.43 (Ph-*C*-4'), 124.45 (*C*-3a,9a), 124.18 (*C*-3,9 or *C*-4,10), 124.07 (N-(Ph-*C*-3'',5'')), 123.19 (*C*-3,9 or *C*-4,10), 121.53 (*C*-2,8), 121.12 (*C*-6b,12b), 120.55 (*C*-3a$_1$,6b$_1$), 50.60 (N-*C*H$_2$), 31.35 (N-CH_2-*C*H$_2$), 31.30 (N-(CH_2)$_4$-*C*H$_2$), 29.41 (Ph-(*C*H)-(CH_3)$_2$), 26.74 (NH-(CH_2)$_3$-*C*H$_2$), 24.27 and 24.22 (Ph-(CH)-(*C*H$_3$)$_2$), 22.50 (NH-(CH_2)$_4$-*C*H$_2$), 14.02 (*C*H$_3$) ppm. **^{11}B{^{1}H} NMR** (160 MHz, $CDCl_3$): δ = 41.01 (br) ppm. **HRMS** (APCI, positive mode): *m/z* $[M+H]^+$ Calcd. for $C_{72}H_{75}{}^{11}B_2N_4O_4$ 1081.59903; found 1081. 59890. **IR** (ATR): υ = 2958 (w), 2924 (w), 2866 (w), 1708 (m), 1670 (s), 1599 (m), 1563 (m), 1446 (m), 1436 (m), 1312 (s), 1280 (m), 1247 (s), 1208 (m), 1109 (m), 1063 (m), 846 (m), 814 (m), 791 (m), 774 (m), 760 (m), 736 (s), 703 (m), 681 (m) cm^{-1}.

1,7-Di(*n*-hexyl)-6,12-di(phenyl)-1,12,6,7-di([1,2]azaborinine)-*N*,*N'*-di(*n*-hexyl)perylene3,4,9,10-tetracarboxylic acid diimide (Ph-BNCDI$^{\text{Hex}}$)

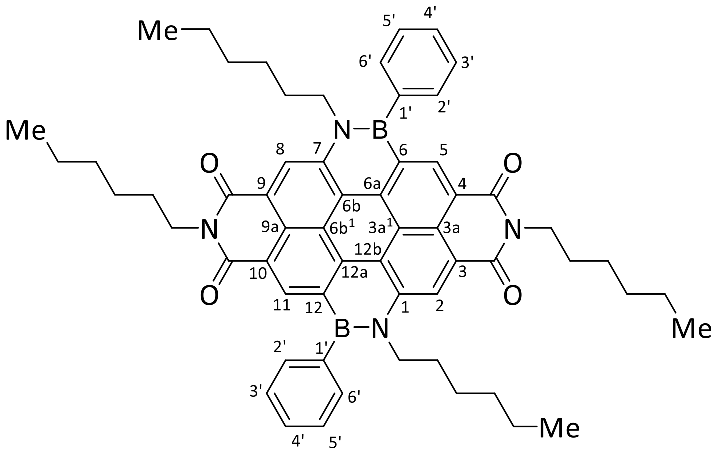

In a nitrogen filled glovebox, a Schlenk tube was charged with 1,7-di(*n*-hexylamino)-*N*,*N'*-di(*n*-hexyl)perylene-3,4,9,10-tetracaboxylic acid diimide (**1,7-DHA-PDI$^{\text{Hex}}$**, 50.0 mg, 66.0 µmol), toluene (10.0 mL), triethylamine (0.5 mL) and dichlorophenyl borane (40.2 mg, 264 µmol). The reaction mixture was stirred for 12 h at 110 °C. After allowing the reaction mixture to cool, the solvent was evaporated and the residue was dissolved in DCM (30 mL), washed with brine (1 x 50 mL), .1 M NaOH (1 x 50 mL) and water (1 x 50 mL). After drying over magnesium sulfate, filtration, and removal of the solvent, the crude product was purified by column (silica, eluent: DCM, R_f = 0.83) to give the product as a red-violet solid (**Ph-BNCDI$^{\text{Hex}}$**, 29.0 mg, 31.1 µmol, 47%).

^{1}H NMR (500 MHz, CDCl$_3$): δ = 9.55 (s, 2H, *H*-2,8), 9.38 (s, 2H, *H*-5,11*)*, 7.76 (dd, ^3J = 7.7 Hz, ^4J = 1.4 Hz, 4H, Ph-*H*-2',6'), 7.62 (m, 6H, Ph-*H*-3',4',5'), 4.71 (t, ^3J = 7.8 Hz, 4H, BN-C*H*$_2$), 4.31 (t, ^3J = 7.6 Hz, 4H, (CO)$_2$N-C*H*$_2$), 2.04 (quin., ^3J = 7.5 Hz, 4H, BN-CH$_2$-C*H*$_2$), 1.85 (quin., ^3J = 7.5 Hz, 4H, (CO)$_2$N-CH$_2$-C*H*$_2$), 1.50 (quin., ^3J = 7.5 Hz, BN-(CH$_2$)$_2$-C*H*$_2$), 1.38 (m, 14H, BN-(CH$_2$)$_4$-C*H*$_2$, (CO)$_2$N-(CH$_2$)$_2$-C*H*$_2$ and BN-CH$_2$-C*H*$_2$), 1.23 (m, 20H, (CO)$_2$N-(CH$_2$)$_4$-C*H*$_2$ and (CO)$_2$N-(CH$_2$)$_4$-C*H*$_2$ and residual grease), 0.91 (t, ^3J = 7.1 Hz, 6H, C*H*$_3$),0.86 (t, ^3J = 6.9 Hz, 6H, C*H*$_3$) ppm. **^{13}C{^{1}H} NMR** (126 MHz, CDCl$_3$): δ = 164.55 ((*C*(O)N)-4,10), 164.53 ((*C*(O)N)-3,9), 139.20 (Ph-*C*-1', only HMBC), 138.72 (*C*-1,7), 137.48 (*C*-5,11), 134.22 (*C*-6a,12a), 132.66 (Ph-*C*-2',6'), 132.41 (br, *C*-6,12), 128.56 (Ph-*C*-4'), 128.39 (Ph-*C*-3',5'), 123.52 (*C*-3,9), 123.43 (*C*-4,10), 122.92 (*C*-3a,9a), 120.78 (*C*-3a^1,6b^1), 120.57 (*C*-6b,12b), 120.18 (*C*-2,8), 50.43 (N-*C*H$_2$), 41.13 ((CO)$_2$N-*C*H$_2$), 31.75 ((BN-(CH$_2$)$_4$-*C*H$_2$), 31.34 (CO)$_2$N-(CH$_2$)$_4$-*C*H$_2$), 31.28 (BN-CH$_2$-*C*H$_2$), 29.85 ((CO)$_2$N-CH$_2$-*C*H$_2$), 28.38 (BN-(CH$_2$)$_3$-*C*H$_2$) and(CO)$_2$N-(CH$_2$)$_3$-*C*H$_2$), 27.09 (BN-(CH$_2$)$_2$-*C*H$_2$), 26.82 ((CO)$_2$N-(CH$_2$)$_2$-*C*H$_2$), 22.76 (BN-(CH$_2$)$_4$-*C*H$_2$), 22.63 ((CO)$_2$N N-(CH$_2$)$_4$-*C*H$_2$), 14.24 (BN-(CH$_2$)$_5$-*C*H$_3$), 14.08 ((CO)$_2$N-(CH$_2$)$_5$-*C*H$_3$) ppm. **^{11}B{^{1}H} NMR** (160 MHz, CDCl$_3$): δ = 40.42 ppm. **HRMS** (APCI): *m/z* [M+H]$^+$ calcd. for $C_{60}H_{67}{}^{11}B_2N_4O_4$ 929.53602; found 929.53628. **IR** (ATR): υ = 2955 (w), 2923 (w), 2865 (w), 1706 (m), 1667 (m), 1600 (m), 1562 (m), 1448 (m), 1436 (m), 1327 (m), 1281 (m), 1247 (s), 1208 (m), 1105 (m), 1029 (m), 1062 (m), 958 (m), 844 (m), 775 (s), 760 (m), 736 (m), 700 (m) cm^{-1}.

1,7-Di(*n*-hexyl)-6,12-di(thiophen-2-yl)-1,12,6,7-di([1,2]azaborinine)-*N*,*N'*-di(cyclohexyl)perylene-3,4,9,10-tetracarboxylic acid diimide (Tph-BNCDI$^{\mathrm{Cy}}$)

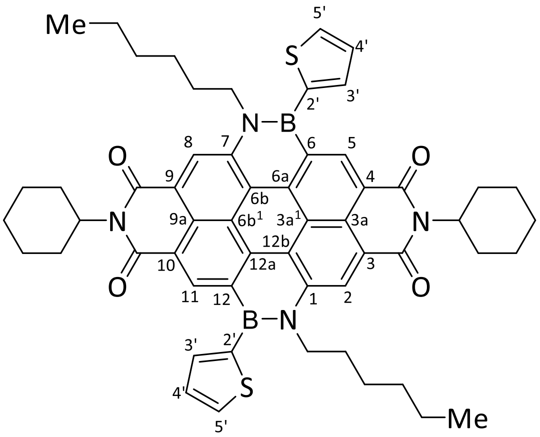

In a nitrogen filled glovebox, a vial was charged with 1,7-di(*n*-hexylamino)-*N*,*N'*-di(cyclohexyl)perylene-3,4,9,10-tetracaboxylic acid diimide (**1,7-DHA-PDI$^{\mathrm{Cy}}$**, 19.0 mg, 25.2 µmol), toluene (5.0 mL), triethylamine (0.5 mL) and dichloro-2-thienyl borane (**$\mathrm{TphBCl_2}$**, 175 mg, 403 µmol). The sealed vial was heated 24 h at 110 °C. After cooling to 25 °C, all volatiles were removed *in vacuo* and the red product was dried (9.7 x 10^{-2} mbar, 70 °C, 2 h). The residue was dissolved in DCM (30 mL), washed with brine (3 x 50 mL), 1 M NaOH (3 x 50 mL) and water (3 x 50 mL). After drying over magnesium sulfate, filtration, removal of the solvent, the product was subjected to column chromatography (silica, eluent: gradient petrol ether to DCM, R_f(DCM) = 0.65) to give the product (**BNCDI$^{\mathrm{Cy}}$**, 23 mg, 24.5 µmol, 97%) as a red-violet solid.

^{1}H NMR (500 MHz, $\mathrm{CDCl_3}$): δ = 9.56 (s, 2H, *H*-2,8), 9.54 (s, 2H, *H*-5,11*)*, 7.87 (dd, ^3J = 4.8 Hz, ^4J = 0.8 Hz, 22H, Tph-*H*-3'), 7.61 (dd, ^3J = 3.2 Hz, ^4J = 0.8 Hz, 2H, Tph-*H*-5'), 6.60 (dd, ^3J = 4.8 Hz, ^3J = 3.2 Hz, 2H, Tph-*H*-4'), 5.23 (tt, ^3J = 12.0, 3.8 Hz, 2H, C*H*), 4.79 (t, ^3J = 7.8 Hz, 4H, N-CH_2), 2.70 (qd, ^3J = 12.0, 3.0 Hz, 4H, CH-CH_{ax}), 2.12 (quin., ^3J = 7.8 Hz, 4H, N-($\mathrm{CH_2}$)-CH_2), 1.98 (d, ^3J = 13.5 Hz, 4H, CH-$\mathrm{CH_2}$-CH_{ax}), 1.91 (d, ^3J = 12.0 Hz, 4H, CH-CH_{eq}), 1.79 (d, ^3J = 13.0 Hz, 2H, CH-$(\mathrm{CH_2})_2$-CH_{ax}), 1.59 - 1.26 (m, 18H, CH-$\mathrm{CH_2}$-CH_{eq}, CH-$(\mathrm{CH_2})_2$-CH_{eq} and N-$(\mathrm{CH_2})_2$-(CH_2)$_3$), 0.90 (t, ^3J = 7.0 Hz, 6H, CH_3) ppm. **^{13}C{^{1}H} NMR** (126 MHz, $\mathrm{CDCl_3}$): δ = 165.06 ((*C*(O)N)-4,10), 165.04 ((*C*(O)N)-3,9), 138.79 (*C*-1,7), 137.33 (*C*-5,11), 136.68 (Tph-*C*-2', only HMBC), 134.22 (Tph-*C*-5'), 133.85 (*C*-6a,12a), 132.51 (*C*-6,12, only HMBC), 130.03 (Tph-*C*-3'), 128.55 (Tph-*C*-4'), 123.70 (*C*-3,9 or *C*-4,10), 123.54 (*C*-3,9 or *C*-4,10), 123.15 (*C*-3a^1,6b^1), 122.67 (*C*-3a,9a), 12089 (*C*-2,8), 120.46 (*C*-6b,12b), 54.56 (*C*H), 50.70 (N-*C*$\mathrm{H_2}$), 31.81 (N-$\mathrm{CH_2}$-*C*$\mathrm{H_2}$), 31.48 (CH-*C*$\mathrm{H_2}$), 29.53 (N-$(\mathrm{CH_2})_2$-*C*$\mathrm{H_2}$), 26.85 (N-$(\mathrm{CH_2})_3$-*C*$\mathrm{H_2}$), 26.85 (CH-$\mathrm{CH_2}$-*C*$\mathrm{H_2}$), 25.70 (CH-$(\mathrm{CH_2})_2$-*C*$\mathrm{H_2}$), 22.74 (N-$(\mathrm{CH_2})_4$-*C*$\mathrm{H_2}$), 14.13 (*C*$\mathrm{H_3}$) ppm. **^{11}B{^{1}H} NMR** (160 MHz, $\mathrm{CDCl_3}$): δ = 38.70 (br) ppm. **HRMS** (EI): *m/z* [M]$^+$ calcd. for $\mathrm{C_{56}H_{58}N_4O_4{}^{11}B_2S_2}$ 936.41460; found 936.41893 (100%). **IR** (ATR): υ = 2921 (m), 2852 (m), 1698 (s), 1654 (s), 1599 (s), 1566 (m), 1450 (s), 1416 (m), 1404 (m), 1343 (w), 1302(s), 1280 (m), 1245 (s), 1202 (m), 1087 (w), 1020 (w), 897 (w), 847 (w), 812 (m), 706 (m), 651 (m), 599 (w) cm^{-1}.

1,7-Di(*n*-hexyl)-6,12-di(thiophen-2-yl)-1,12,6,7-di([1,2]azaborinine)-*N*,*N*'-bis(2,6-di(*iso*proypyl)phenyl)perylene-3,4,9,10-tetracarboxylic acid diimide (Tph-BNCDI$^{\mathrm{Dip}}$)

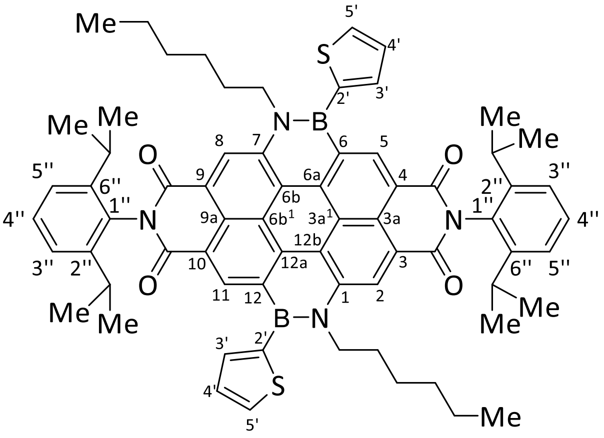

In a nitrogen filled glovebox, a pressure tube (50 mL) was charged with 1,7-di(*n*-hexylamino)-*N*,*N*'-*bis*(di*iso*propylphenyl)perylene-3,4,9,10-tetracaboxylic acid diimide (**1,7-DHA-PDI$^{\mathrm{Dip}}$**, 120 mg, 132 µmol), toluene (4.8 mL), triethylamine (200 µL) and dichloro-2-thienyl borane (100 mg, 607 µmol). The sealed tube was heated for 10 h at 110 °C. After cooling to 25 °C, the reaction mixture was dissolved in DCM (30 mL), washed with brine (3 x 50 mL), 1 M NaOH (3 x 50 mL) and water (3 x 50 mL). After drying over magnesium sulfate, filtration, and removal of the solvent *in vacuo*, the crude product was purified by column chromatography (silica, eluent: DCM, R$_f$(DCM) = 0.81) to give the red/violet product (**BNCDI$^{\mathrm{Dip}}$**, 120 mg, 110 µmol, 83%).

^{1}H NMR (500 MHz, CDCl$_3$): δ = 9.75 (s, 2H, *H*-5,11), 9.74 (s, 2H, *H*-2,8), 7.86 (dd, ^3J = 4.8 Hz, ^4J = 0.8 Hz, 2H, Tph-*H*-3'), 7.67 (dd, ^3J = 3.3 Hz, ^4J = 0.8 Hz, 2H, Tph-*H*-5'), 7.53 (t, ^3J = 7.9 Hz, 2H, Ph-*H*-4''), 7.50 (dd, ^3J = 4.8 Hz, ^3J = 3.3 Hz, 2H, Tph-*H*-4'), 7.40 (d, ^3J = 7.9 Hz, 4H, Ph-*H*-3'',5''), 4.79 (m$_c$, 4H, N-C*H*$_2$), 2.91 (m$_c$, 4H, Ph-(C*H*)-(CH$_3$)$_2$), 2.20 (m$_c$, 4H, NH-C*H*$_2$), 1.54 (m$_c$, 4H, N-(CH$_2$)-C*H*$_2$), 1.51 - 1.21 (m, 8H, NH-(CH$_2$)$_2$-(C*H*$_2$)$_3$), 1.22 (t, ^3J = 6.8 Hz, 24H, Ph-(CH)-(C*H*$_3$)$_2$), 0.87 (t, ^3J = 7.0 Hz, 6H, C*H*$_3$) ppm. **^{13}C{^{1}H} NMR** (126 MHz, CDCl$_3$): δ = 164.69 ((*C*(O)N)-4,10), 164.49 ((*C*(O)N)-3,9), 145.84 (Ph-*C*-2'',6''), 139.16 (*C*-1,7), 138.02 (*C*-2,8), 136.60 (Tph-*C*-2'), 134.59 (*C*-6a,12a), 134.42 (Tph-*C*-5'), 132.71 (*C*-6,12, only HMBC), 131.06 (Ph-*C*-1''), 130.13 (Tph-*C*-3'), 129.71 (Ph-*C*-4''), 128.62 (Tph-*C*-4'), 124.20 (Ph-*C*-3'',5''), 123.92 (*C*-3a$_1$,6b$_1$), 123.24 (*C*-3,4/9,10), 121.63 (*C*-3a,9a), 121.14 (*C*-5,11), 120.61 (*C*-6b,12b), 50.92 (NH-C*H*$_2$), 31.90 (NH-CH$_2$-*C*H$_2$), 31.42 (NH-(CH$_2$)$_2$-*C*H$_2$), 29.42 (Ph-(*C*H)-(CH$_3$)$_2$), 26.75 (NH-(CH$_2$)$_3$-*C*H$_2$), 24.25 and 24.23 (Ph-(CH)-(*C*H$_3$)$_2$), 22.58 (NH-(CH$_2$)$_4$-*C*H$_2$), 14.08 (*C*H$_3$) ppm. **^{11}B{^{1}H} NMR** (160 MHz, CDCl$_3$): δ = 38.21 (br) ppm. **HRMS** (APCI, MeOH/toluene, positive mode): *m/z* [M+H]$^+$ calcd. For $C_{68}H_{71}{}^{11}B_2N_4O_4S_2$ 1093.51179; found 1093.51256. **HRMS** (APCI, MeOH/toluene, negative mode): *m/z* [M]$^{\cdot-}$ Calcd. for $C_{68}H_{70}{}^{11}B_2N_4O_4S_2$ 1092.50507; found 1092.50602. **IR** (ATR): υ = 2956 (w), 2921 (w), 2851 (w), 1707 (m), 1669 (m), 1600 (m), 1562 (m), 1436 (m), 1311 (s), 1280 (m), 1245 (s) 1207 (m), 1192 (m), 1053 (m), 847 (m), 813 (m), 792 (m), 759 (m), 753 (m), 720 (m), 700 (s) cm^{-1}.

1,7-Di(*n*-hexyl)-6,12-*bis*(4-(diphenylamino)phenyl)-1,12,6,7-*di*([1,2]azaborinine)-*N*,*N'*-di(cyclo-hexyl)perylene-3,4,9,10-tetracarboxylic acid diimide (TPA-BNCDI^{Cy})

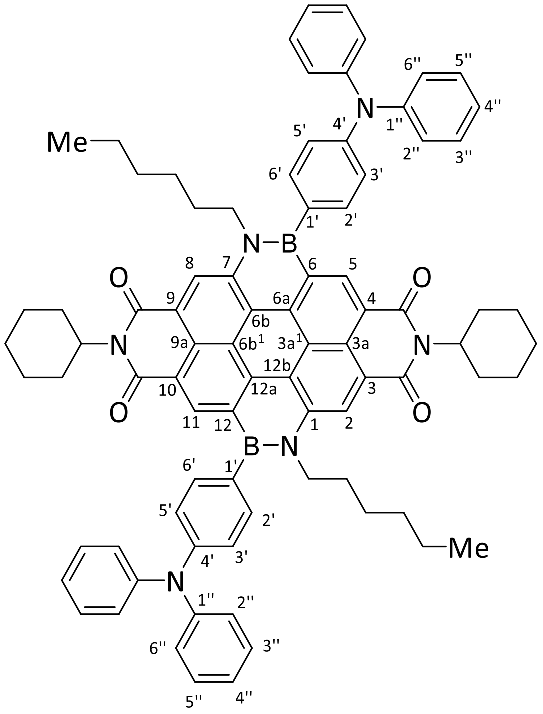

The precursor 4-(dichloroboranyl)-*N*,*N*-diphenylaniline was generated *in situ* from (4-(trimethylsilyl)phenyl)-diphenylamine (1.00 g, 3.15 mmol) using boron trichloride (3.50 mL, 3.50 mmol, 1 M in DCM) in DCM (10 mL). After stirring at 25 °C for 14 h, all volatiles were removed, and the resulting yellow oil was directly used.[8] In a nitrogen filled glovebox, a Schlenk tube was charged with 1,7-di(*n*-hexylamino)-*N*,*N'*-di(cyclohexyl)perylene-3,4,9,10-tetracaboxylic acid diimide (**1,7-DHA-PDI^{Cy}**, 111 mg, 150 µmol), toluene (10.0 mL), triethylamine (1.0 mL) and 4-(dichloroboranyl)-*N*,*N*-diphenylaniline (**TPABCl$_2$**, 1.02 g, 3.15 mmol). The sealed tube was stirred for 4 h at 110 °C. Afterwards all volatiles were removed *in vacuo* and the residue was dissolved in DCM (50 mL), washed with brine (3 x 50 mL), 1 M NaOH (3 x 50 mL) and water (3 x 50 mL). After drying over magnesium sulfate, filtration and removal of all volatiles *in vacuo*, the material was mixed with *n*-pentane (200 mL, 2x) and heated to 50 °C and the solution was discarded. The residual blue/violet solid was subjected to column chromatography. (silica, eluent: gradient *n*-pentane to DCM, R_f(DCM) = 0.75) to give the product (**TPA-BNCDI^{Cy}**, 134 mg, 0.11 mmol, 71%) as a red-violet solid.

^{1}H NMR (500 MHz, CDCl$_3$): δ = 9.59 (s, 2H, *H*-2,8), 9.54 (s, 2H, *H*-5,11), 7.62 (d, ^{3}J = 8.4 Hz, 4H, B-Ph-*H*-2',6'), 7.39 - 7.30 (m, 20H, B-Ph-*H*-3',5' and TPA-Ph-*H*-2'',3'',5'',6''), 7.10 (t, ^{3}J = 8.4 Hz, 4H, TPA-Ph-*H*-4''), 5.24 (tt, ^{3}J = 12.1 Hz , ^{4}J = 3.6 Hz, 2H, C*H*), 4.77 (t, ^{3}J = 8.0 Hz, 4H, N-CH_2), 2.71 (qd, ^{3}J = 12.6 Hz , ^{4}J = 3.3 Hz, 4H, CH-CH_{ax}), 2.07 (m$_c$, 4H, N-(CH$_2$)-CH_2), 1.98 (d, ^{3}J = 10.9 Hz, 4H, CH-(CH$_2$)CH_{ax}), 1.90 (d, ^{3}J = 10.2 Hz, 4H, CH-CH_{eq}), 1.79 (d, ^{3}J = 12.8 Hz, 2H, CH-(CH$_2$)$_2$-CH_{ax}), 1.62 - 1.40 (m, 20H, N-(CH$_2$)-CH_2, N-(CH$_2$)-CH_2 and CH-(CH$_2$)$_2$-CH_{eq}), 1.37-1.15 (m, 30H, (CH_2)$_2$-CH$_3$ and CH-(CH$_2$)CH_{eq}), 0.90 (t, ^{3}J = 7.0 Hz, 6H, CH_3) ppm. **^{13}C{^{1}H} NMR** (126 MHz, CDCl$_3$): δ = 164.83 ((*C*(O)N)-4,10), 164.66 ((*C*(O)N)-3,9), 148.08 (B-Ph-*C*-4'), 147.87 (TPA-Ph-*C*-1''), 138.97 (*C*-1,7), 137.49 (*C*-5,11), 134.26 (*C*-6a,12a), 134.01 (B-Ph-*C*-2',6'), 132.61 (*C*-6,12 only HMBC), 131.94 (B-Ph-*C*-1' only HMBC), 129.55 (TPA-Ph-*C*-3'',5''), 125.18 (TPA-Ph-*C*-2'',6''), 123.65/123.48 (*C*-3,9/4,10), 123.38 (*C*-3a,9a) 123.36 (TPA-Ph-*C*-4''), 122.63 (B-Ph-*C*-3',5'), 120.86 (*C*-6b,12b), 120.70 (*C*-3a^1,6b^1), 120.54 (*C*-2,8), 54.47 (*C*H), 50.37 (N-*C*H$_2$), 31.35 (N-(CH$_2$)-

*C*H$_2$ and N-(CH$_2$)$_3$-*C*H$_2$), 29.55 (CH-*C*H$_2$), 26.83 (CH-(CH$_2$)*C*H$_2$), 25.68 (CH-(CH$_2$)$_2$-*C*H$_2$), 22.73 (N-(CH$_2$)$_4$-*C*H$_2$), 14.14 (*C*H$_3$). **^{11}B{^{1}H} NMR** (160 MHz, CDCl$_3$): δ = 40.57 (br) ppm. **HRMS** (ESI): *m/z* [M-B$_2$]$^{2+}$ calcd. $C_{84}H_{80}N_6O_4$ 618.3115; found 618.31106. **IR** (ATR): υ = 2924 (w), 2856 (w), 1693 (m), 1654 (m), 1593 (s), 1566 (m), 1508 (m), 1486 (m), 1449 (m), 1436 (m), 1412 (m), 1362 (m), 1324 (m), 1299 (m), 1268 (s), 1256 (m), 1245 (m), 1194 (m), 1181 (m), 1102 (m), 813 (s), 755(s), 696 (s) cm^{-1}.

1,7-Di(*n*-hexyl)-6,12-*bis*(4-(diphenylamino)phenyl)-1,12,6,7-di([1,2]azaborinine)-*N,N'*-bis(2,6-di(*iso*proypyl)phenyl)perylene-3,4,9,10-tetracarboxylic acid diimide (TPA-BNCDI^{Dip})

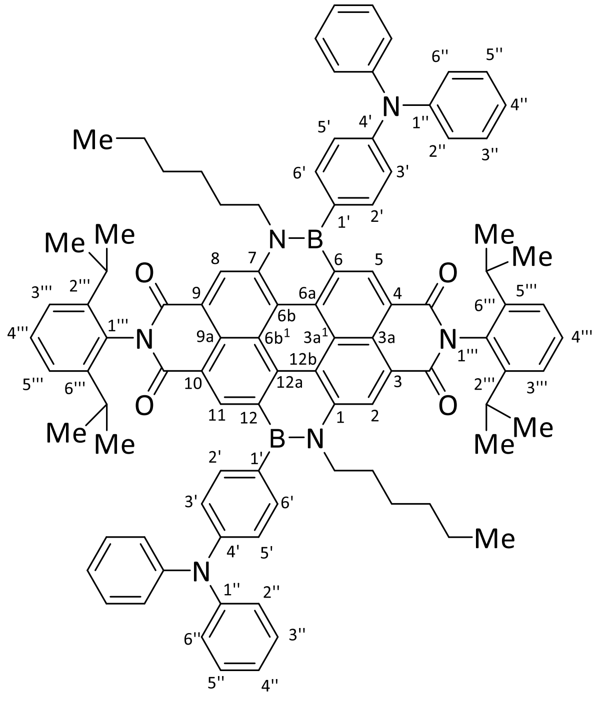

The precursor 4-(dichloroboranyl)-*N,N*-diphenylaniline was generated *in situ* from (4-(trimethylsilyl)phenyl)-diphenylamine (317 mg, 1.00 mmol) using boron trichloride (1.11 mL, 1.11 mmol, 1 M in DCM) in DCM (10 mL). After stirring at 25 °C for 14 h, all volatiles were removed, and the resulting yellow oil was directly used.[8] In a nitrogen filled glovebox, a sealable vial was charged with 1,7-di(*n*-hexylamino)-*N,N'*-*bis*(2,6-di(*iso*propyl)phenyl)perylene-3,4,9,10-tetracaboxylic acid diimide (**1,7-DHA-PDI^{Dip}**, 98 mg, 0.10 mmol), toluene (5.0 mL), triethylamine (0.5 mL) and 4-(dichloroboranyl)-*N,N*-diphenylaniline (**TPA-BCl$_2$**, 326 mg, 1.00 mmol). The reaction mixture was stirred for 12 h at 110 °C. After the reaction mixture was cooled to 25 °C, it was mixed with DCM (30 mL), washed with brine (3 x 50 mL), 1 M NaOH (3 x 50 mL) and water (3 x 50 mL). After drying of the organic phase over magnesium sulfate, filtration and evaporation of all volatiles, the residue was mixed with *n*-pentane (200 mL, 2x) and heated to 50 °C where the solution was discarded. The product was subjected to column chromatography (silica, eluent: gradient *n*-pentane to DCM, R$_f$ = 0.72) to give the product (71 mg, 0.05 mmol, 50%) as a red-violet solid.

^{1}H NMR (500 MHz, CDCl$_3$): δ = 9.72 (s, 2H, *H*-2,8), 9.66 (s, 2H, *H*-5,11), 7.66 (d, ^3J = 8.2 Hz, 4H, B-Ph-*H*-2',6'), 7.53 (t, ^3J = 7.9 Hz, 2H, (CO)$_2$N-Ph-*H*-4'''), 7.39 (d, ^3J = 8.3 Hz, 4H, (CO)$_2$N-Ph-*H*-3''',5'''), 7.37 - 7.24 (m, 12H, B-Ph-*H*-3',5' and TPA-Ph-*H*-3'',5''), 7.29 - 7.27 (m, 8H, and TPA-Ph-*H*-2'',6''), 7.08 (tt, ^3J = 7.2 Hz, ^4J = 1.0 Hz, 4H, TPA-Ph-*H*-4''), 4.84 (t, ^3J = 8.0 Hz, 4H, N-C*H*$_2$), 2.92 (sept., ^3J = 6.8 Hz, 4H, Ph-(C*H*)-(CH$_3$)$_2$), 2.23-2.17 (m, 4H, N-CH$_2$-C*H*$_2$), 1.52 - 1.44 (m, 4H, NH-(CH$_2$)$_2$-C*H*$_2$), 1.33- 1.27 (m, 8H, N-(CH$_2$)$_3$-(C*H*$_2$)$_2$), 1.26 - 1.18 (t, ^3J = 6.8 Hz, 24H, Ph-(CH)-(C*H*$_3$)$_2$), 0.87 (t, ^3J = 6.8 Hz, 6H, C*H*$_3$) ppm. **^{13}C{^{1}H}**

NMR (126 MHz, CDCl$_3$): *δ* = 164.83 ((*C*(O)N)-3,9), 164.66 ((*C*(O)N)-4,10), 148.24 (B-Ph-*C*-4’), 147.82 (TPA-Ph-*C*-1’’), 145.88 ((CO)$_2$N-Ph-*C*-2’’’,6’’’), 139.23 (*C*-1,7), 138.13 (*C*-5,11), 134.80 (*C*-6a,12a), 133.90 (B-Ph-*C*-2’,6’), 132.77 (*C*-6,12, only HMBC), 131.78 (B-Ph-*C*-1’, only HMBC), 131.19 ((CO)$_2$N-Ph-*C*-1’’’), 129.75 ((CO)$_2$N-Ph-*C*-4’’’), 129.55 (TPA-Ph-*C*-3’’,5’’), 125.21 (TPA-Ph-*C*-2’’,6’’), 124.39 (*C*-3a,9a), 124.26/124.10 ((CO)$_2$N-Ph-*C*-3’’’,5’’), 123.40 (TPA-Ph-*C*-4’’), 123.10/123.00 (*C*-3,9/4,10), 122.54 (B-Ph-*C*-3’,5’), 121.51 (*C*-2,8), 121.10 (*C*-6b,12b), 120.45 (*C*-3a^1,6b^1), 50.50 (N-C*H*$_2$), 31.36 (N-CH$_2$-*C*H$_2$), 31.29 (N-(CH$_2$)$_2$-*C*H$_2$), 29.42 (Ph-(*C*H)-(CH$_3$)$_2$), 26.81 (N-(CH$_2$)$_3$-*C*H$_2$), 24.30 and 24.24 (Ph-(CH)-(*C*H$_3$)$_2$), 22.60 (N-(CH$_2$)$_4$-*C*H$_2$), 14.07 (*C*H$_3$) ppm. **^{11}B{^{1}H} NMR** (160 MHz, CDCl$_3$): *δ* = 39.10 (br) ppm. **HRMS** (ESI, IMPACT II): *m/z* [M+Na]$^+$ calcd. $C_{96}H_{92}{}^{11}B_2N_6O_4Na$ 1437.72849; found 1437.72860. **IR** (ATR): υ = 2960 (w), 2927 (w), 2868 (w), 1706 (m), 1670 (m), 1601 (m), 1589 (m), 1566 (m), 1508 (m), 1488 (m), 1448 (m), 1438 (m), 1314 (m), 1249 (s), 1211 (m), 1195 (m), 1107 (w), 1056 (w), 988 (w), 847 (m), 815 (m), 793 (m), 739 (m), 697 (s) cm^{-1}.

NMR Spectra

Perylene-3,4,9,10-tetra-*n*-butylester (PTBE)

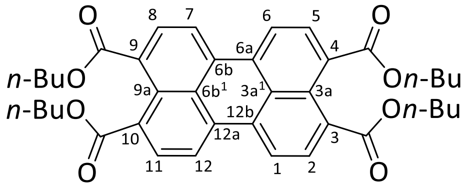

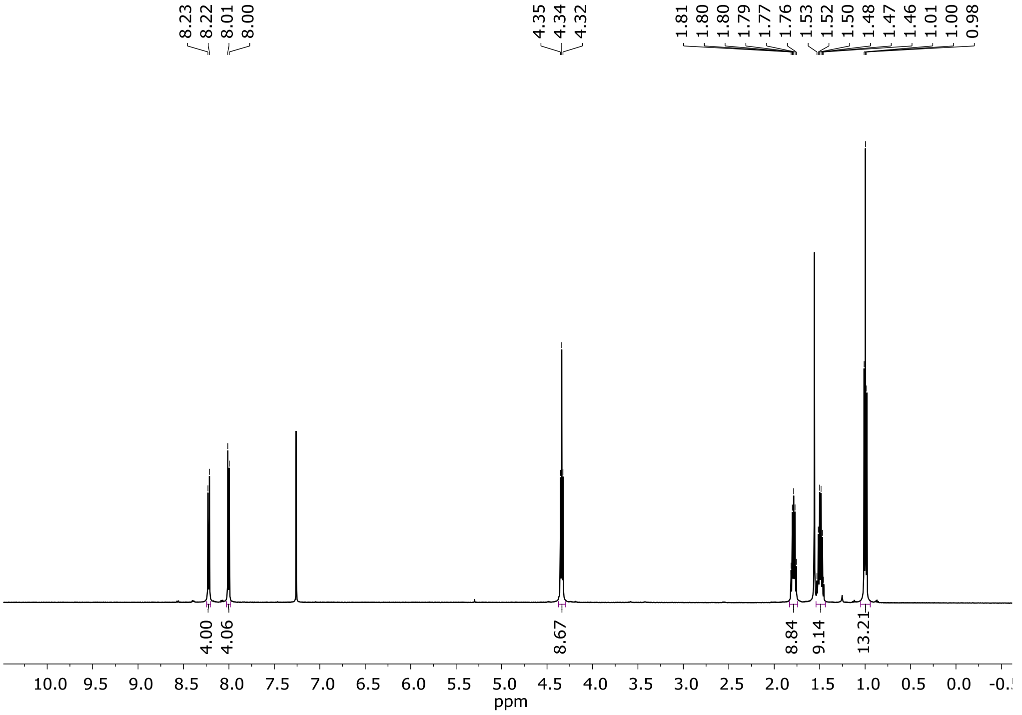

Fig. S1: ^{1}H NMR (500 MHz, $CDCl_3$) spectrum of **PTBE**.

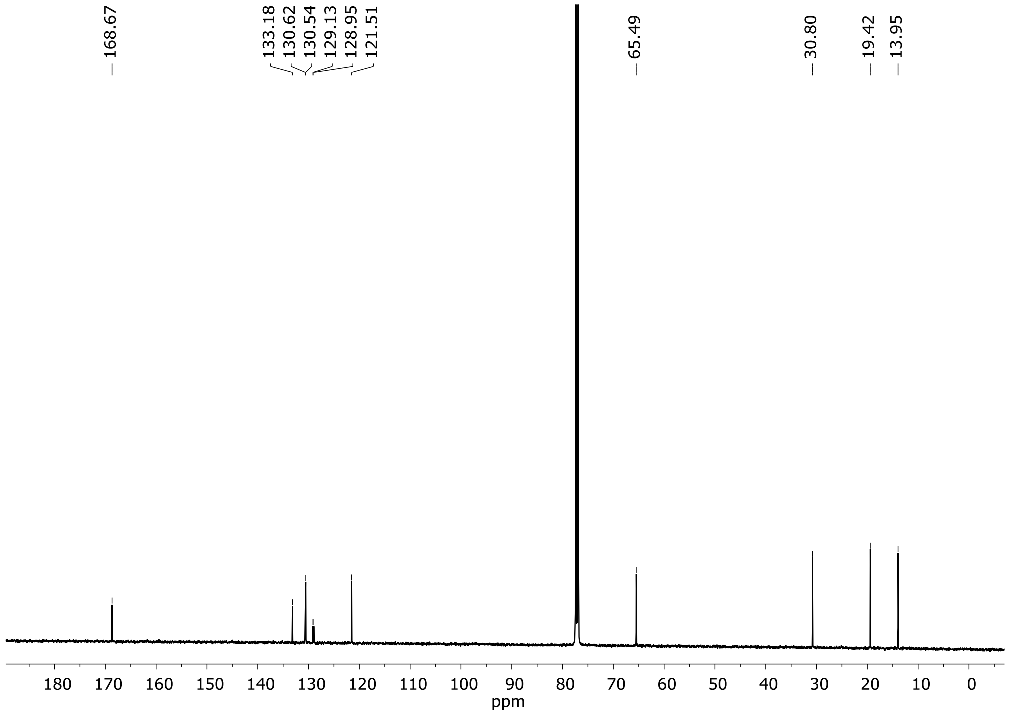

Fig. S2: $^{13}C\{^1H\}$ NMR (125 MHz, $CDCl_3$) spectrum of **PTBE**.

1,7-Dibromoperylene-3,4,9,10-tetra-*n*-butylester (1,7-DB-PTBE)

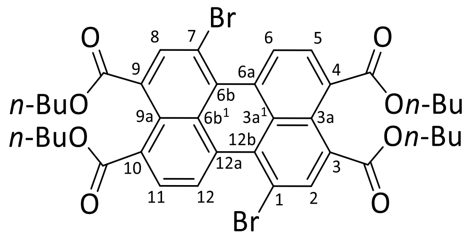

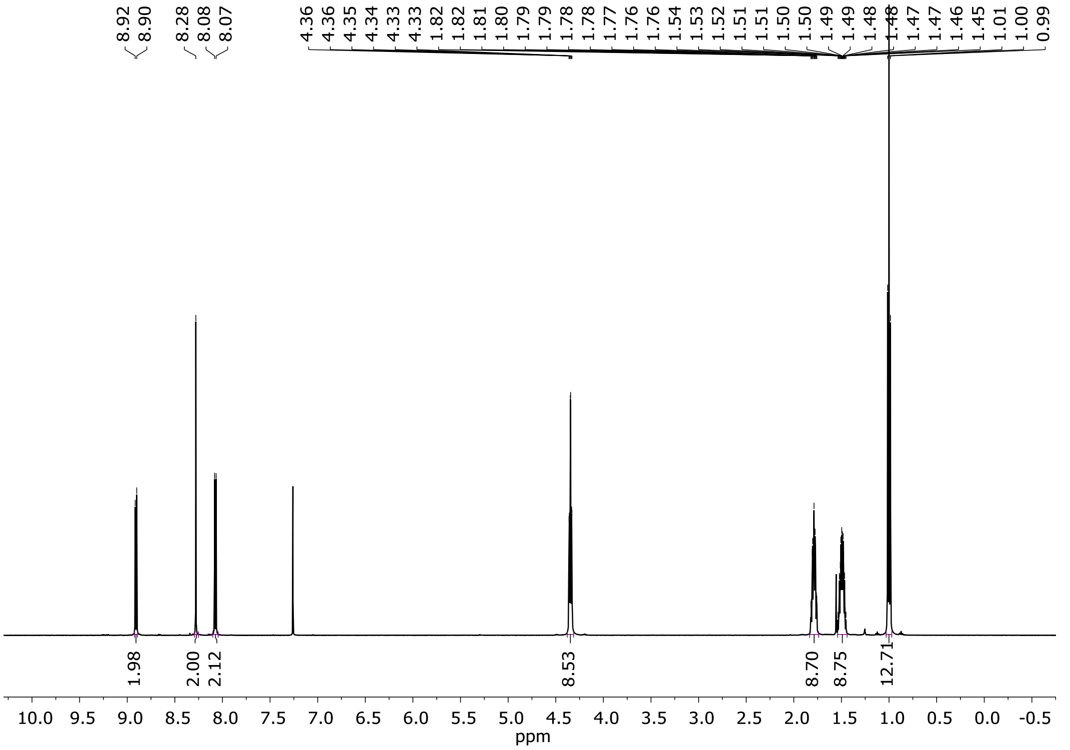

Fig. S3: ^{1}H NMR (500 MHz, CDCl$_3$) spectrum of **1,7-DB-PTBE**.

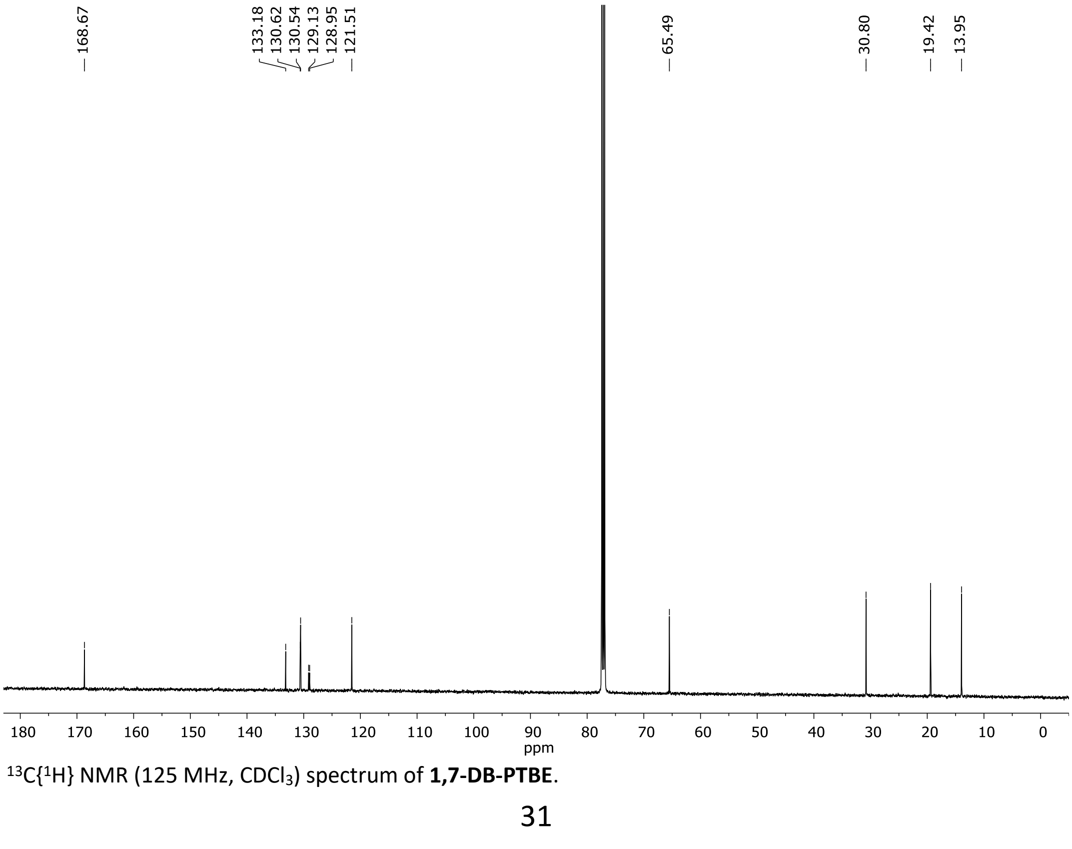

Fig. S4: ^{13}C{^{1}H} NMR (125 MHz, CDCl$_3$) spectrum of **1,7-DB-PTBE**.

1,7-Dibromoperylene-3,4,9,10-tetracaboxylic dianhydride (1,7-DB-PTCDA)

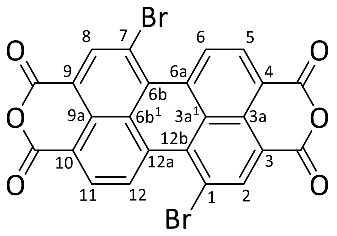

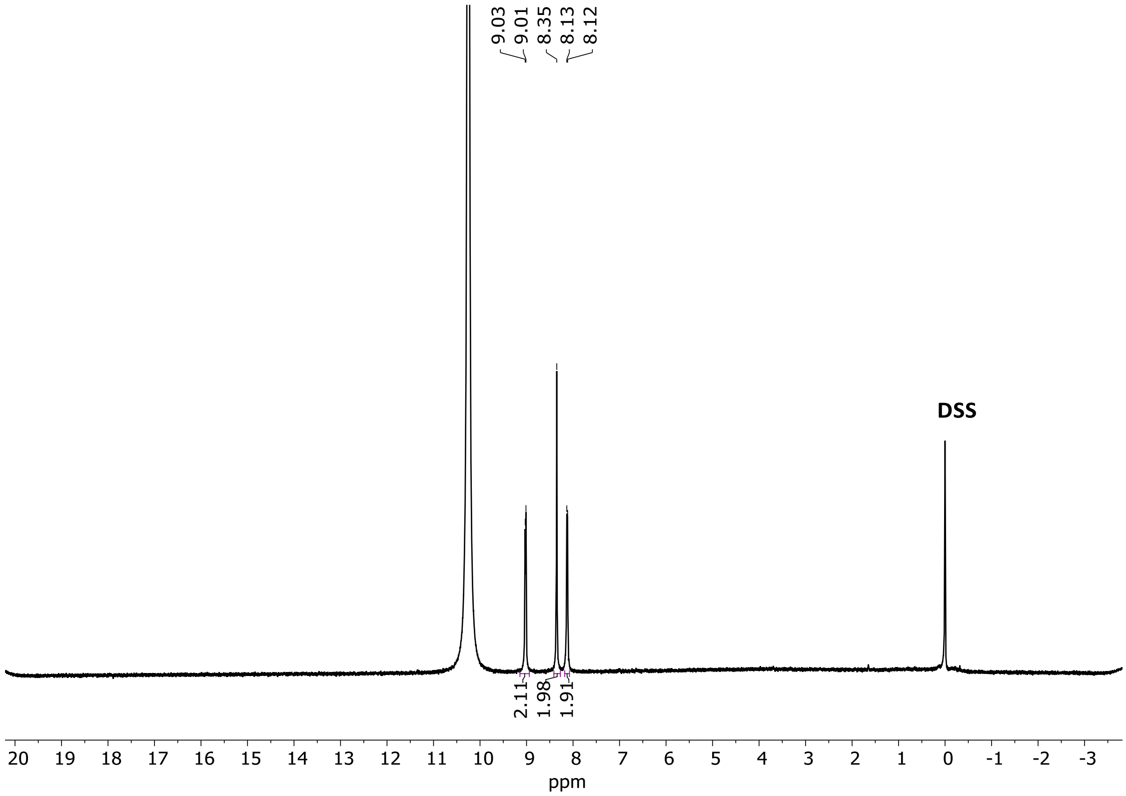

Fig. S5: ^{1}H NMR (500 MHz, D_2SO_4+DSS) spectrum of **1,7-DB-PTCDA**.

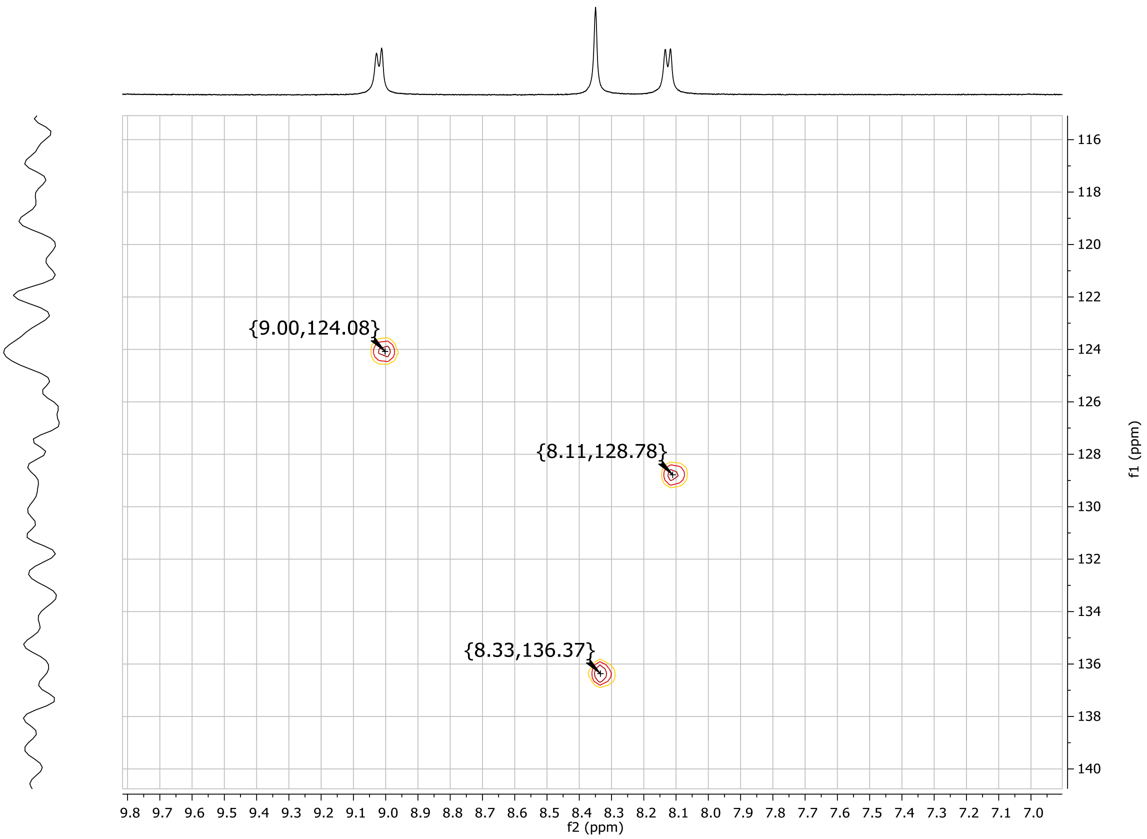

Fig. S6: ^{1}H-^{13}C{^{1}H} HSQC spectrum of **1,7-DB-PTCDA**.

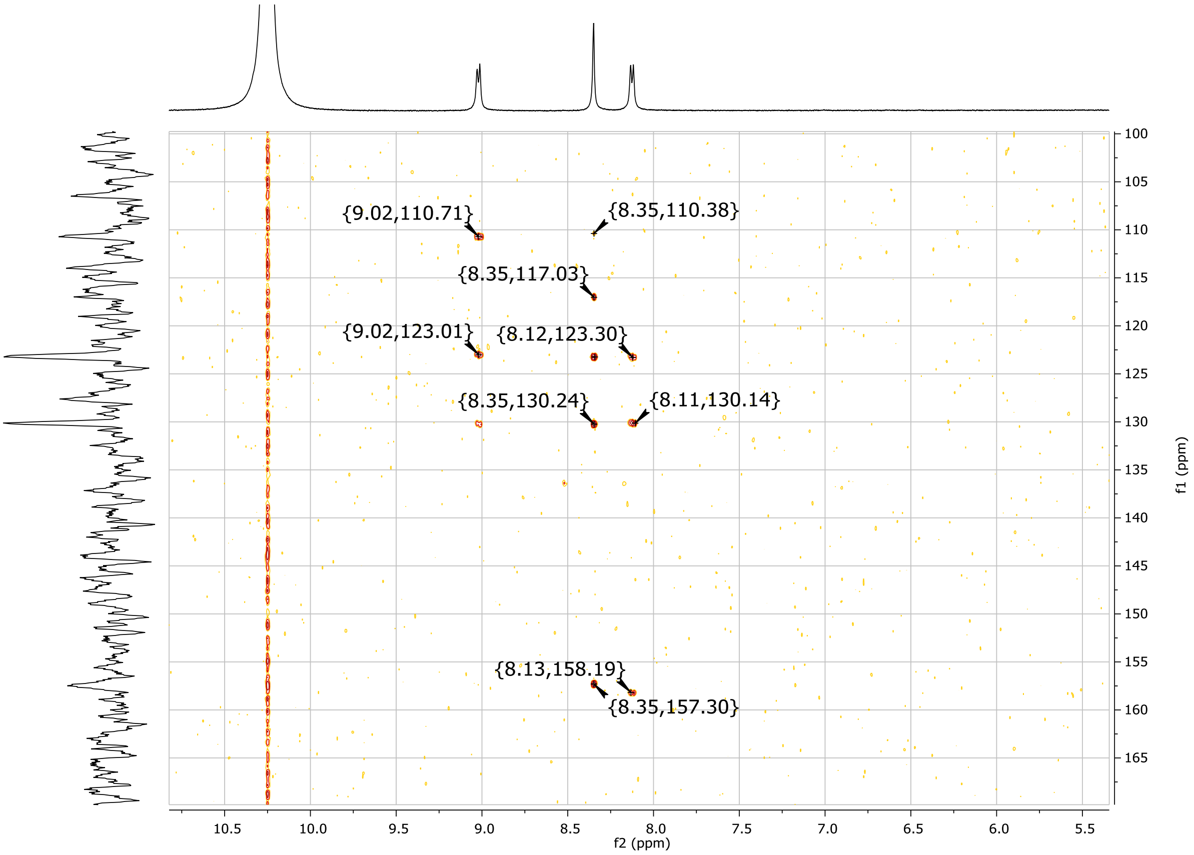

Fig. S7: ^{1}H-^{13}C{^{1}H} HMBC spectrum of **1,7-DB-PTCDA**.

1,7-Dibromo-*N*,*N'*-dicyclohexylperylene-3,4,9,10-tetracaboxylic acid diimide (1,7-DB-PDI^{Cy})

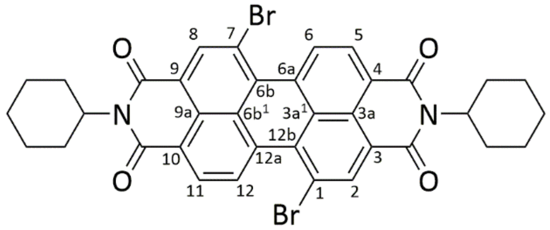

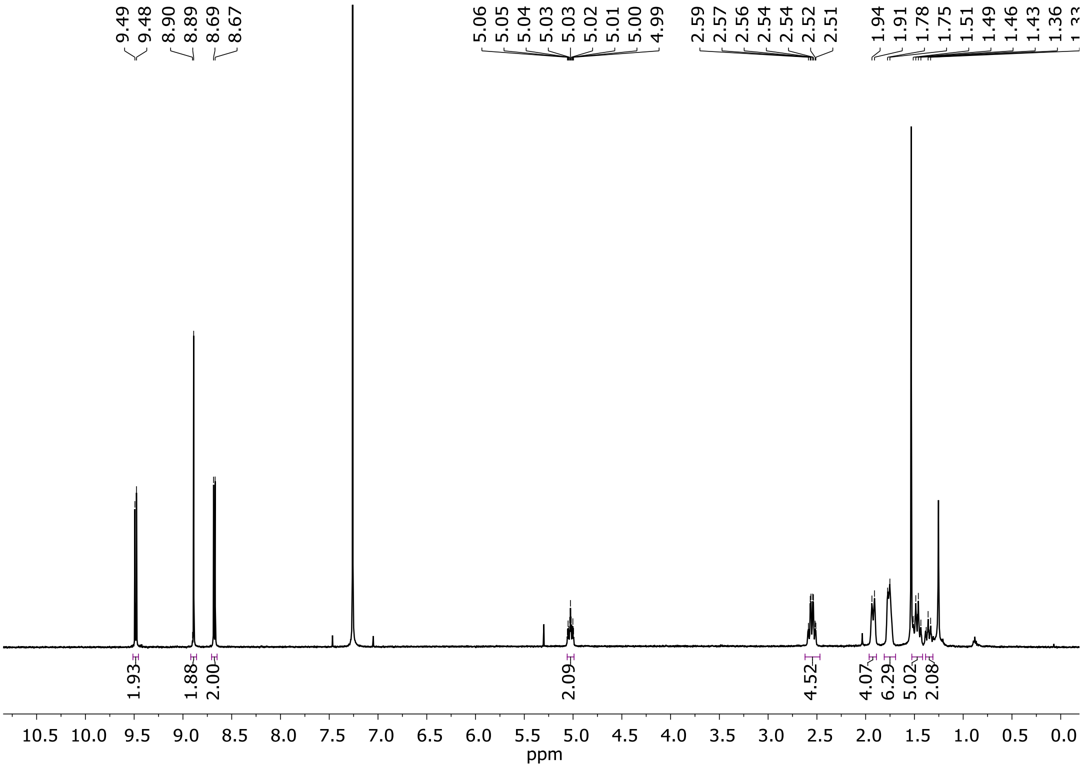

Fig. S8: ^{1}H NMR (500 MHz, CDCl$_3$) spectrum of **1,7-DB-PDI^{Cy}**.

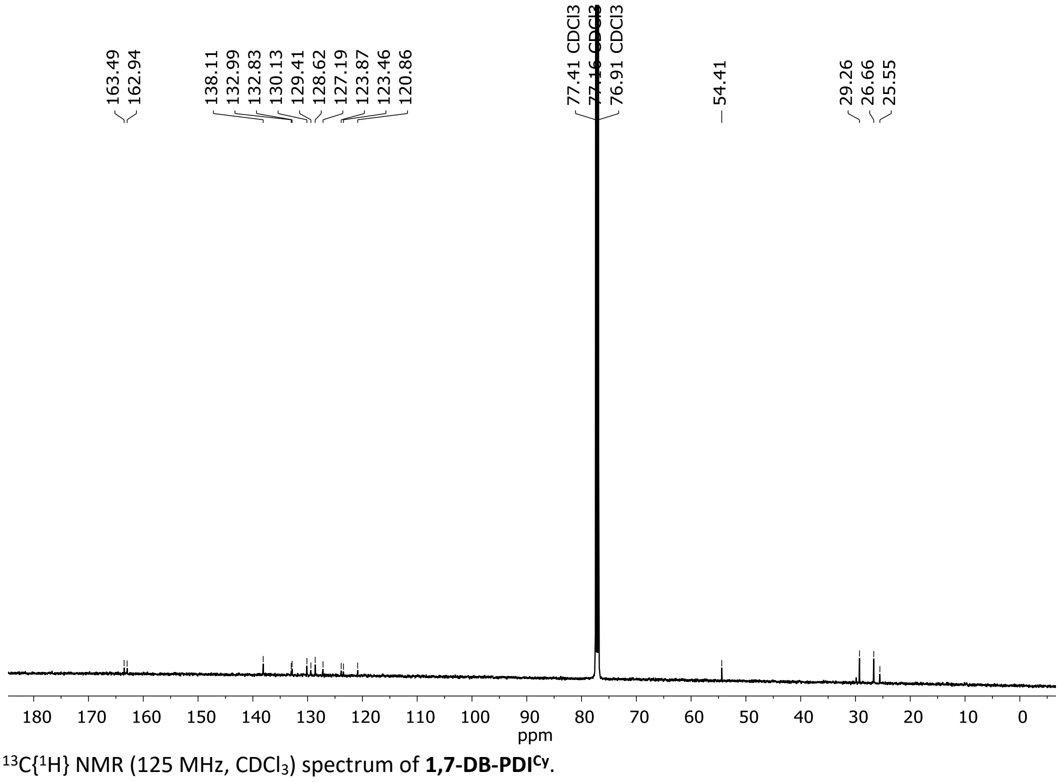

Fig. S9: ^{13}C{^{1}H} NMR (125 MHz, CDCl$_3$) spectrum of **1,7-DB-PDI^{Cy}**.

1,7-Dibromo-*N*,*N'*-(Di*iso*propylphenyl)-perylene-3,4,9,10-tetracaboxylic acid diimide (1,7-DB-PDI^{Dip})

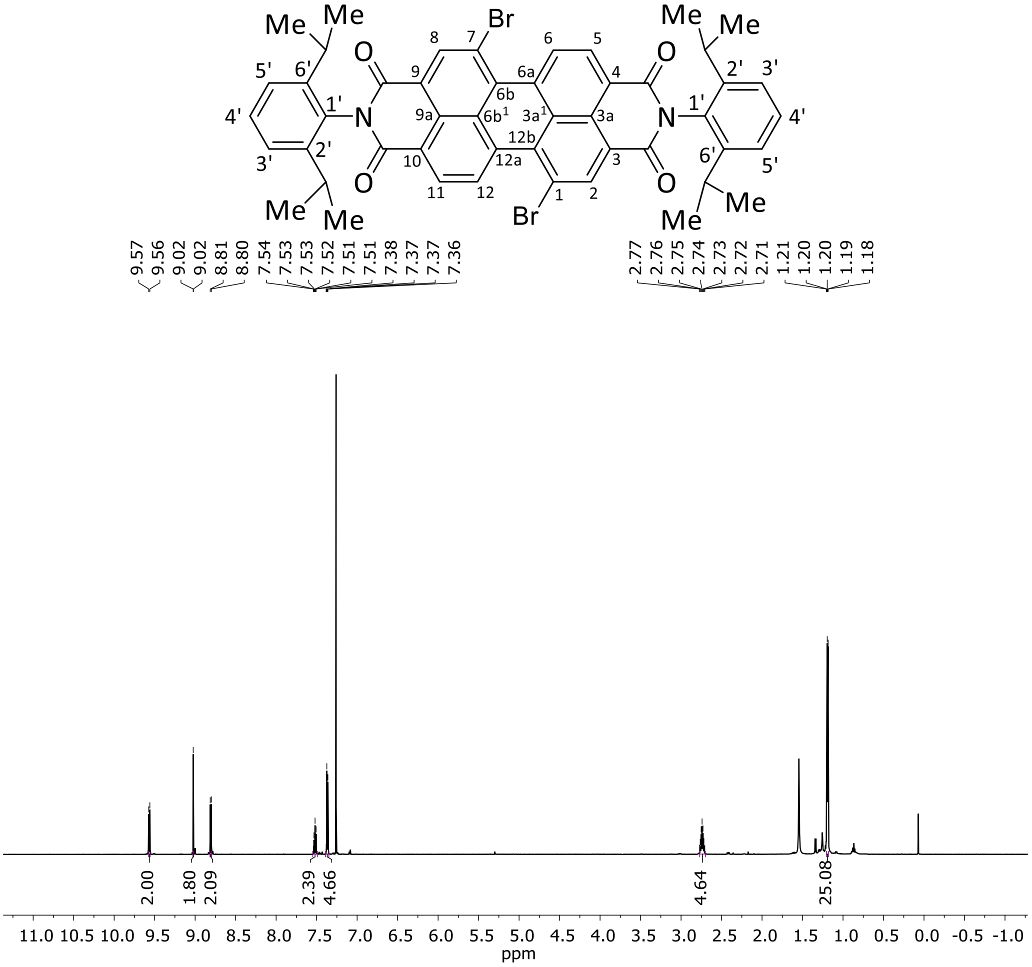

Fig. S10: ^{1}H NMR (601 MHz, CDCl$_3$) spectrum of **1,7-DB-PDI^{Dip}**.

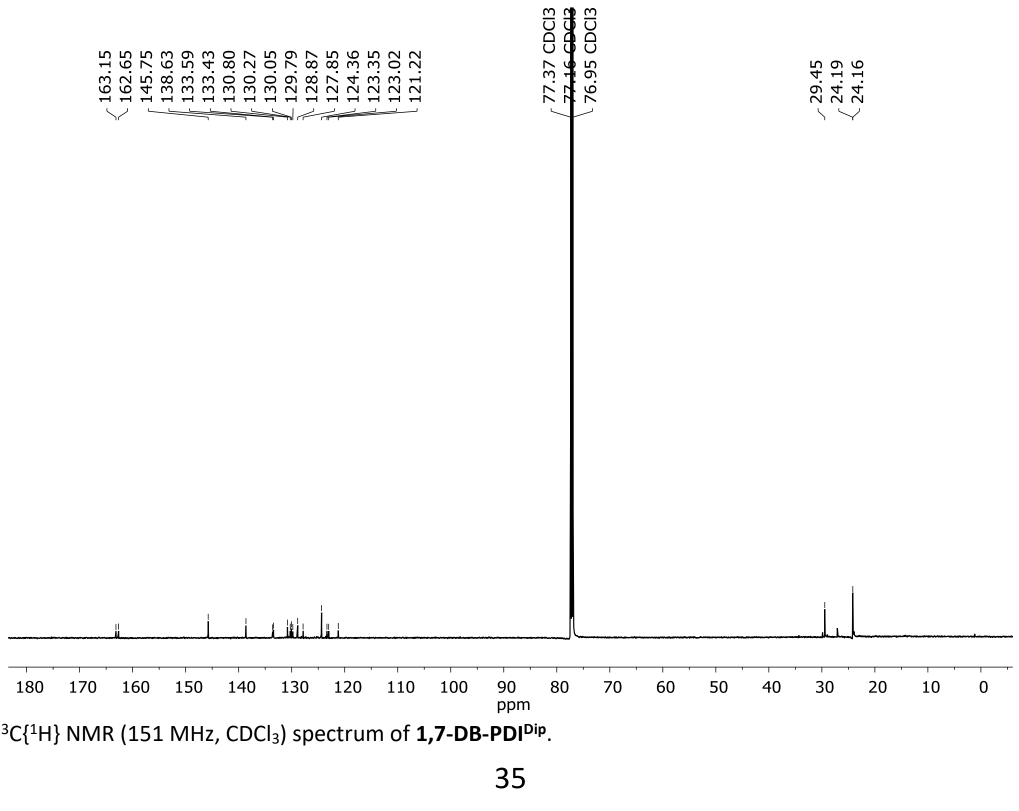

Fig. S11: ^{13}C{^{1}H} NMR (151 MHz, CDCl$_3$) spectrum of **1,7-DB-PDI^{Dip}**.

1,7-Di(*n*-hexylamino)-*N*,*N'*-di(cyclohexyl)perylene-3,4,9,10-tetracaboxylic acid diimide (1,7-DHA-PDI^{Cy})

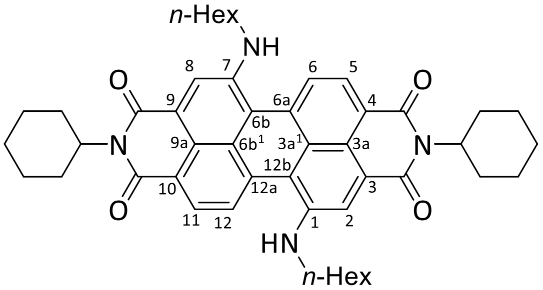

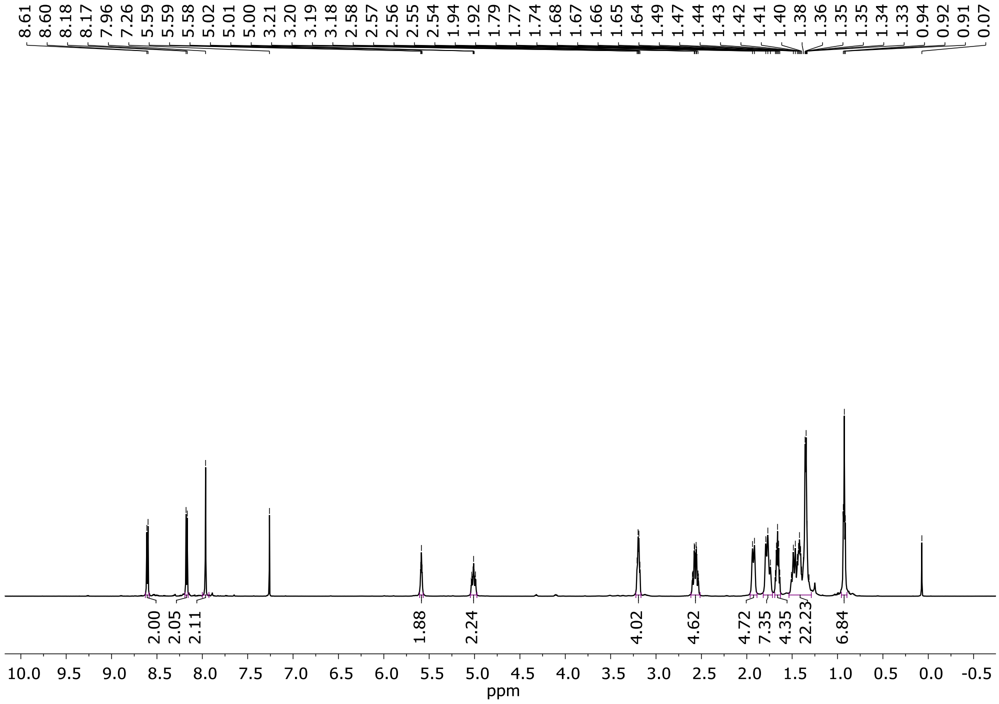

Fig. S12: ^{1}H NMR (600 MHz, $CDCl_3$) spectrum of **1,7-DHA-PDI^{Cy}**.

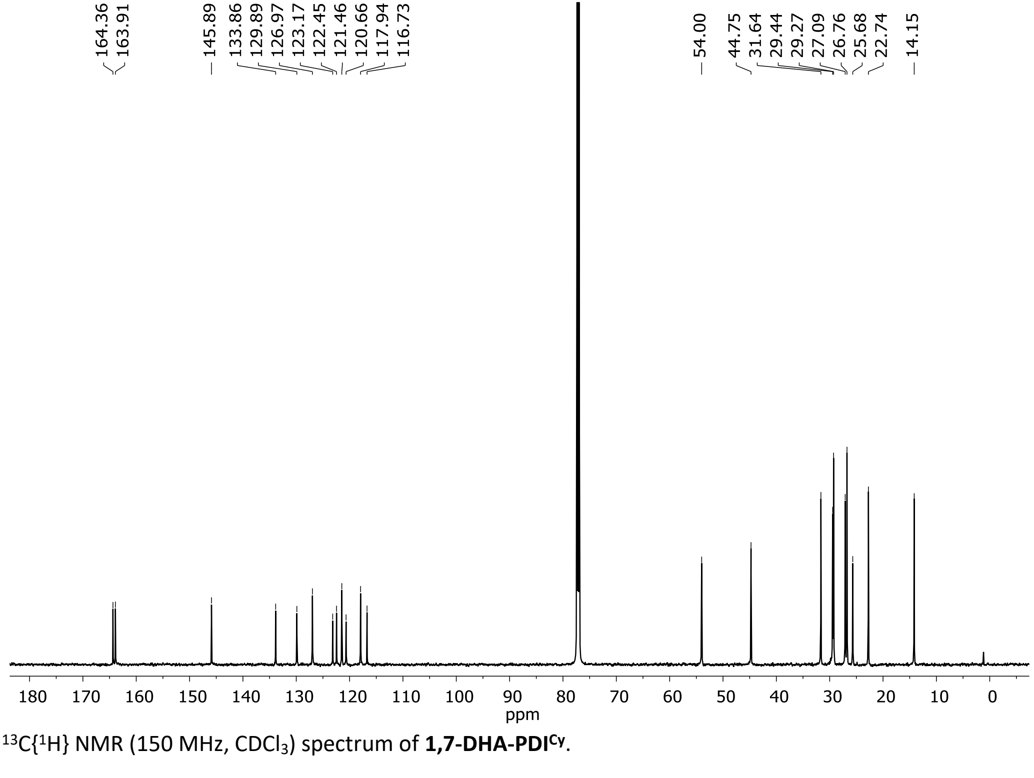

Fig. S13: $^{13}C\{^1H\}$ NMR (150 MHz, $CDCl_3$) spectrum of **1,7-DHA-PDI^{Cy}**.

1,7-Di(*n*-hexylamino)-*N*,*N'*-bis(2,6-di*iso*propylphenyl)perylene-3,4,9,10-tetracaboxylic acid diimide (1,7-DHA-PDI$^{\mathrm{Dip}}$)

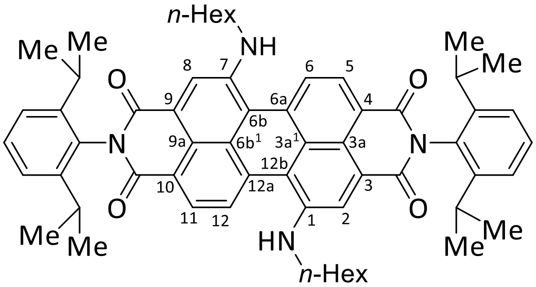

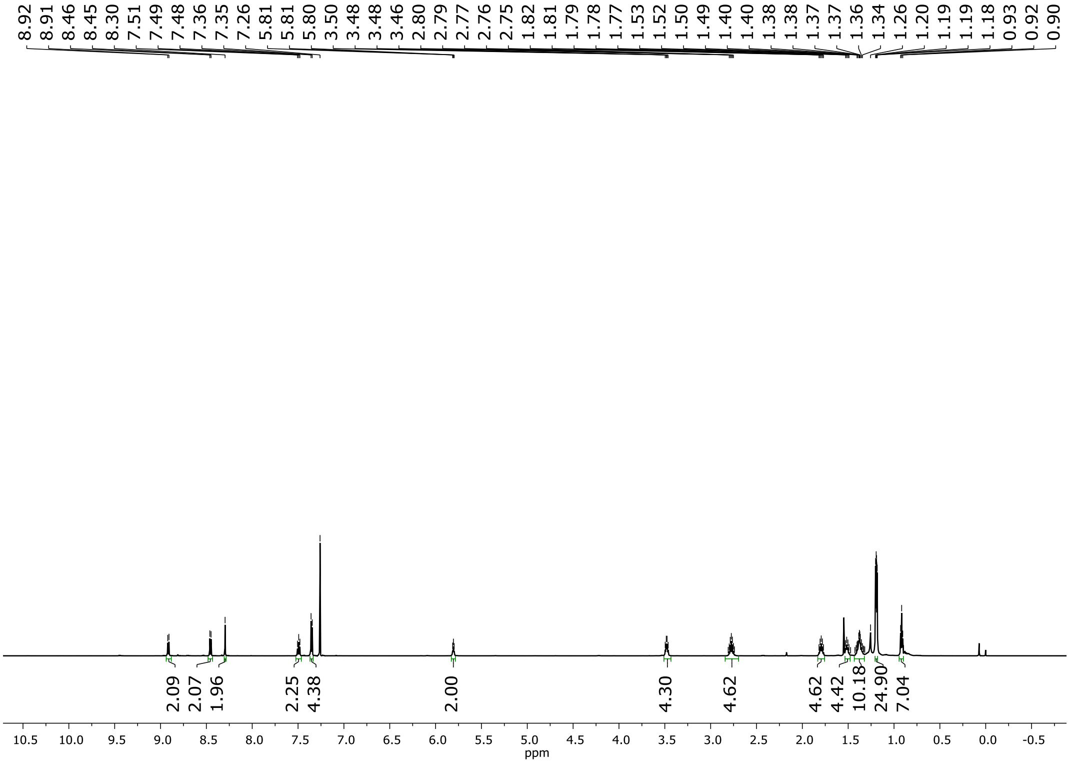

Fig. S14: ^{1}H NMR (600 MHz, CDCl$_3$) spectrum of **1,7-DHA-PDI$^{\mathrm{Dip}}$**.

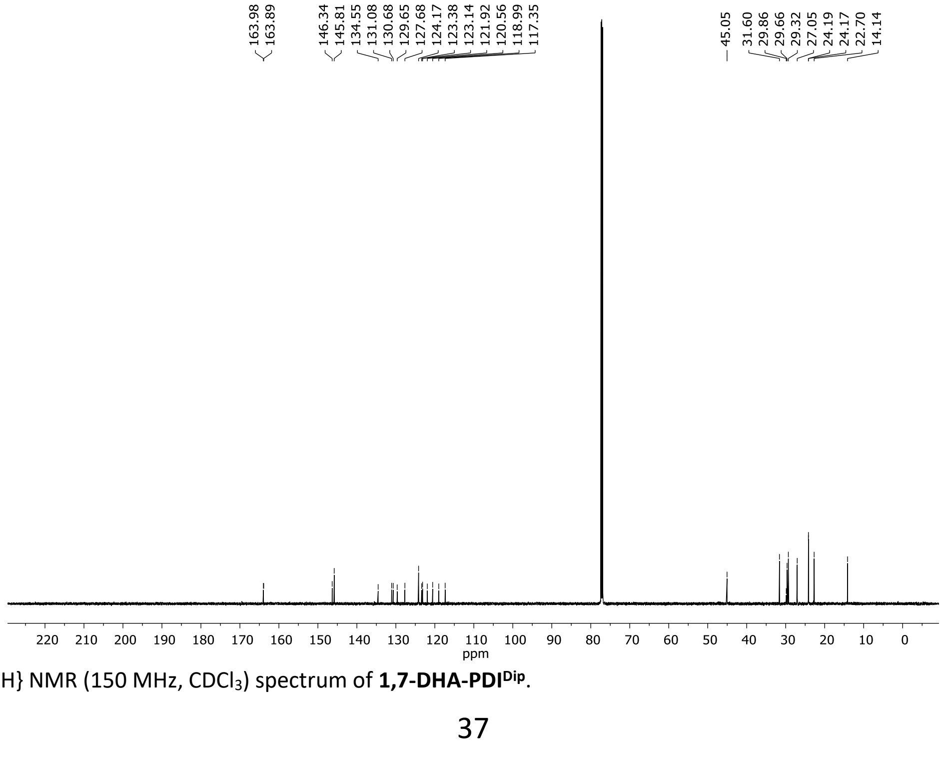

Fig. S15: ^{13}C{^{1}H} NMR (150 MHz, CDCl$_3$) spectrum of **1,7-DHA-PDI$^{\mathrm{Dip}}$**.

1,7-Di(*n*-hexylamino)-*N*,*N'*-di(*n*hexyl)perylene-3,4,9,10-tetracaboxylic acid diimide (1,7-DHA-PDI$^{\text{Hex}}$)

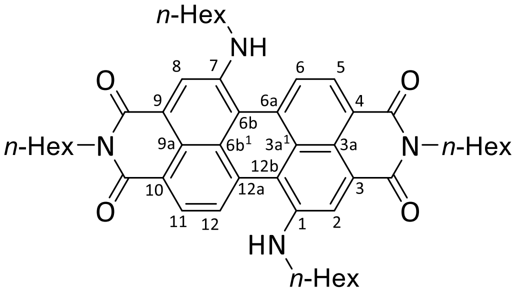

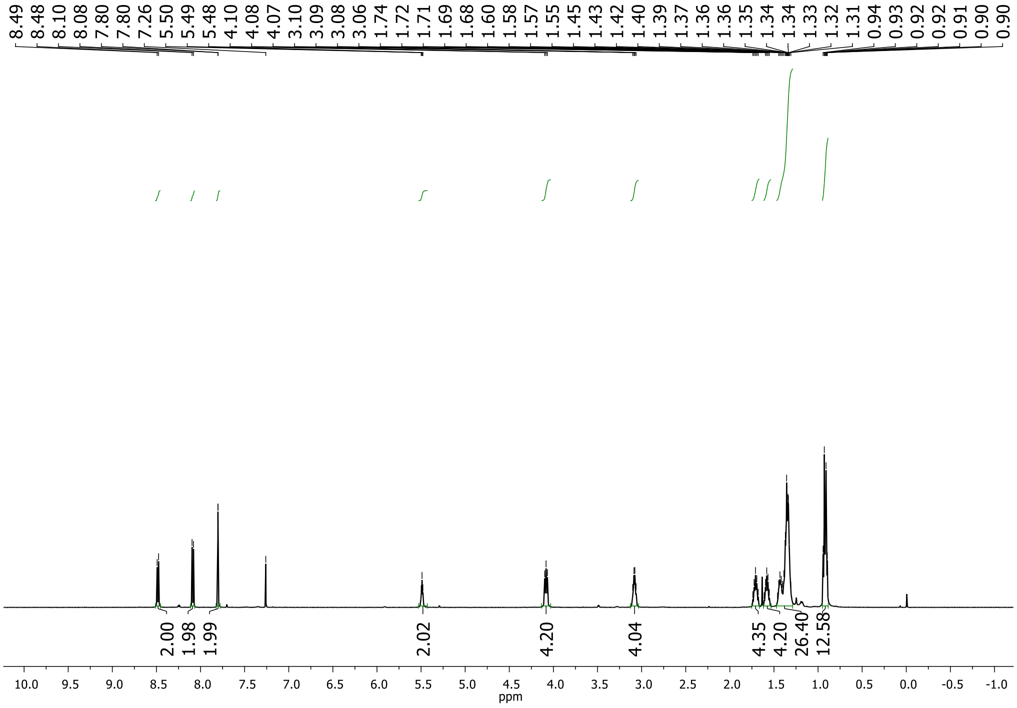

Fig. S16: ^{1}H NMR (500 MHz, CDCl$_3$) spectrum of compound **1,7-DHA-PDI$^{\text{Hex}}$**.

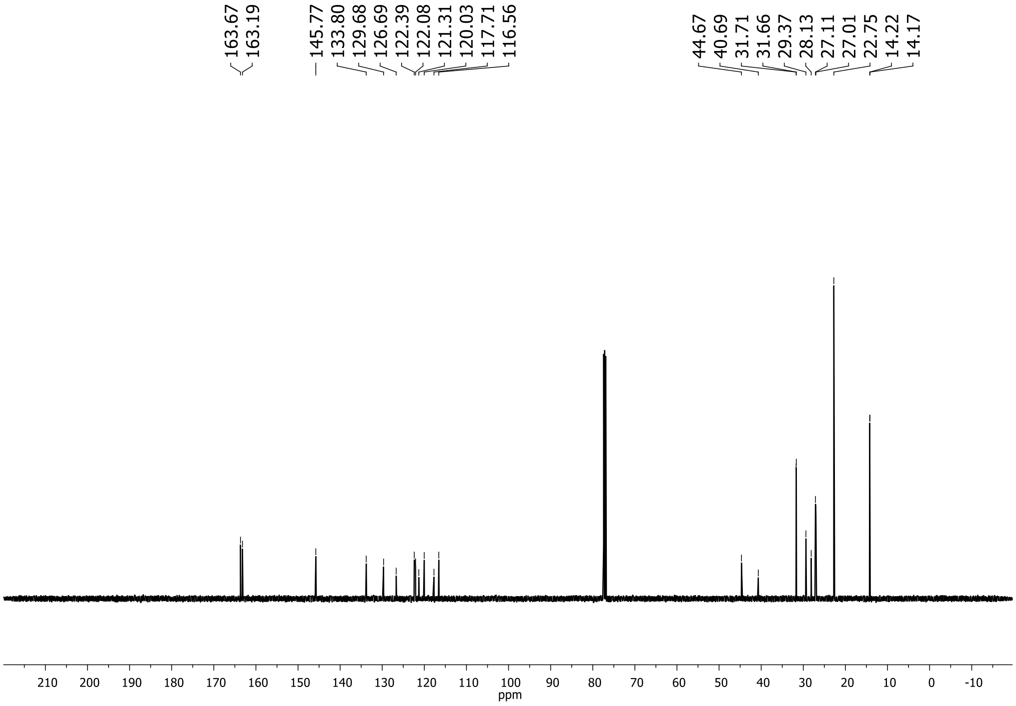

Fig. S17: ^{13}C{^{1}H} NMR (125 MHz, CDCl$_3$) spectrum of compound **1,7-DHA.PDI$^{\text{Hex}}$**.

2-(Trimethylsilyl)thiophene (TphTMS)

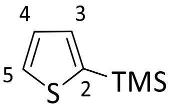

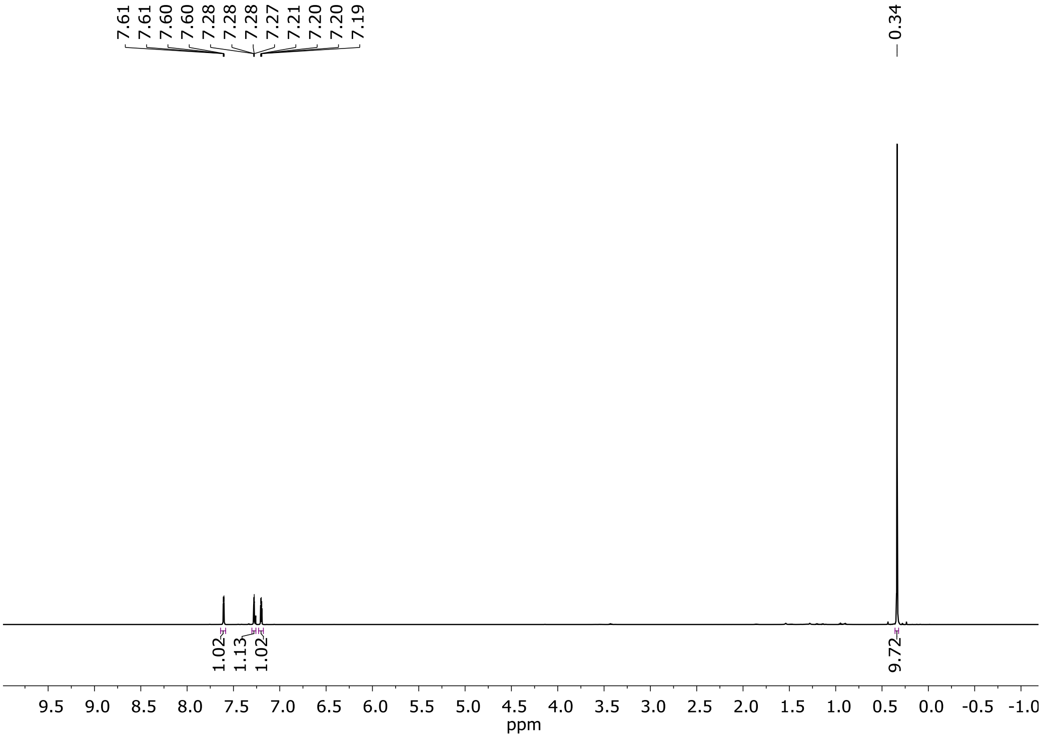

Fig. S18: ^{1}H NMR (600 MHz, CDCl$_3$) spectrum of **TphTMS**.

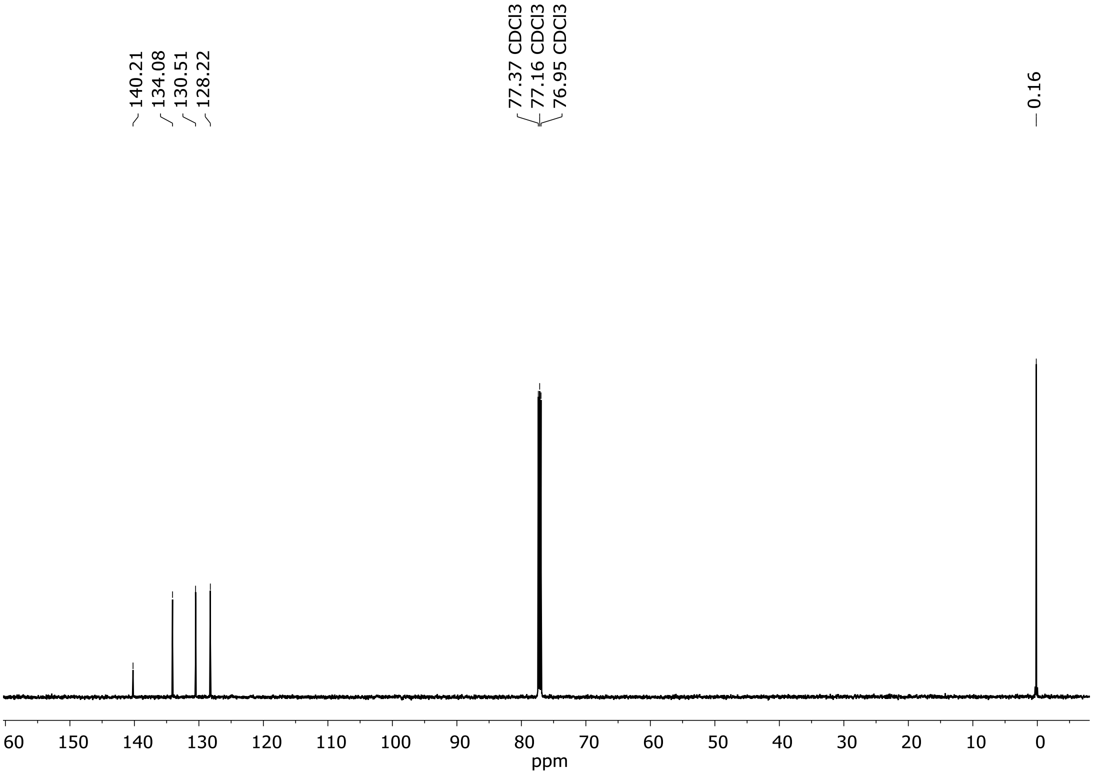

Fig. S19: ^{13}C{^{1}H} NMR (151 MHz, CDCl$_3$) spectrum of **TphTMS**.

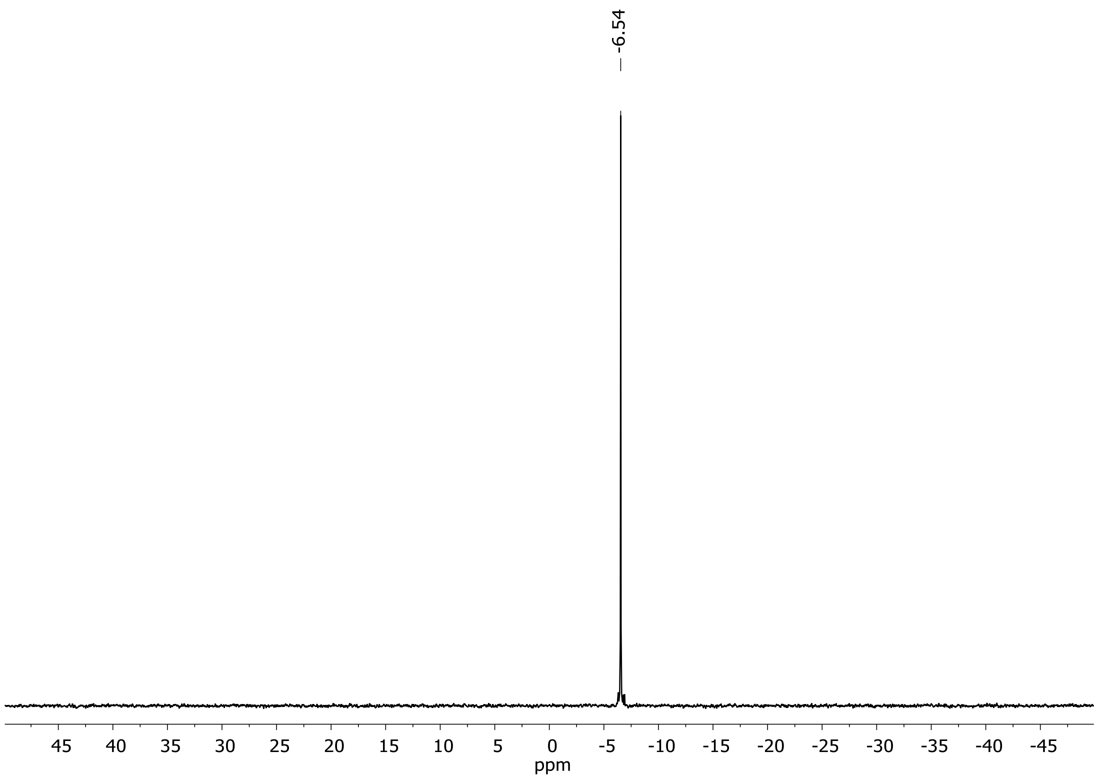

Fig. S20: $^{29}Si\{^1H\}$ NMR (119 MHz, $CDCl_3$) spectrum of **TphTMS**.

Dichloro-2-thienyl borane (TphBCl$_2$)

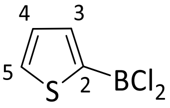

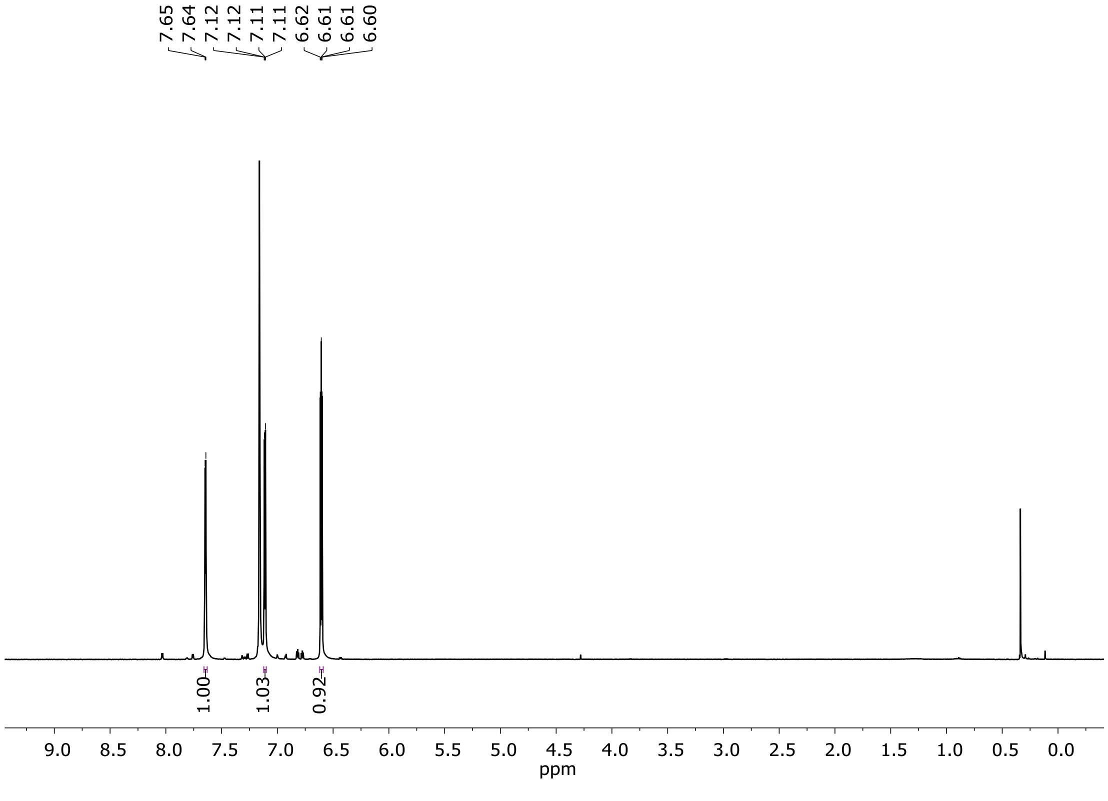

Fig. S21: ^1H NMR (500 MHz, C_6D_6) spectrum of **TphBCl$_2$**.

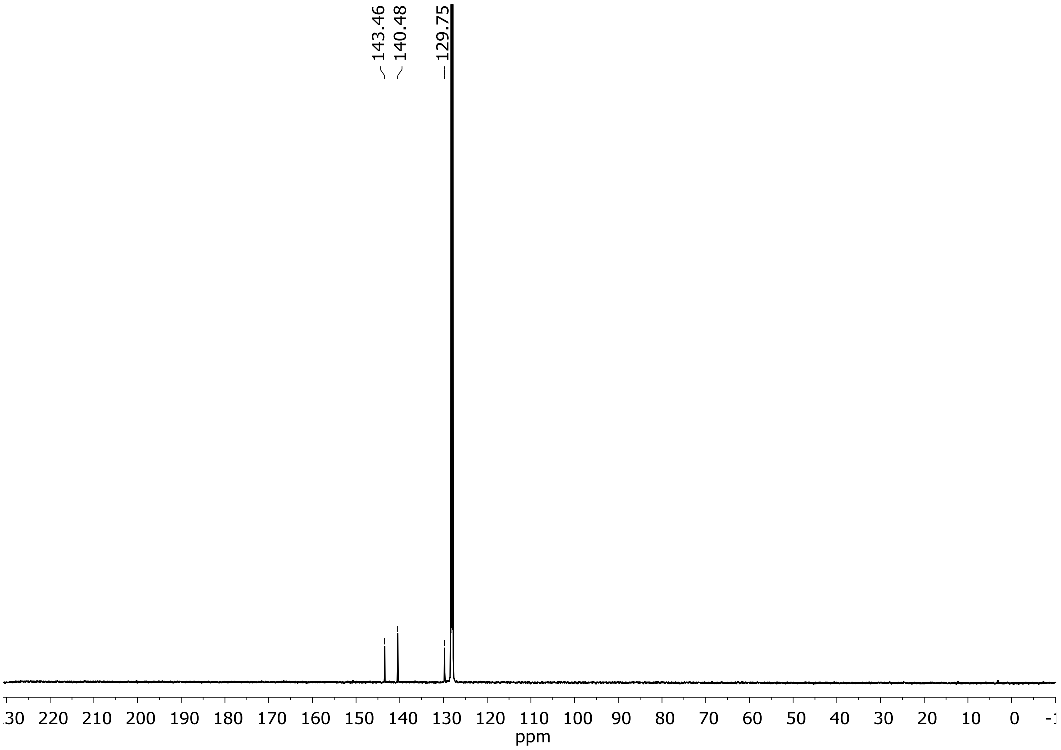

Fig. S22: $^{13}C\{^{1}H\}$ NMR (126 MHz, C_6D_6) spectrum of **TphBCl$_2$**.

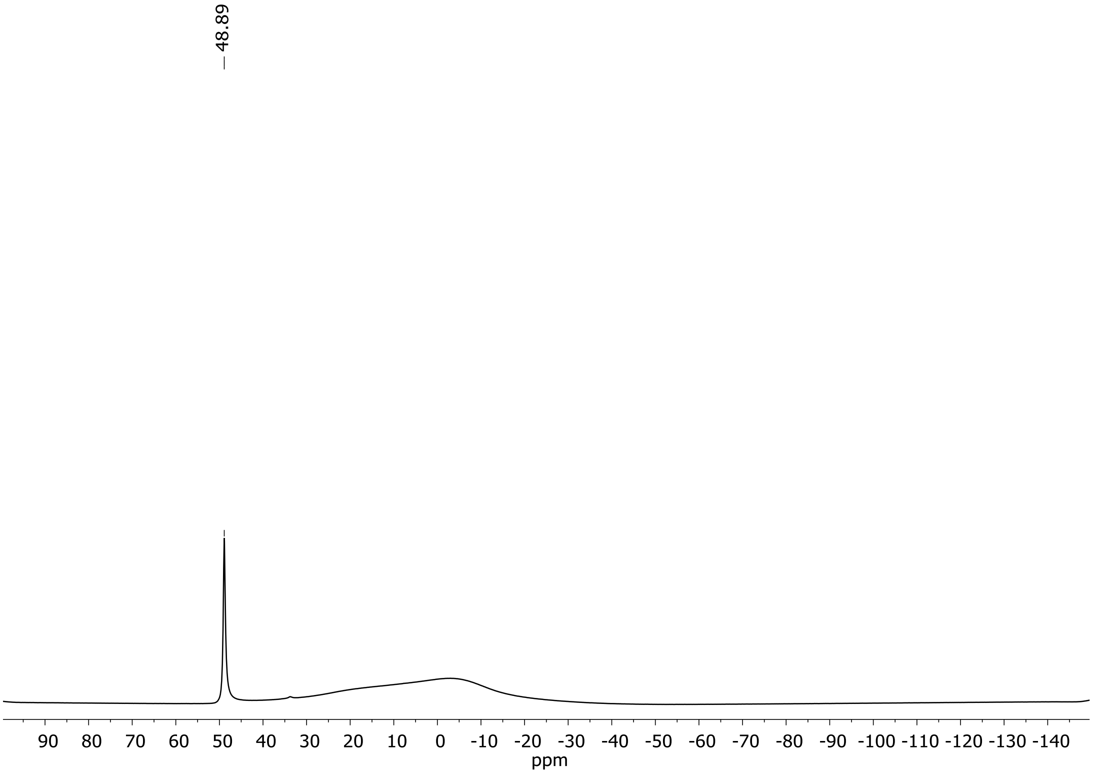

Fig. S23: $^{11}B\{^{1}H\}$ NMR (160 MHz, C_6D_6) spectrum of **TphBCl$_2$**.

4-(Trimethylsilyl)triphenylamine (TPATMS)

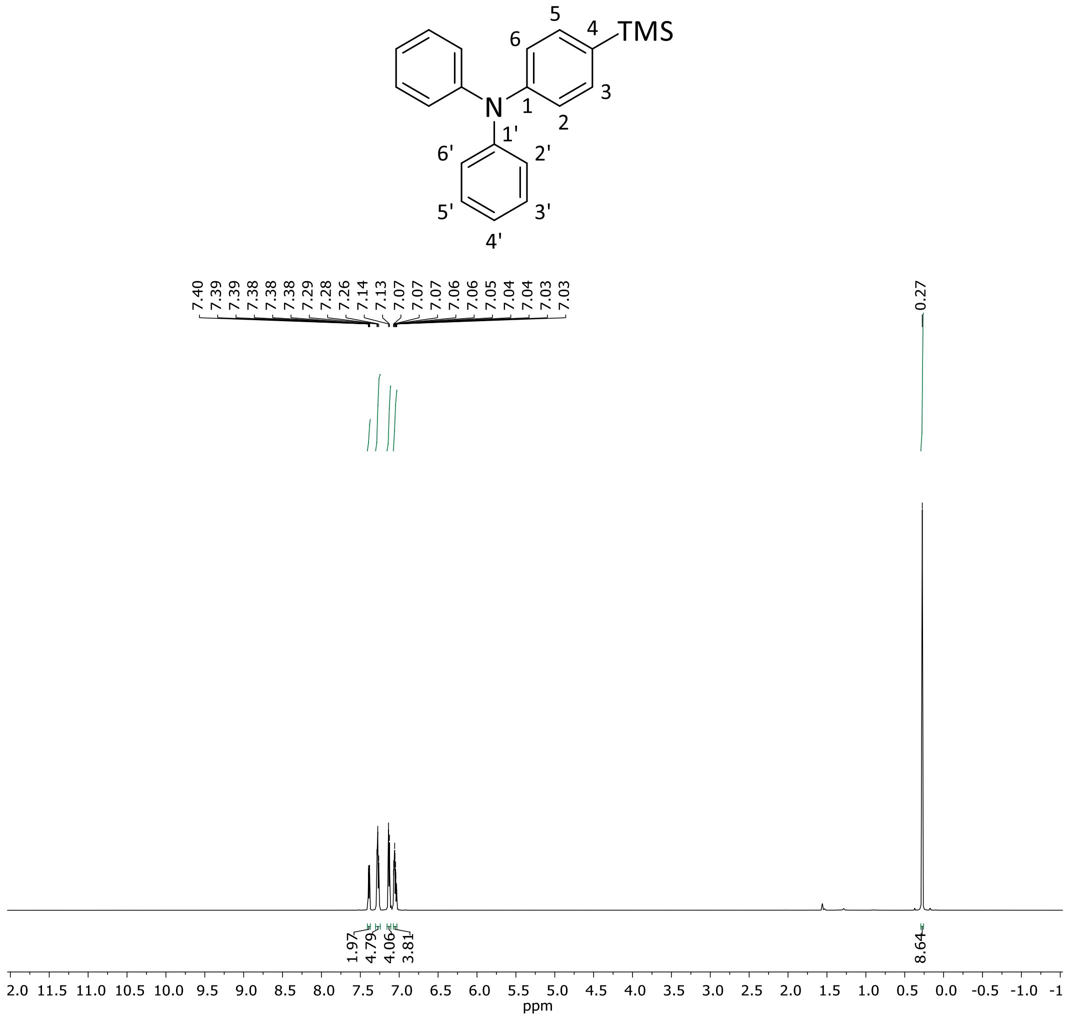

Fig. S24: ^{1}H NMR (600 MHz, $CDCl_3$) spectrum of compound **TPATMS**.

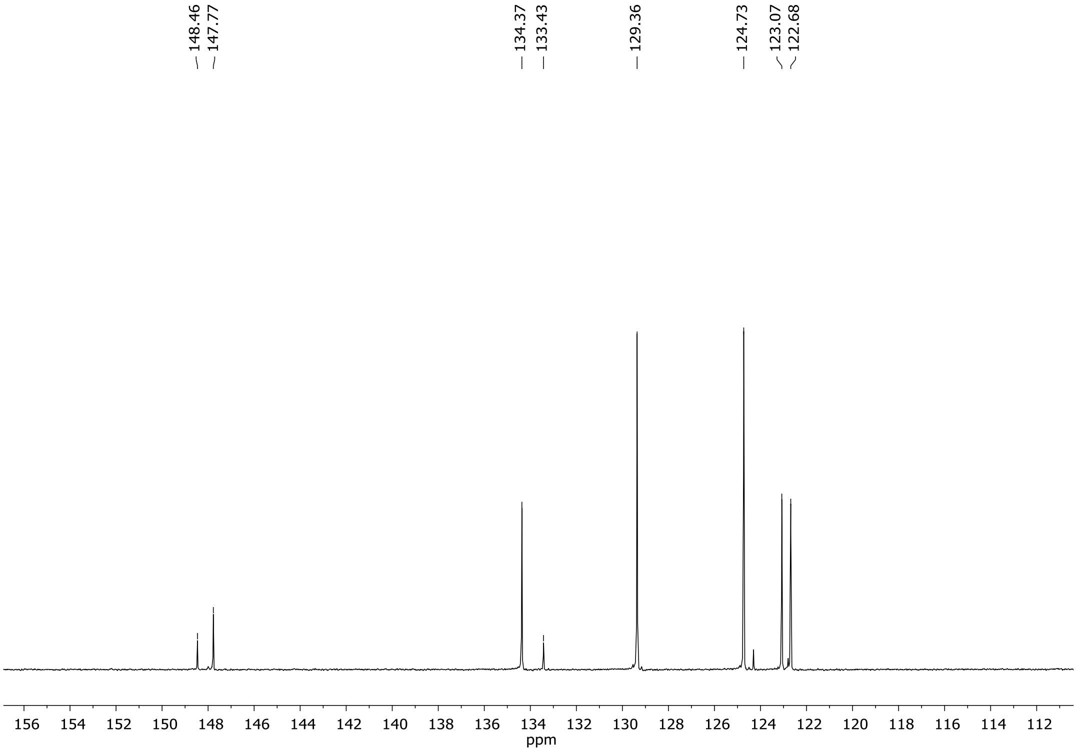

Fig. S25: $^{13}C\{^1H\}$ NMR (151 MHz, $CDCl_3$) spectrum of compound **TPATMS**.

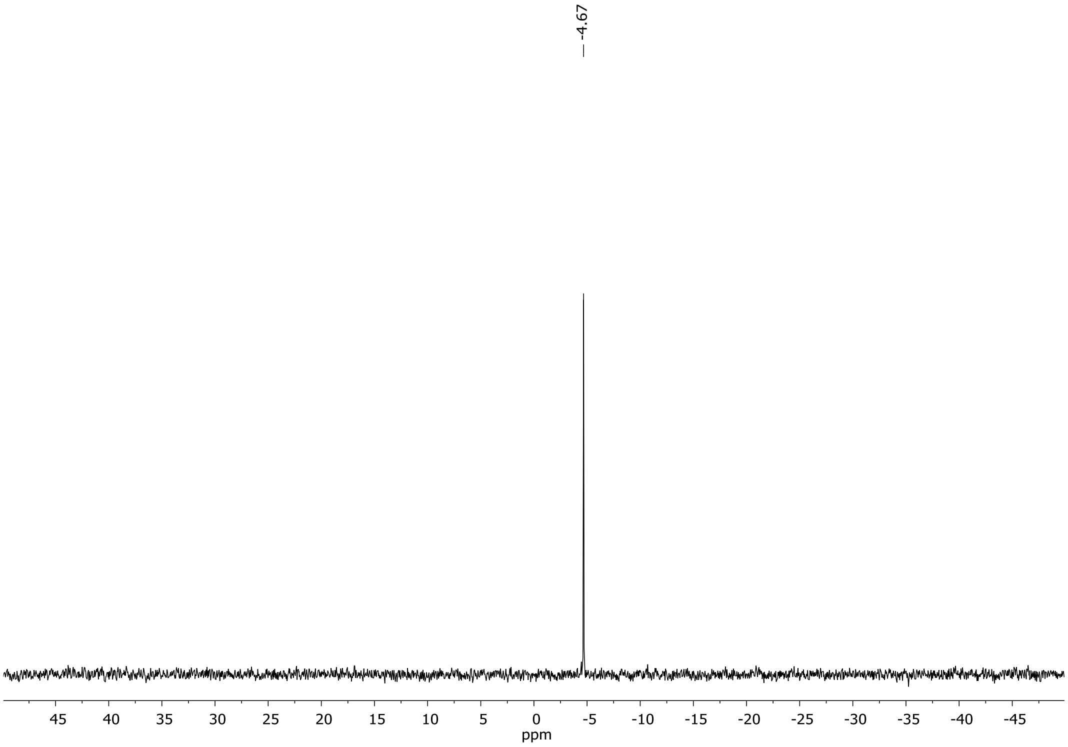

Fig. S26: $^{29}Si\{^1H\}$ NMR (119 MHz, $CDCl_3$) spectrum of compound **TPATMS**.

1,7-Di(*n*-hexyl)-6,12-di(phenyl)-1,12,6,7-di([1,2]azaborinine)-*N*,*N'*-di(cyclohexyl)perylene-3,4,9,10-tetracarboxylic acid diimide (Ph-BNCDI^{Cy})

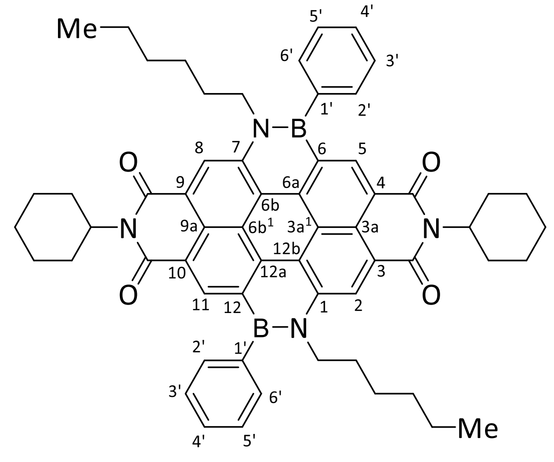

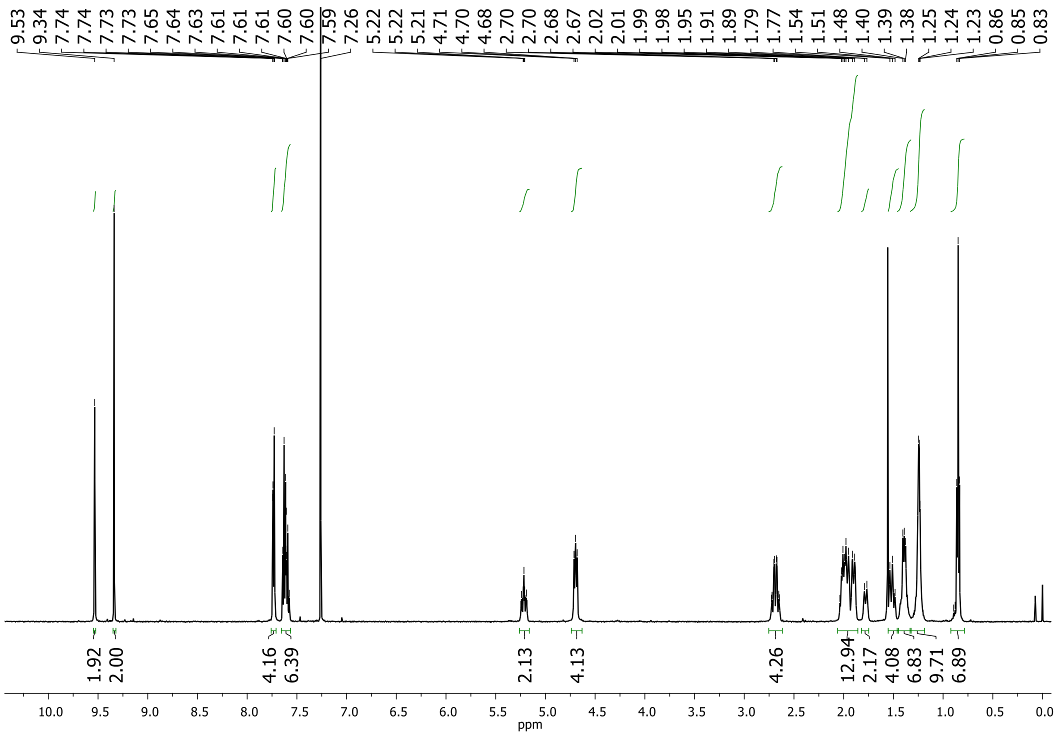

Fig. S27: ^{1}H NMR (500 MHz, CDCl$_3$) spectrum of compound **Ph-BNCDI^{Cy}**.

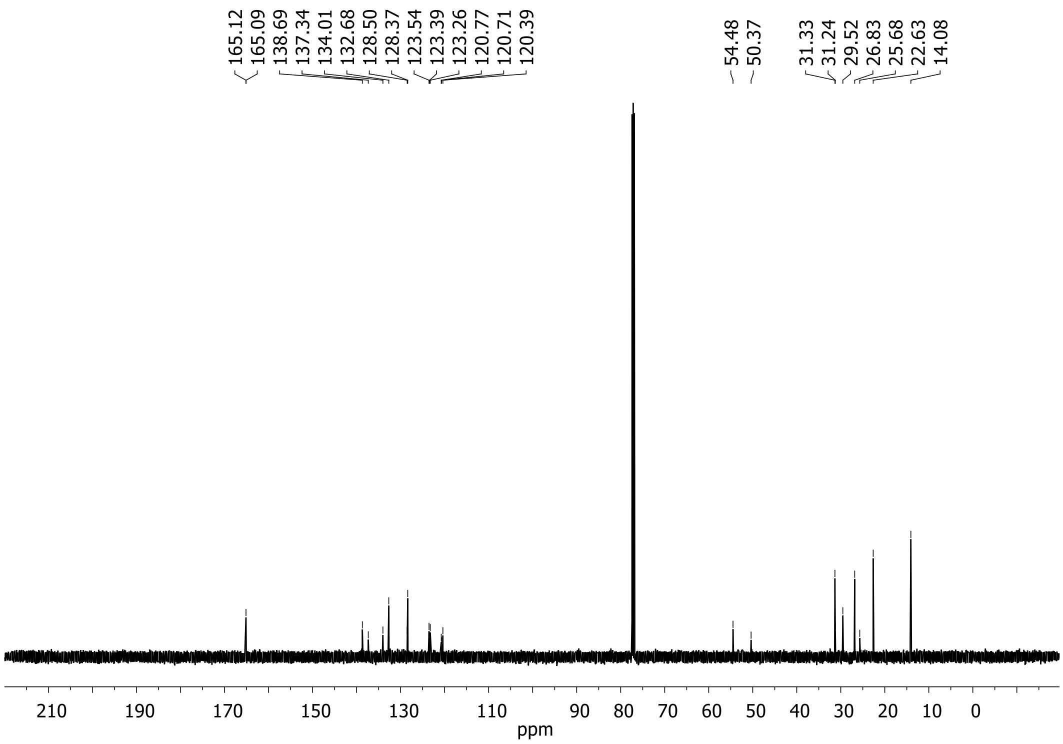

Fig. S28: $^{13}C\{^{1}H\}$ NMR (125 MHz, $CDCl_3$) spectrum of compound **Ph-BNCDI^{Cy}**.

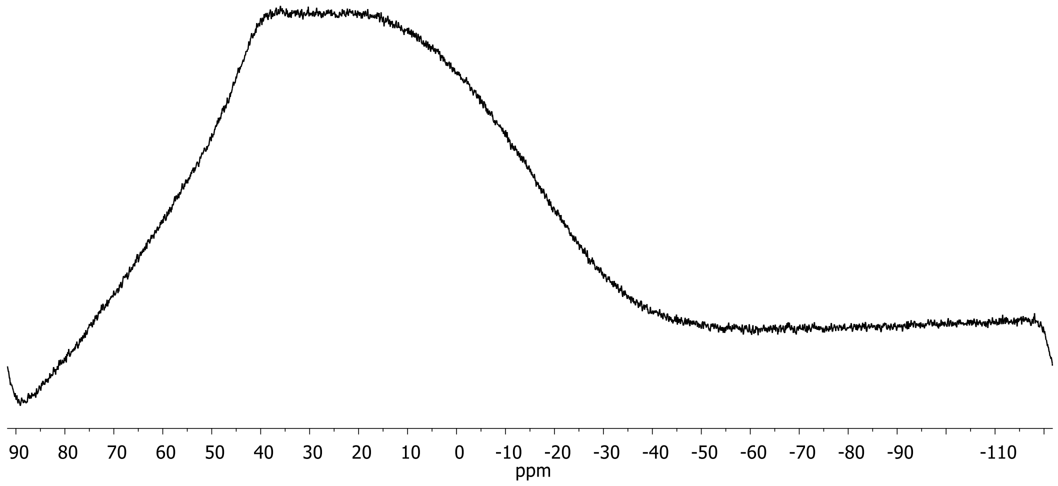

Fig. S29: $^{11}B\{^{1}H\}$ NMR (160 MHz, $CDCl_3$) spectrum of compound **Ph-BNCDI^{Cy}**.

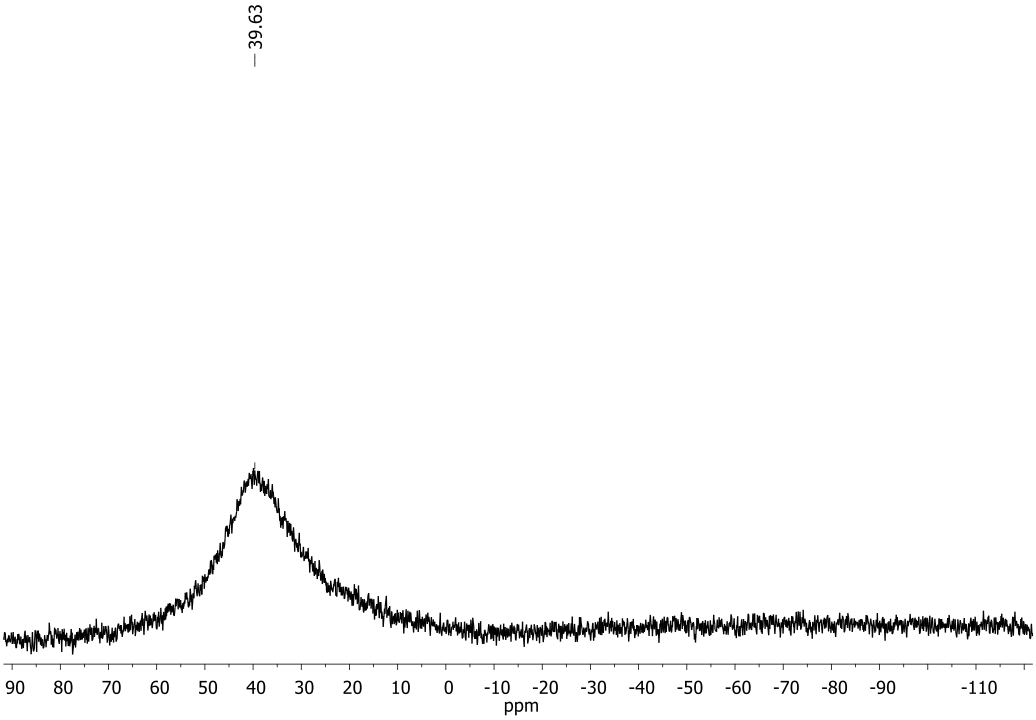

Fig. S30: $^{11}B\{^1H\}$ NMR (160 MHz, $CDCl_3$) differential spectrum of $CDCl_3$ and compound **Ph-BNCDI^{Cy}**.

1,7-Di(*n*-hexyl)-6,12-di(phenyl)-1,12,6,7-di([1,2]azaborinine)-*N*,*N'*-bis(2,6-di*iso*propylphenyl)perylene-3,4,9,10-tetracarboxylic acid diimide (Ph-BNCDI^{Dip})

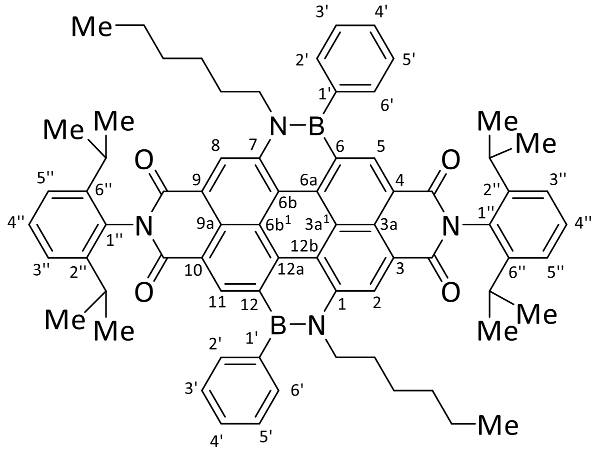

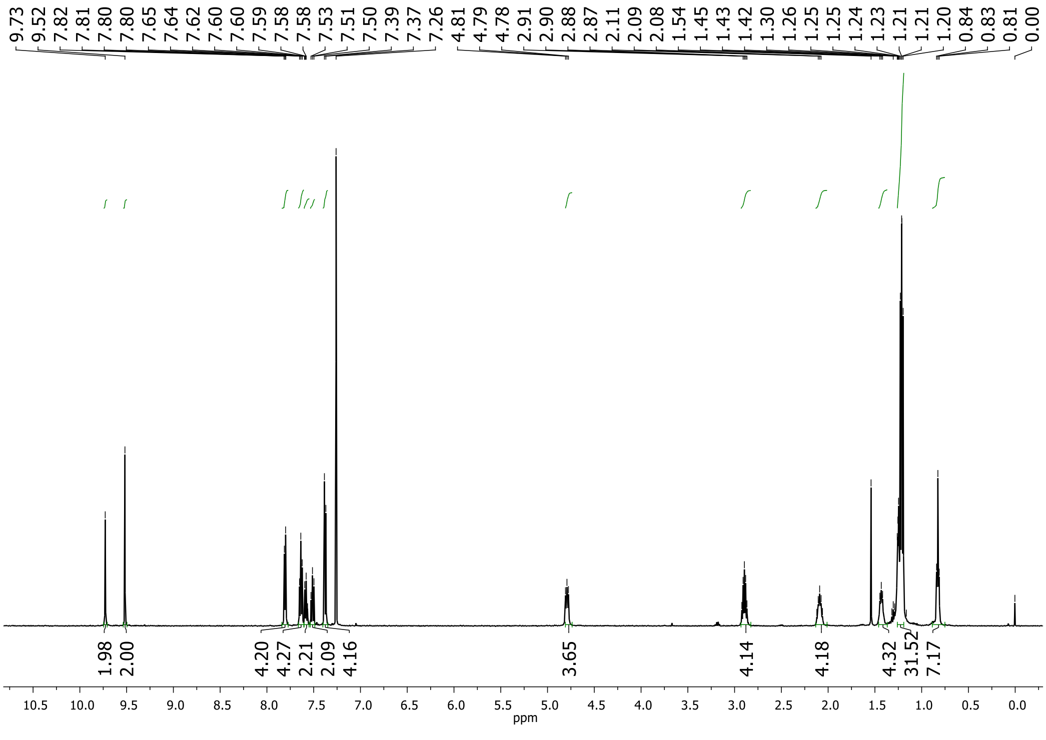

Fig. S31: ^{1}H NMR (500 MHz, CDCl$_3$) spectrum of compound **Ph-BNCDI^{Dip}**.

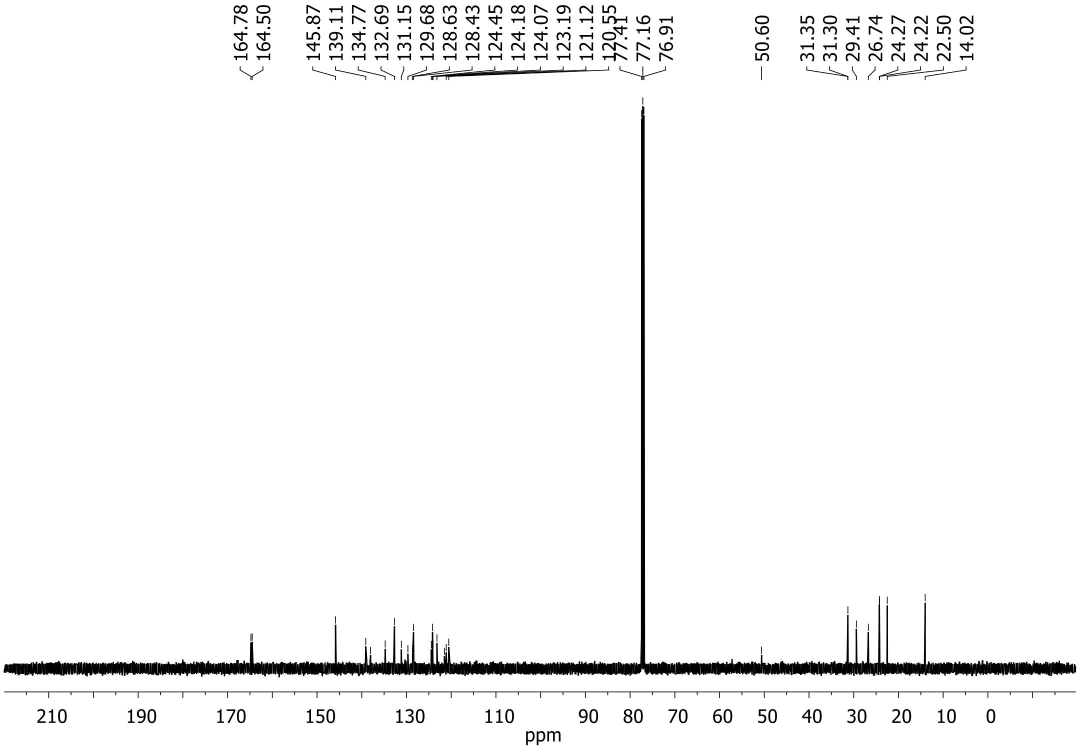

Fig. S32: $^{13}C\{^{1}H\}$ NMR (125 MHz, $CDCl_3$) spectrum of compound **Ph-BNCDI^{Dip}**.

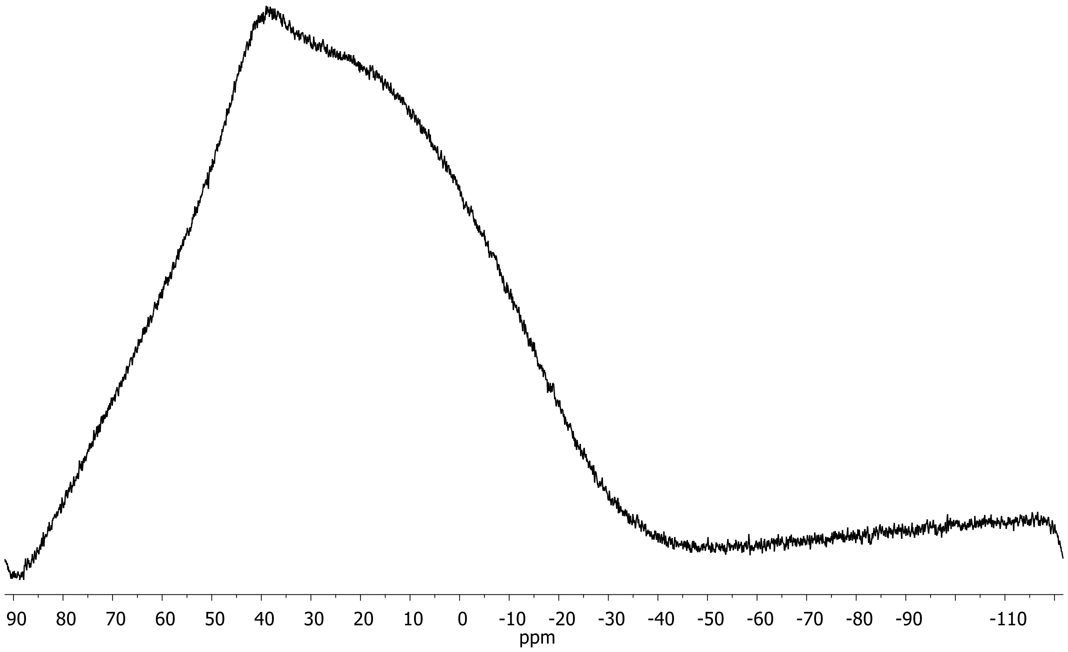

Fig. S33: $^{11}B\{^{1}H\}$ NMR (160 MHz, $CDCl_3$) spectrum of compound **Ph-BNCDI^{Dip}**.

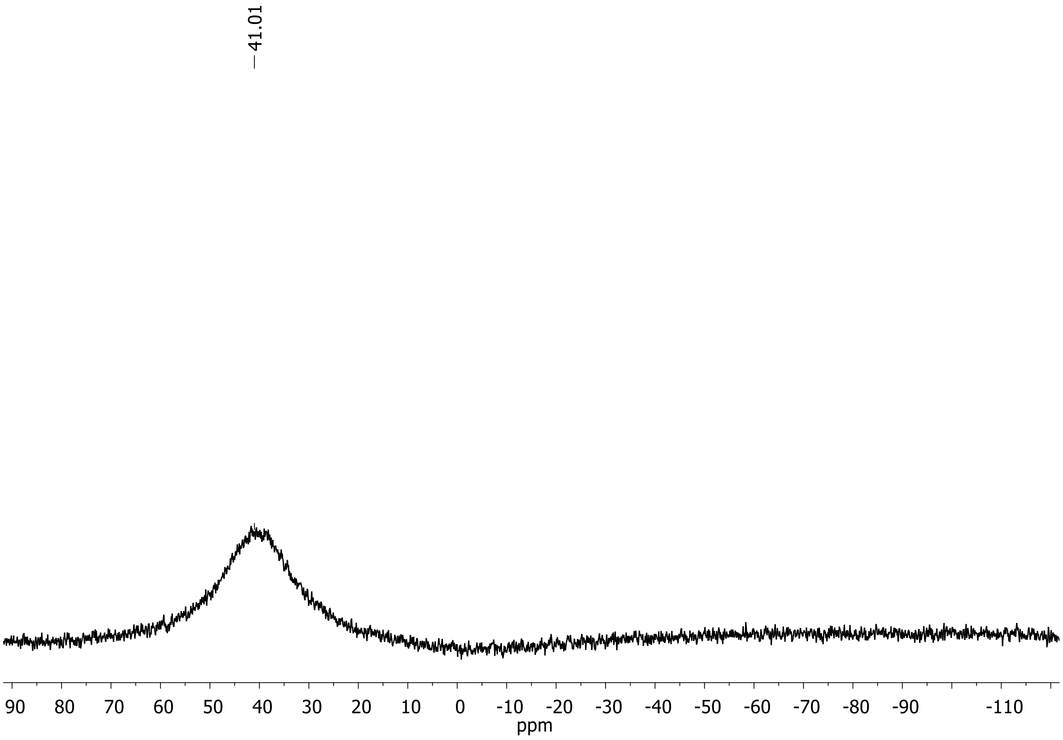

Fig. S34: $^{11}B\{^{1}H\}$ NMR (160 MHz, $CDCl_3$) differential spectrum of $CDCl_3$ and compound **Ph-BNCDI$^{\mathbf{Dip}}$**.

1,7-Di(*n*-hexyl)-6,12-di(phenyl)-1,12,6,7-di([1,2]azaborinine)-***N*,*N'***-di(*n*-hexyl)perylene3,4,9,10-tetracarboxylic acid diimide (Ph-BNCDI^{Hex})

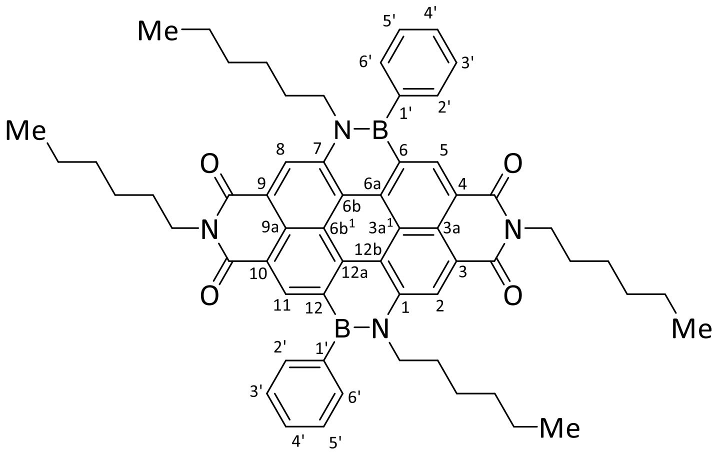

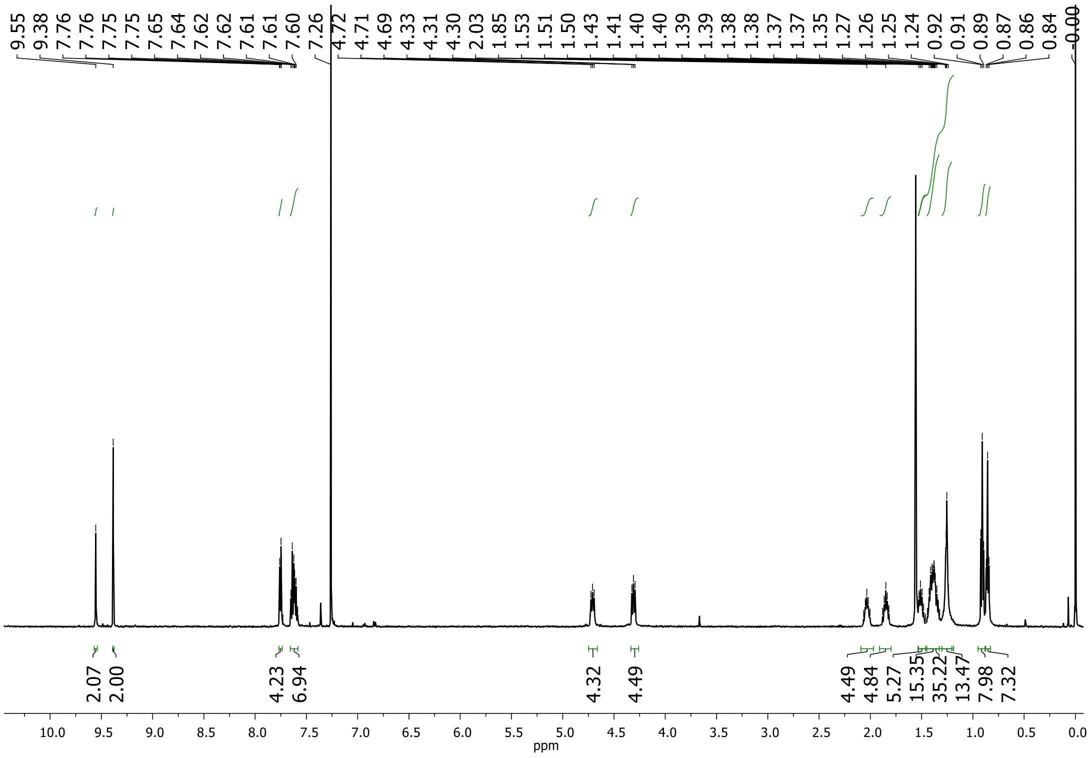

Fig. S35: ^{1}H NMR (500 MHz, CDCl$_3$) spectrum of compound **Ph-BNCDI^{Hex}**.

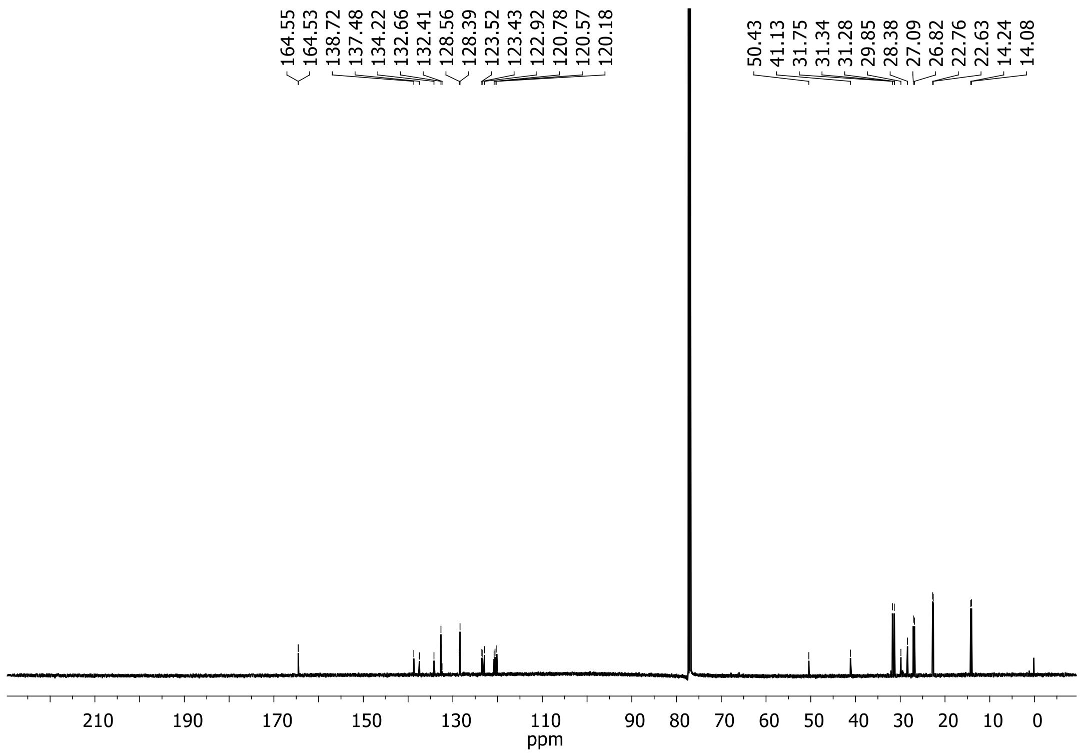

Fig. S36: $^{13}C\{^{1}H\}$ NMR (125 MHz, $CDCl_3$) spectrum of compound **Ph-BNCDI^{Hex}**.

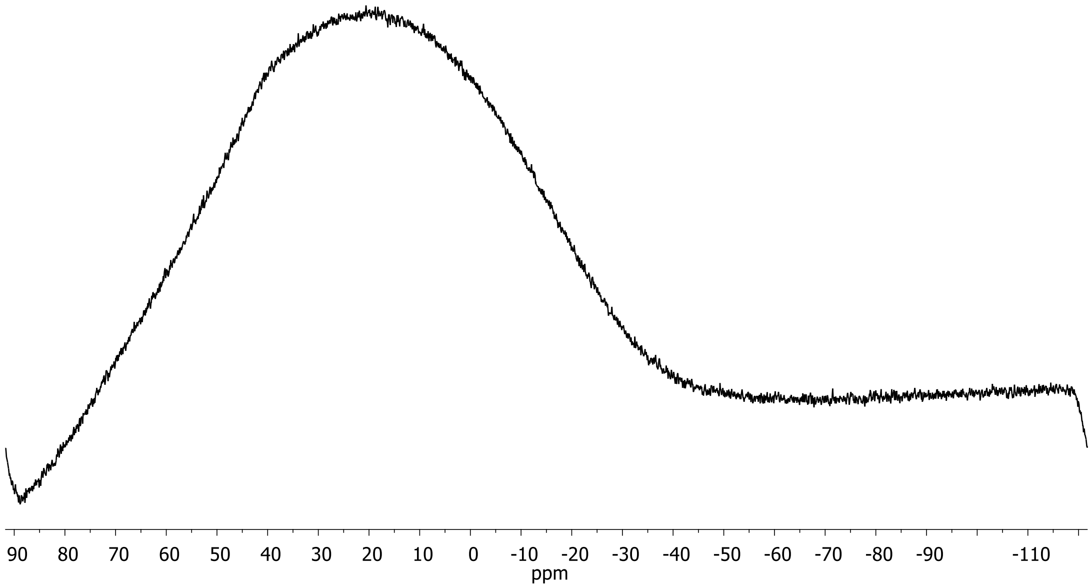

Fig. S37: $^{11}B\{^{1}H\}$ NMR (160 MHz, $CDCl_3$) spectrum of compound **Ph-BNCDI^{Hex}**.

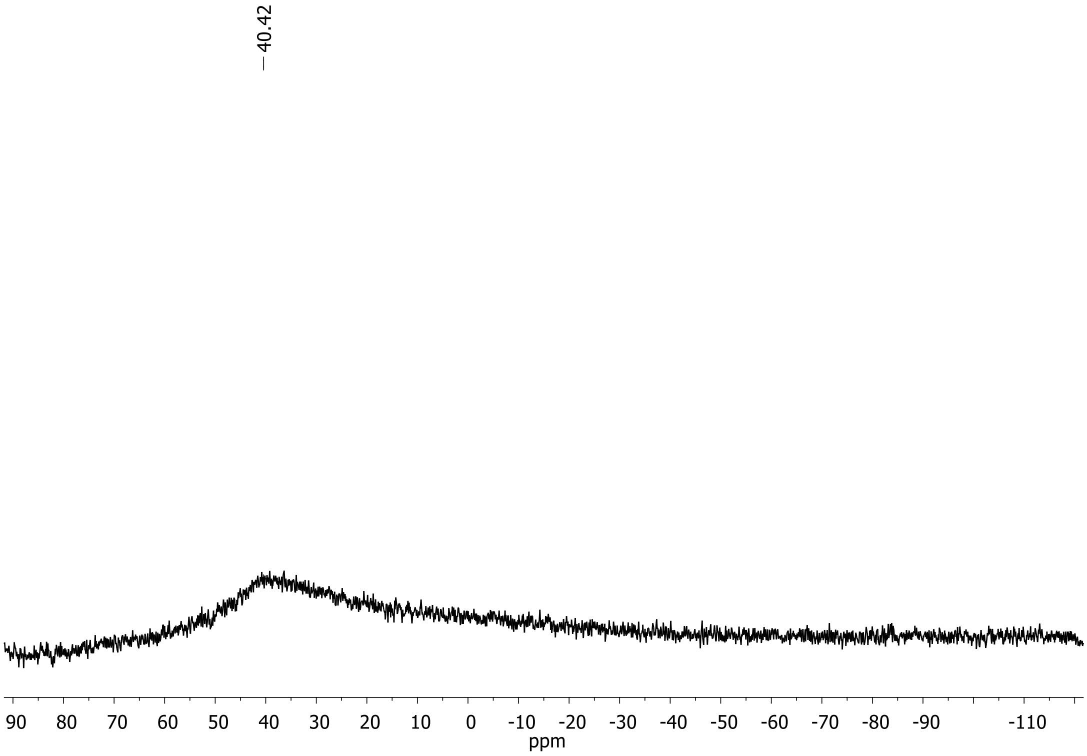

Fig. S38: $^{11}B\{^{1}H\}$ NMR (160 MHz, $CDCl_3$) differential spectrum of $CDCl_3$ and compound **Ph-BNCDI^{Hex}**.

1,7-Di(*n*-hexyl)-6,12-di(thiophen-2-yl)-1,12,6,7-di([1,2]azaborinine)-*N*,*N'*-di(cyclohexyl)perylene-3,4,9,10-tetracarboxylic acid diimide (Tph-BNCDI^{Cy})

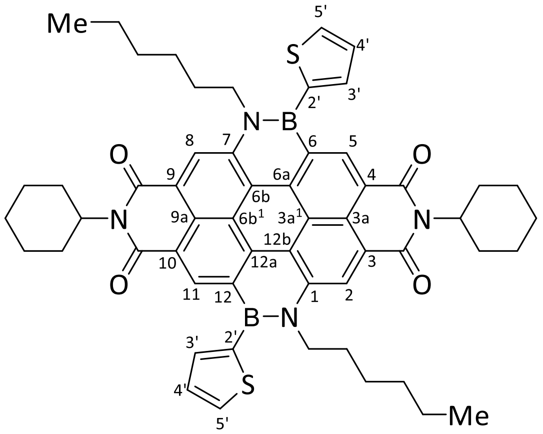

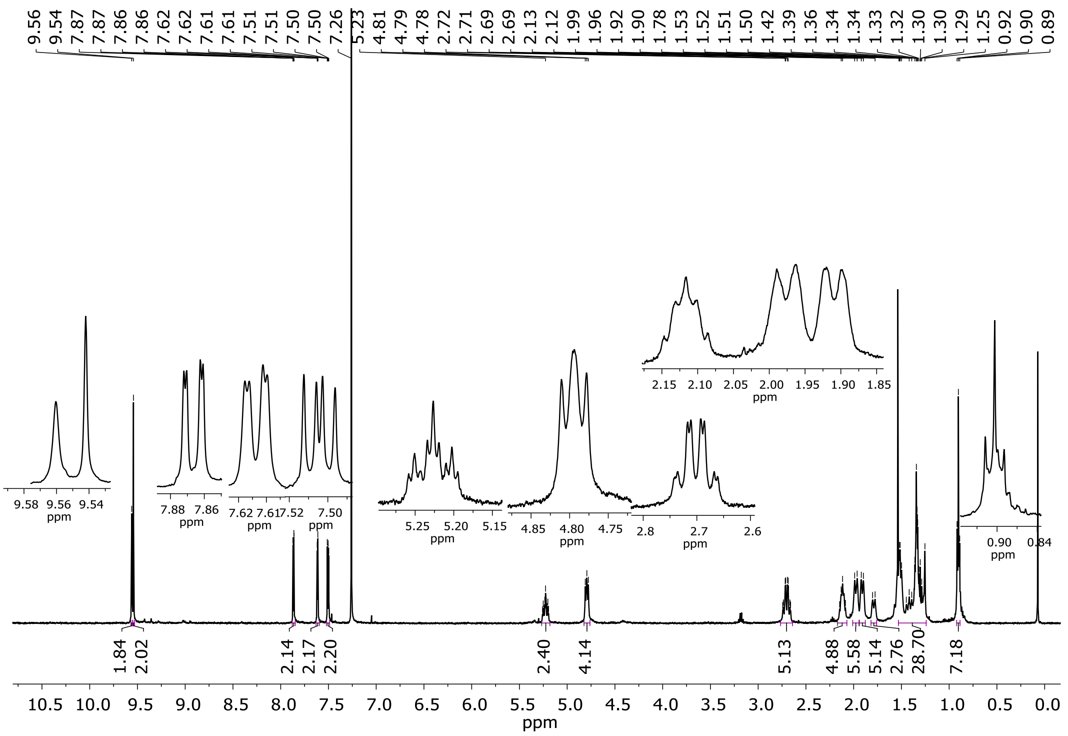

Fig. S39: ^{1}H NMR (500 MHz, CDCl$_3$) spectrum of **Tph-BNCDI^{Cy}**.

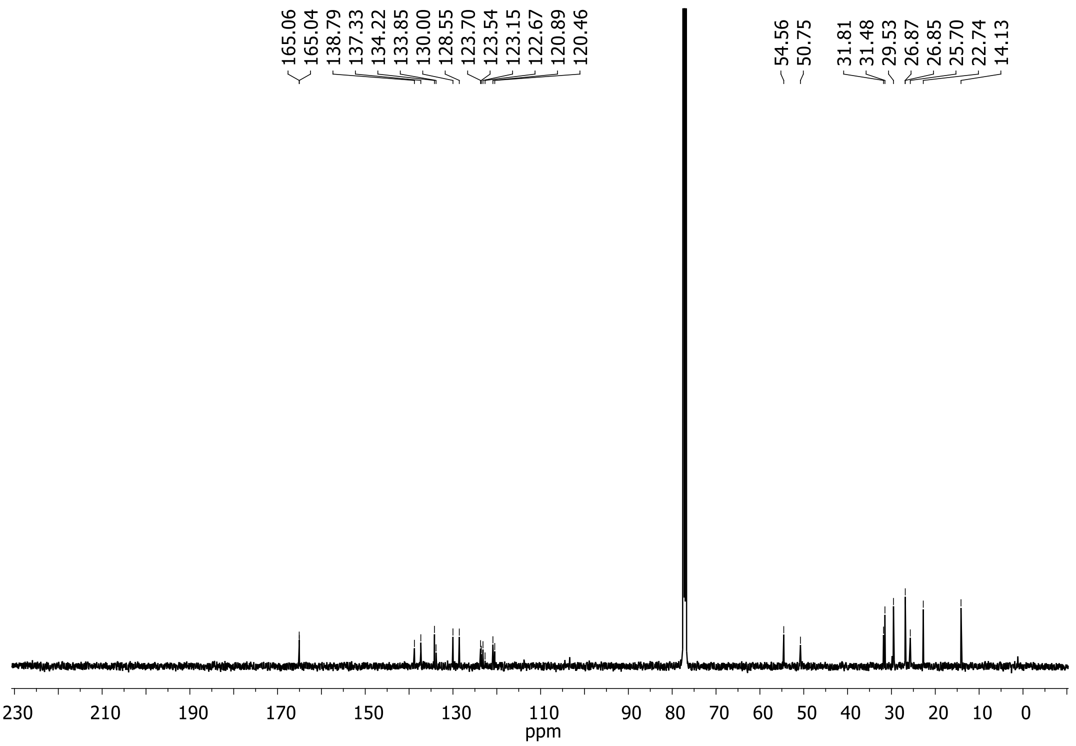

Fig. S40: ^{13}C{^{1}H} NMR (126 MHz, CDCl$_3$) spectrum of **Tph-BNCDI^{Cy}**.

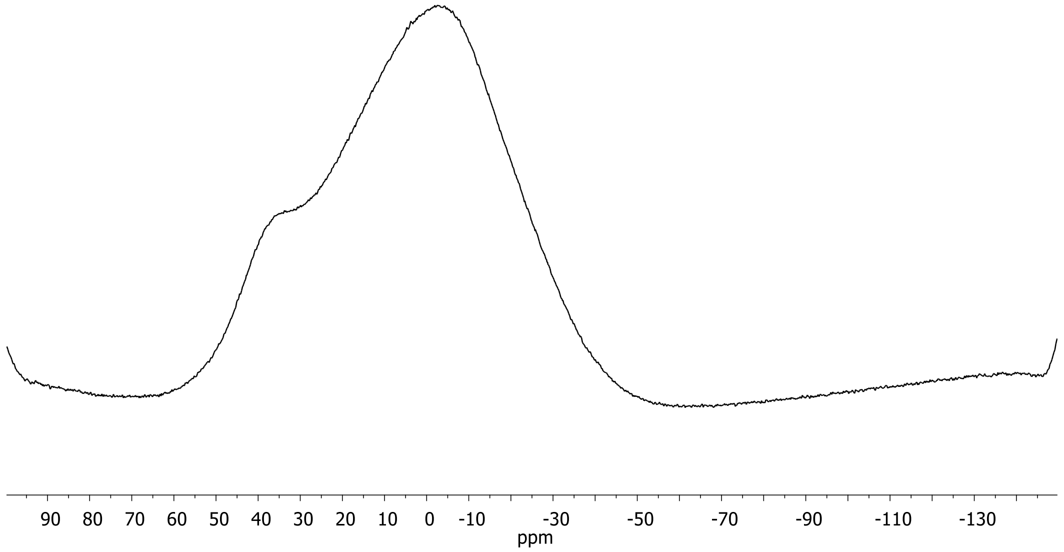

Fig. S41: ^{11}B{^{1}H} NMR (160 MHz, CDCl$_3$) spectrum of **Tph-BNCDI^{Cy}**.

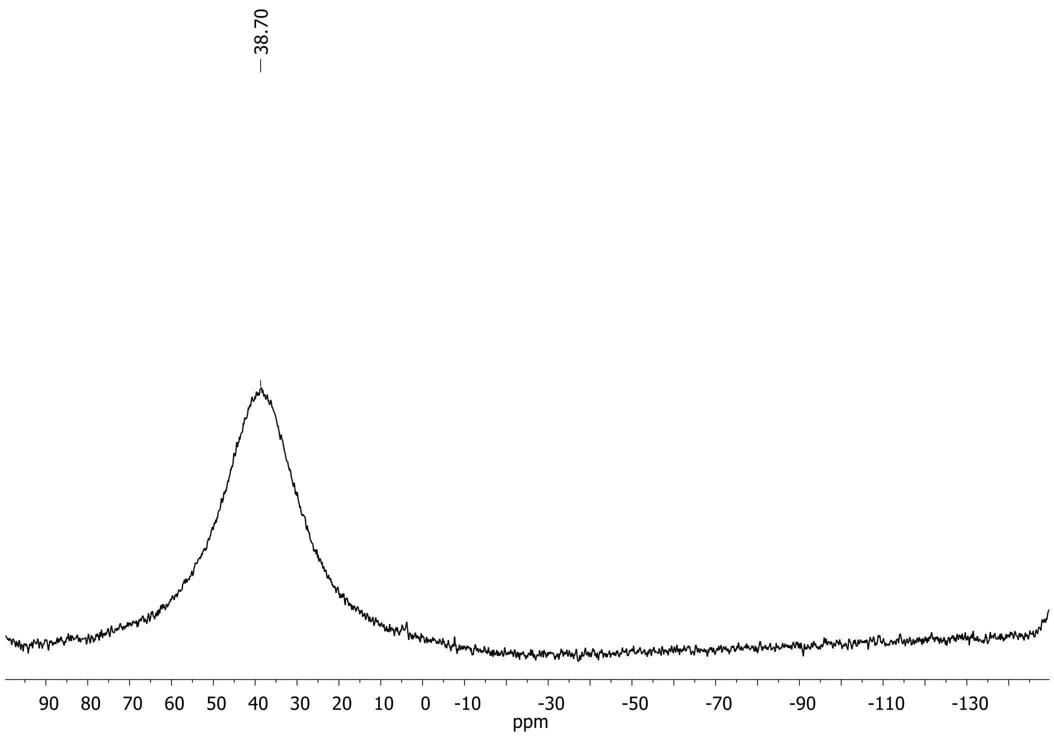

Fig. S42: $^{11}B\{^{1}H\}$ NMR (160 MHz, $CDCl_3$) differential spectrum of $CDCl_3$ and **Tph-BNCDI^{Cy}**.

1,7-Di(*n*-hexyl)-6,12-di(thiophen-2-yl)-1,12,6,7-di([1,2]azaborinine)-*N*,*N'*-bis(2,6-di*iso*propylphenyl)perylene-3,4,9,10-tetracarboxylic acid diimide (Tph-BNCDI^{Dip})

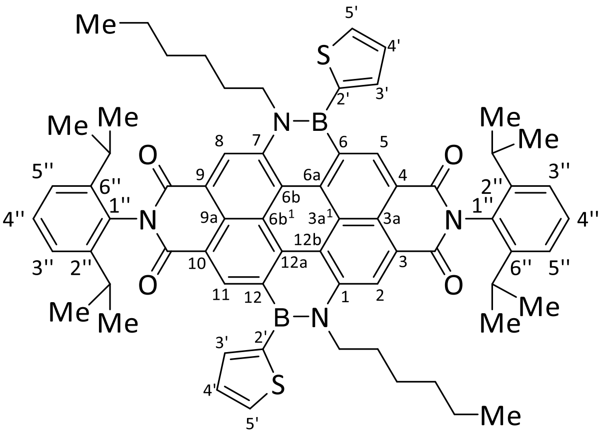

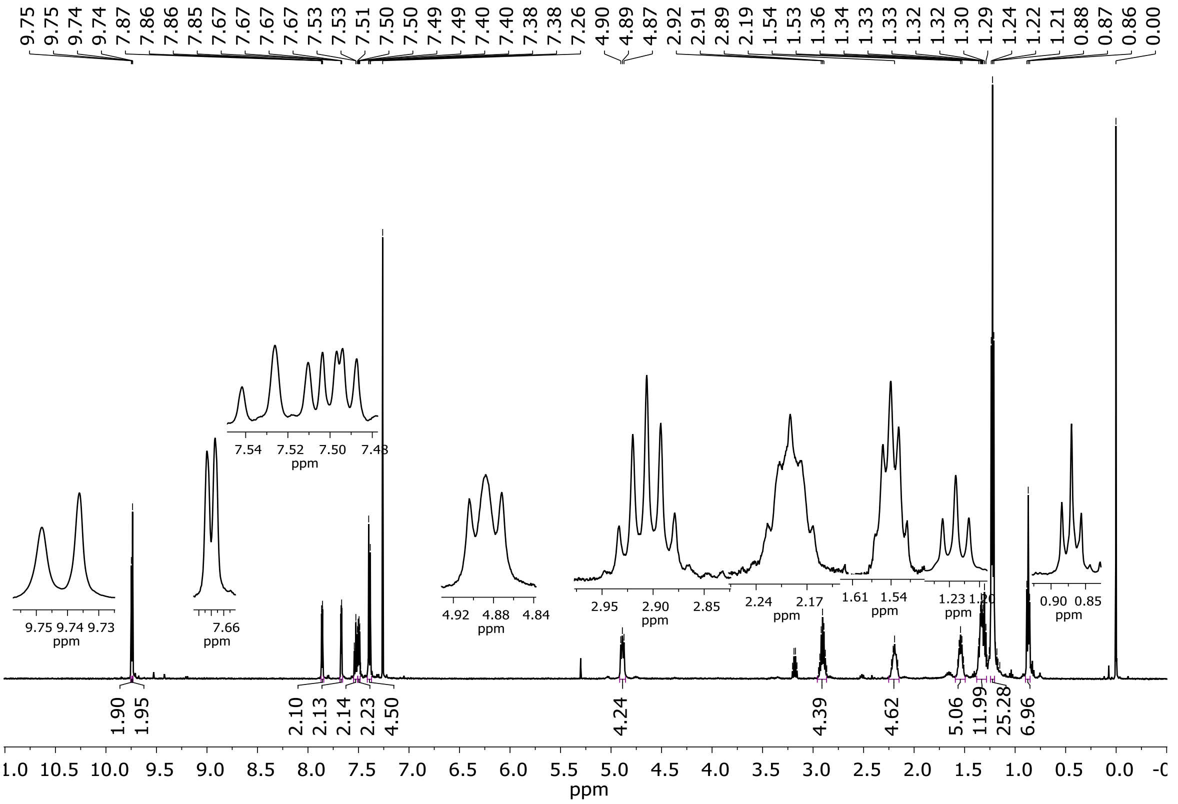

Fig. S43: ^1H NMR (500 MHz, $CDCl_3$) spectrum of **Tph-BNCDI^{Dip}**.

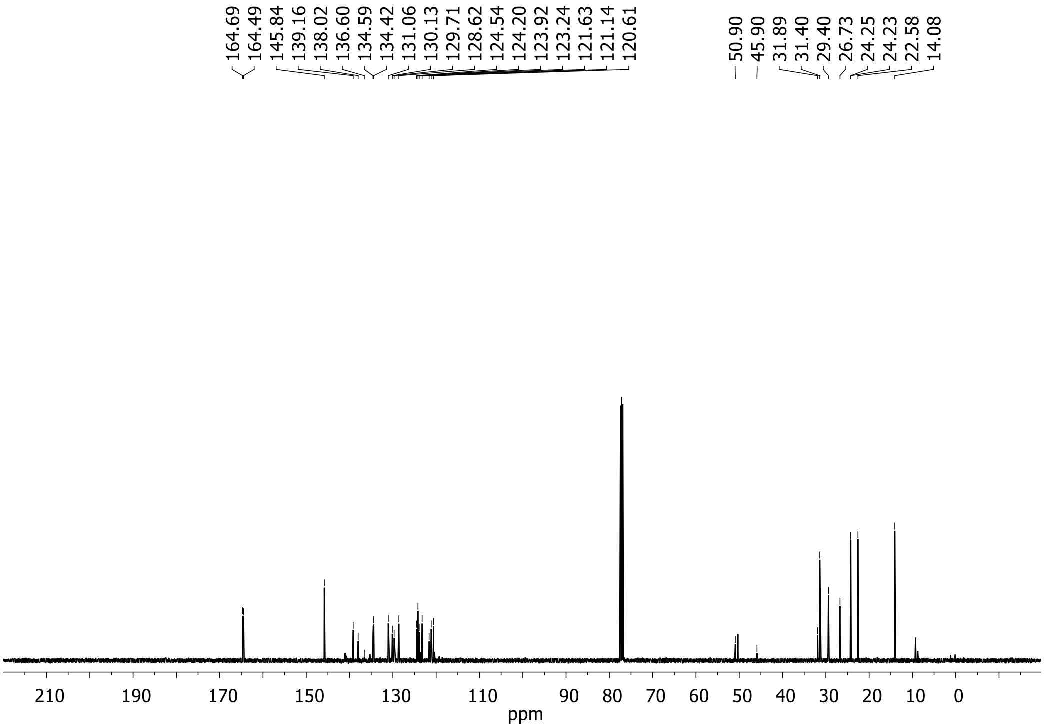

Fig. S44: $^{13}C\{^1H\}$ NMR (126 MHz, $CDCl_3$) spectrum of **Tph-BNCDI^{Dip}**.

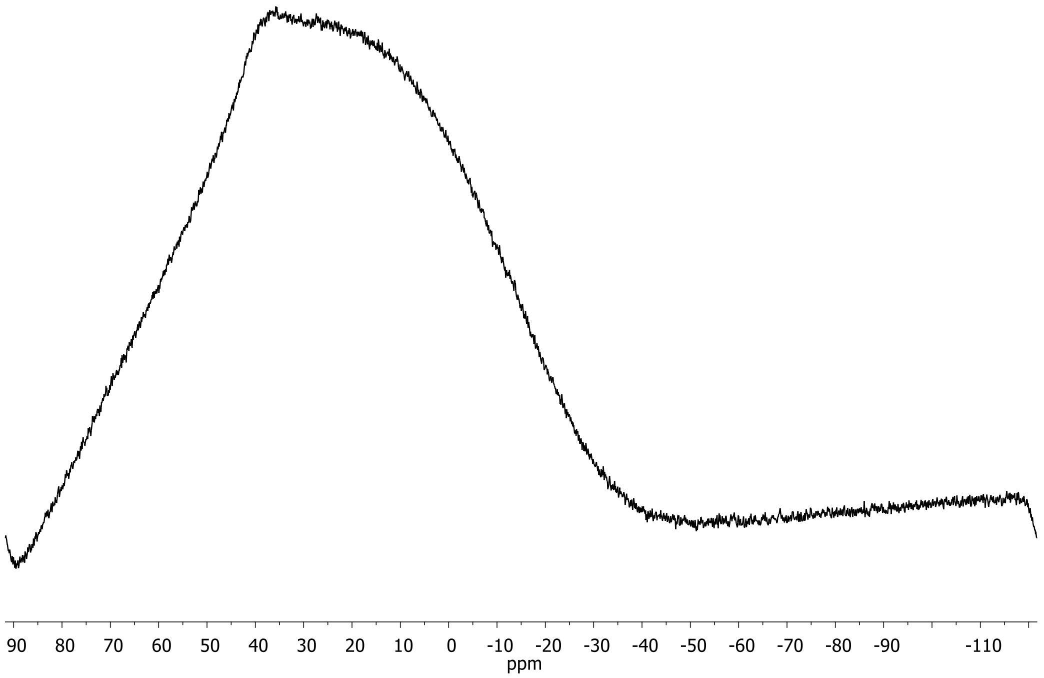

Fig. S45: $^{11}B\{^1H\}$ NMR (160 MHz, $CDCl_3$) spectrum of **Tph-BNCDI^{Dip}**.

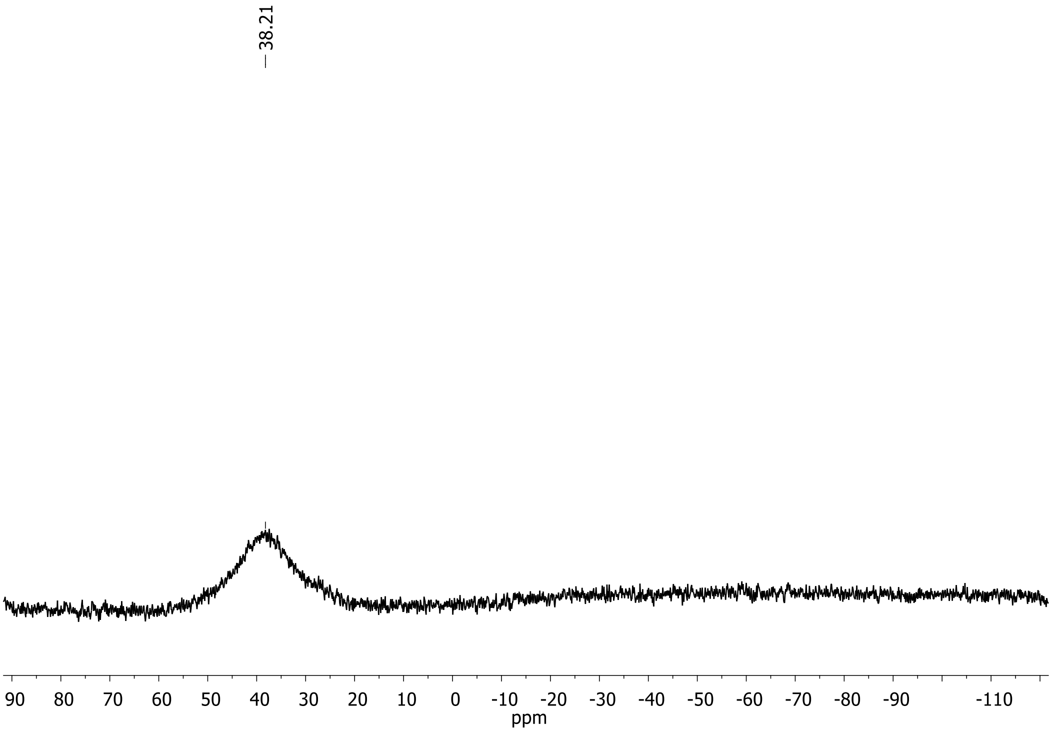

Fig. S46: $^{11}B\{^1H\}$ NMR (160 MHz, $CDCl_3$) differential spectrum of $CDCl_3$ and **Tph-BNCDI^{Dip}**.

1,7-Di(*n*-hexyl)-6,12-*bis*(4-(diphenylamino)phenyl)-1,12,6,7-*di*([1,2]azaborinine)-***N*,*N*'**-dicyclo-hexylperylene-3,4,9,10-tetracarboxylic acid diimide (TPA-BNCDI^{Cy})

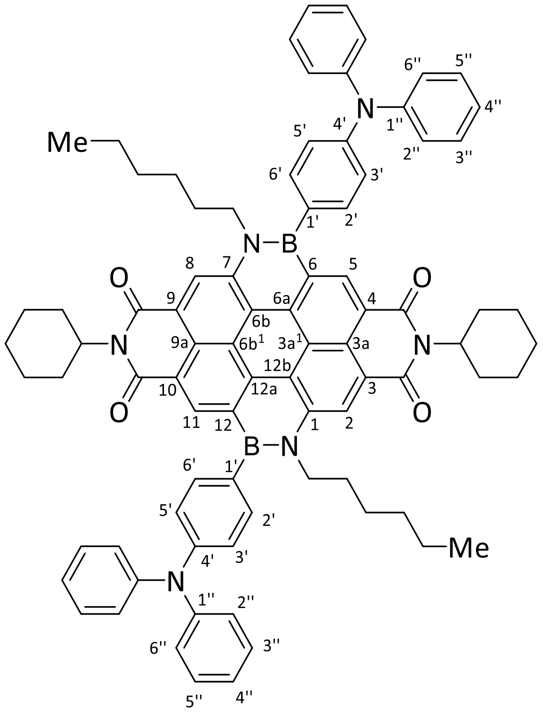

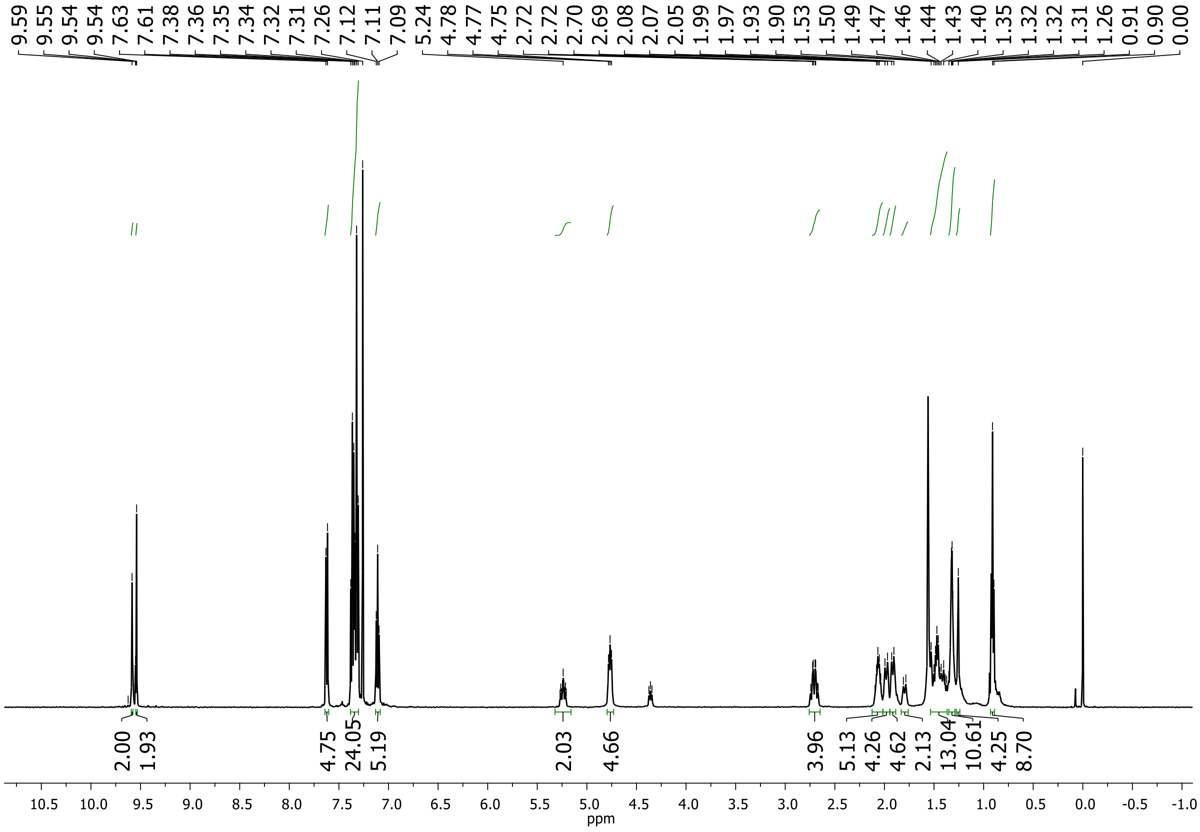

Fig. S47: ^{1}H NMR (500 MHz, CDCl$_3$) spectrum of compound **TPA-BNCDI^{Cy}**.

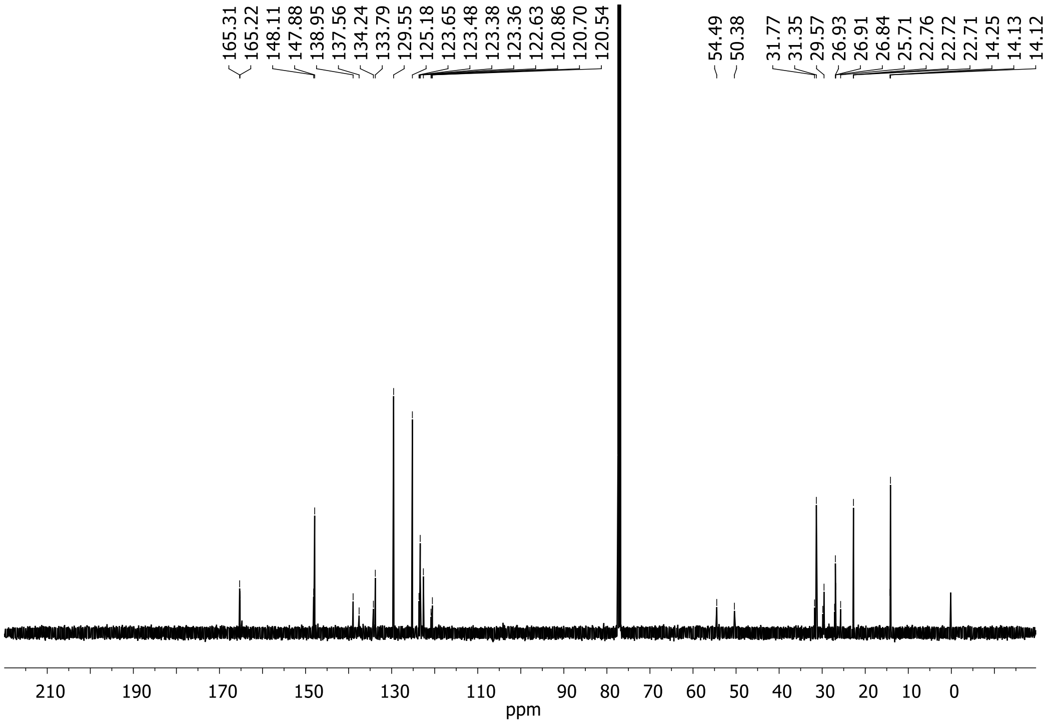

Fig. S48: $^{13}C\{^{1}H\}$v NMR (125 MHz, $CDCl_3$) spectrum of compound **TPA-BNCDI^{Cy}**.

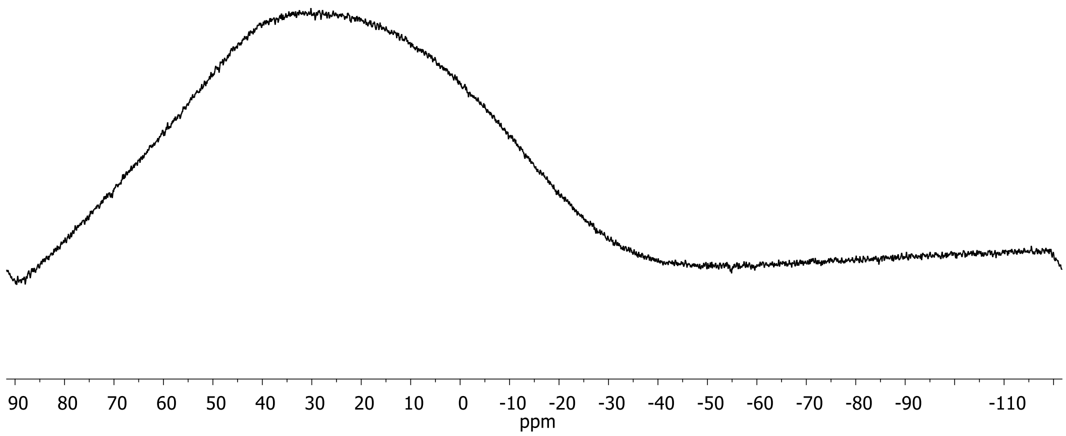

Fig. S49: $^{11}B\{^{1}H\}$ NMR (160 MHz, $CDCl_3$) spectrum of compound **TPA-BNCDI^{Cy}**.

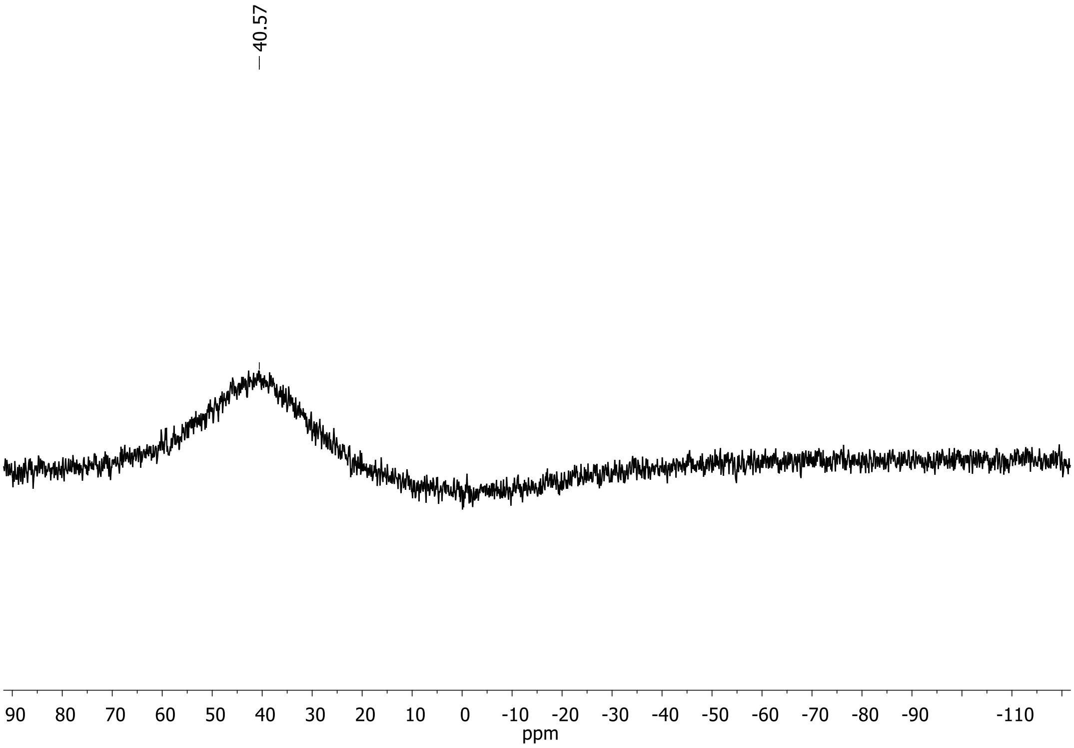

Fig. S50: $^{11}B\{^{1}H\}$ NMR (160 MHz, $CDCl_3$) differential spectrum of $CDCl_3$ and compound **TPA-BNCDI^{Cy}**.

1,7-Di(*n*-hexyl)-6,12-*bis*(4-(diphenylamino)phenyl)-1,12,6,7-di([1,2]azaborinine)-*N*,*N'*-bis(2,6-di*iso*propylphenyl)perylene-3,4,9,10-tetracarboxylic acid diimide (TPA-BNCDI^{Dip})

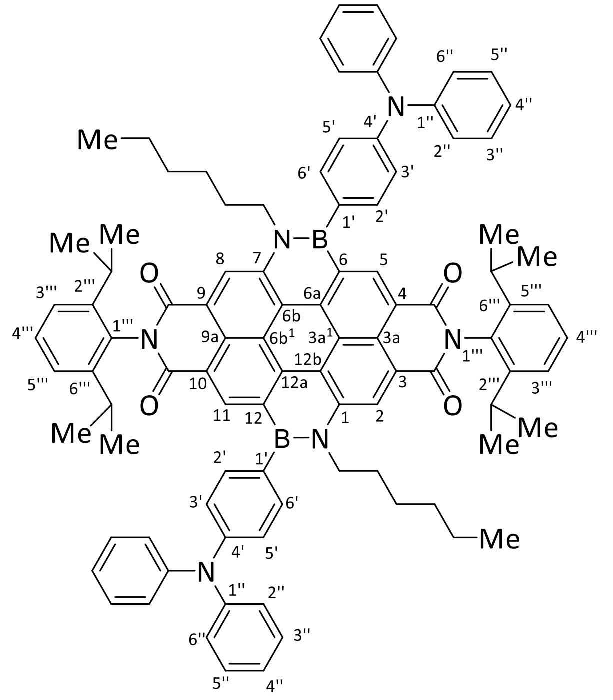

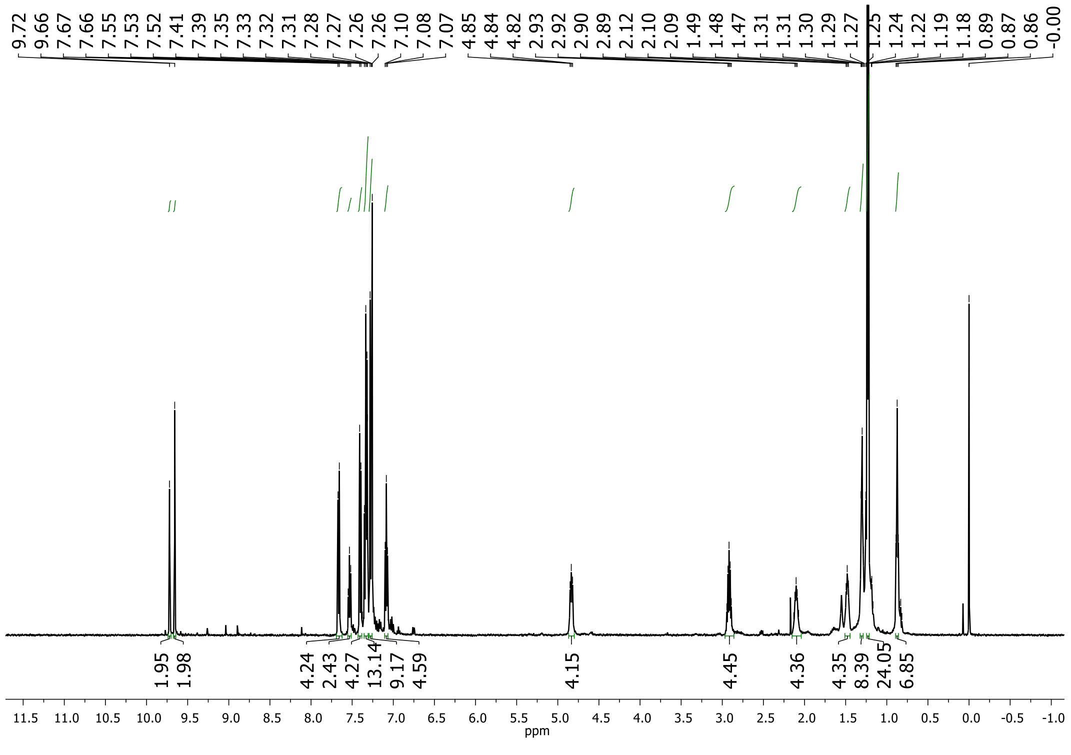

Fig. S51: ^{1}H NMR (500 MHz, $CDCl_3$) spectrum of compound **TPA-BNCDI^{Dip}**.

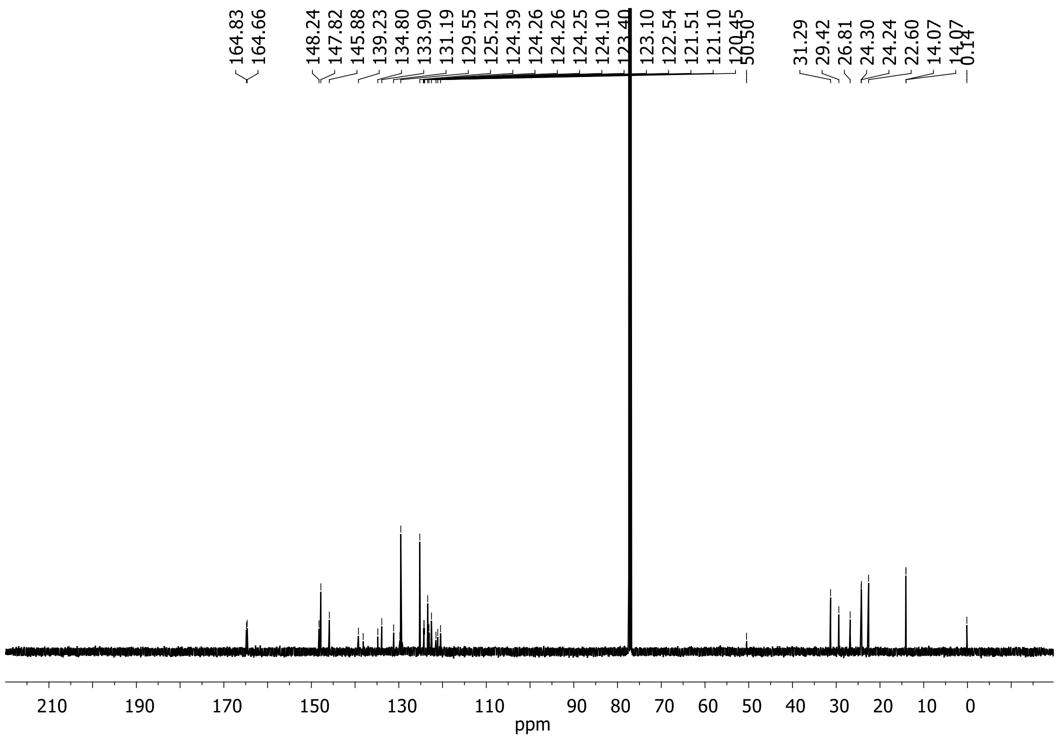

Fig. S52: $^{13}C\{^1H\}$ NMR (125 MHz, $CDCl_3$) spectrum of compound **TPA-BNCDI^{Dip}**.

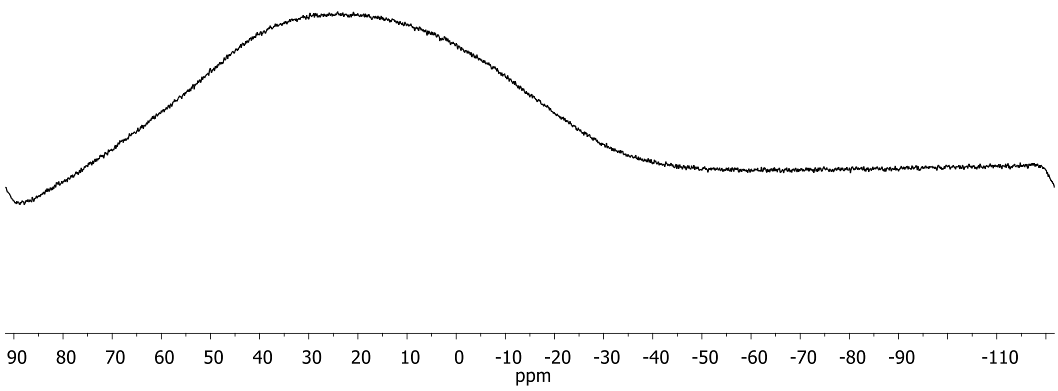

Fig. S53: $^{11}B\{^1H\}$ NMR (160 MHz, $CDCl_3$) spectrum of compound **TPA-BNCDI^{Dip}**.

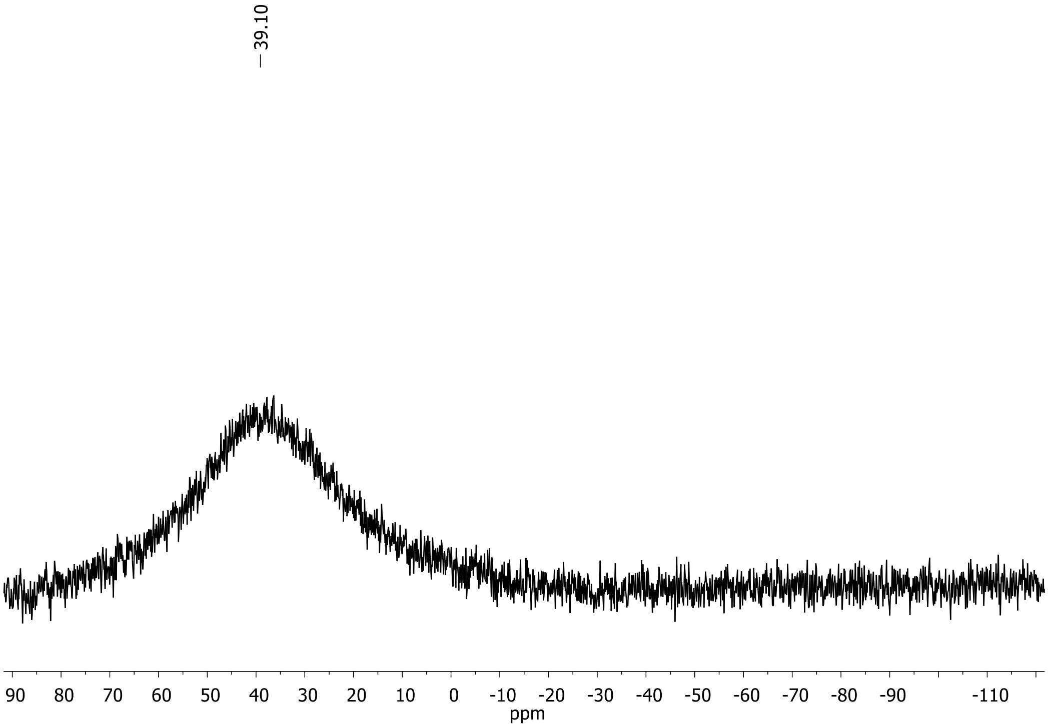

Fig. S54: $^{11}B\{^{1}H\}$ NMR (160 MHz, $CDCl_3$) differential spectrum of $CDCl_3$ and compound **TPA-BNCDI^{Dip}**.

UV/Vis Absorption, Fluorescence and Excitation

Overview

Tab. S4: Overview of the optical and thermal properties of all **BNCDI**s.

compound	$\lambda_{abs}{}^{a}$ / nm	Lg(ε)^{a}	E_{opt} /eV^{b}	$\lambda_{lum}{}^{a}$ / nm	$\Delta\nu_{stokes}{}^{a}$ /cm^{-1}	$\Phi_{lum}{}^{c}$
Ph-BNCDI^{Cy}	536	4.80	2.30	544	285	0.95
Ph-BNCDI^{Dip}	539	4.91	2.23	543	137	0.88
Ph-BNCDI^{nHex}	536	4.75	2.25	546	342	0.91
TPA-BNCDI^{Cy}	540	4.68	2.19	581	1307	< 0.01
TPA-BNCDI^{Dip}	541	4.66	2.16	574	1158	< 0.01
Tph-BNCDI^{Cy}	535	4.74	2.24	544	310	0.95
Tph-BNCDI^{Dip}	538	4.85	2.23	546	272	0.94

[a] Measured in DCM solutions (10^{-5}-10^{-6} M) [b] Calculated from the offset wavelength derived from the lowest energy absorption band. [c] Referenced externally against fluorescein in 0.1 M NaOH.

Ph-BNCDI^{Cy}

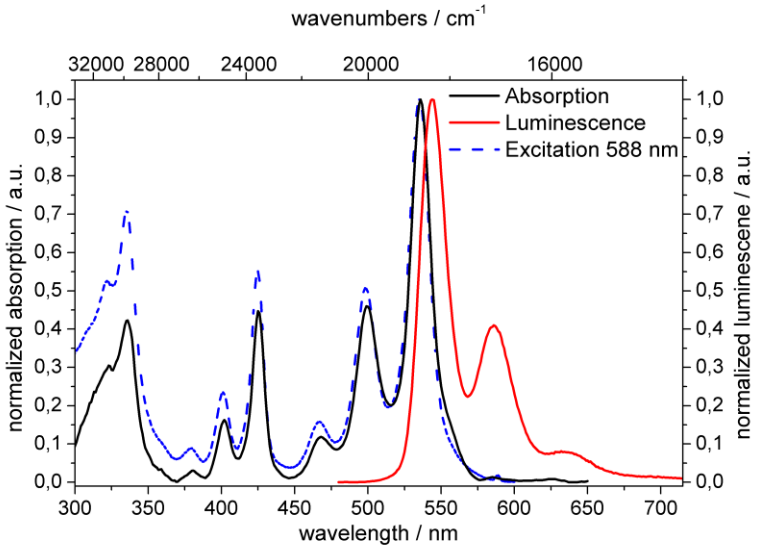

Fig. S55: Absorption/Emission/Excitation spectra of compound **Ph-BNCDI^{Cy}** in dichloromethane.

Ph-BNCDI^{Dip}

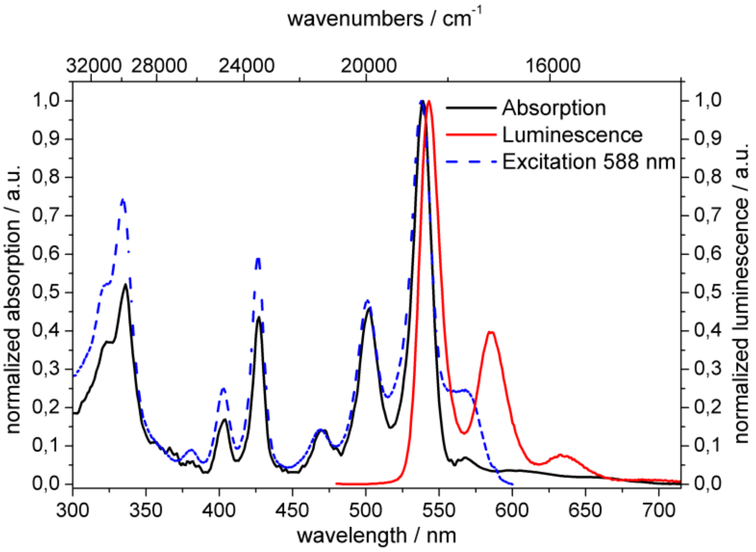

Fig. S56: Absorption/Emission/Excitation spectra of compound **Ph-BNCDI^{Dip}** in dichloromethane.

Ph-BNCD^{Hex}

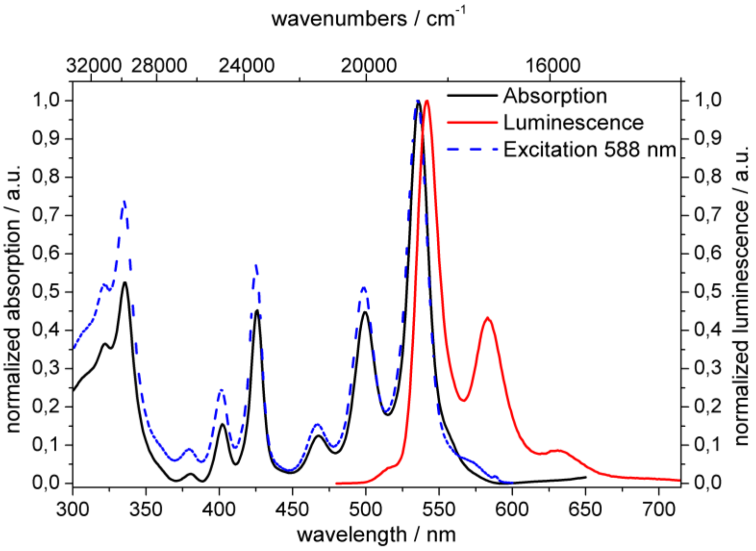

Fig. S57: Absorption/Emission/Excitation spectra of compound **Ph-BNCDI^{Hex}** in dichloromethane.

Tph-BNCDI^{Cy}

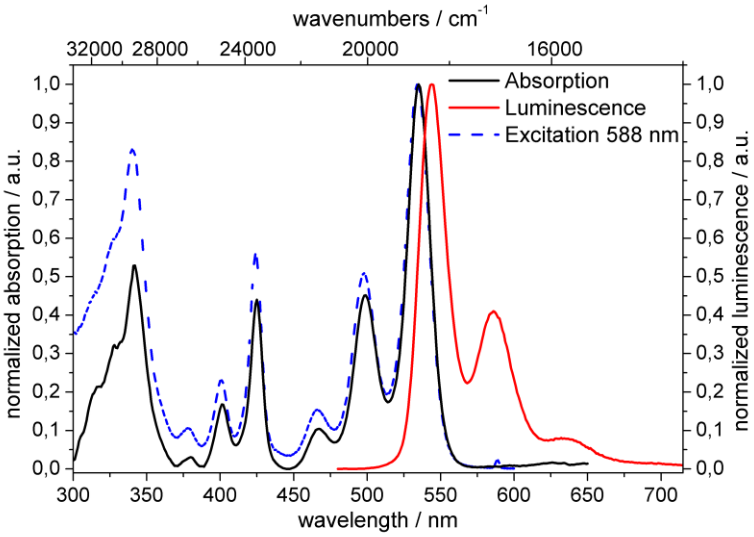

Fig. S58: Absorption/Emission/Excitation spectra of **Tph-BNCDI^{Cy}** in dichloromethane (10^{-6} M).

Tph-BNCDI^{Dip}

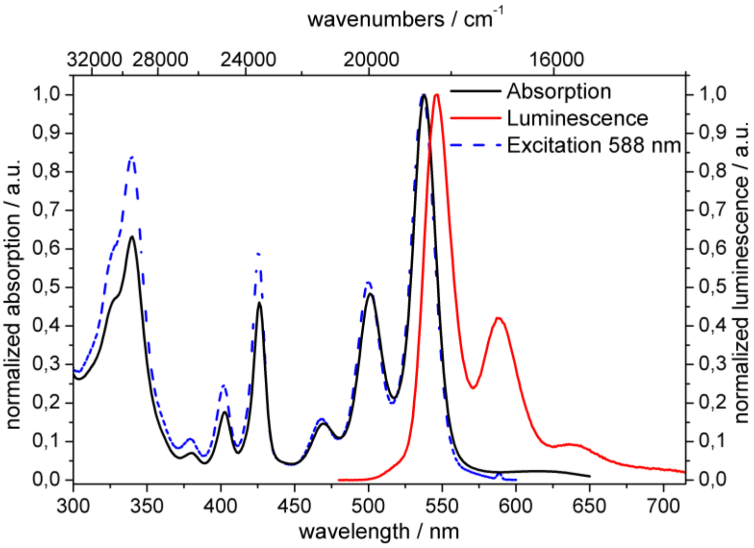

Fig. S59: Absorption/Emission/Excitation spectra of **Tph-BNCDI^{Dip}** in dichloromethane (10^{-6} M).

TPA-BNCDI^{Cy}

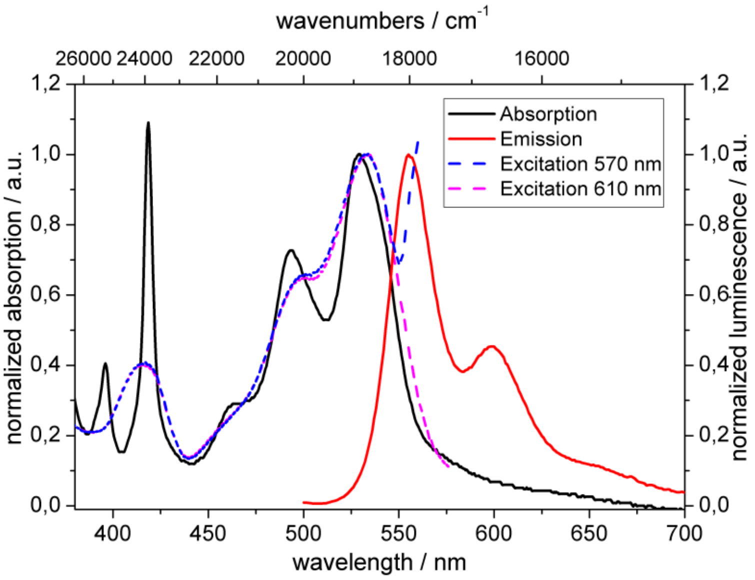

Fig. S60: Absorption/Emission/Excitation spectra of compound **TPA-BNCDI^{Cy}** in cyclohexane.

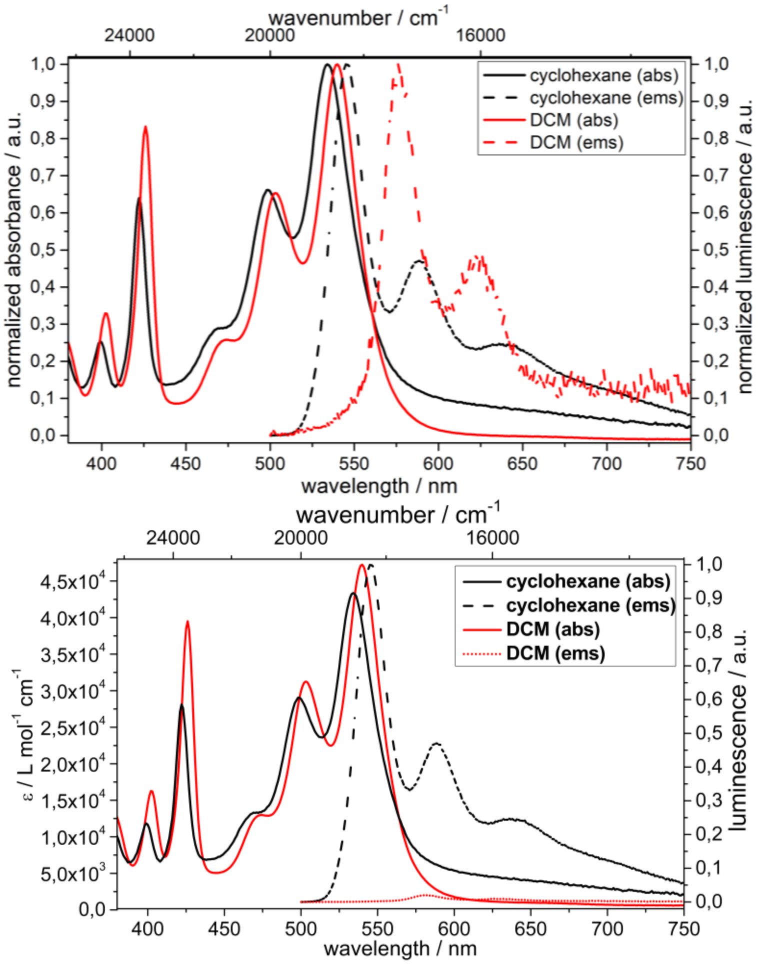

Fig. S61: Absorption/Emission spectra of compound **TPA-BNCDI^{Cy}** in cyclohexane and DCM normalized (top) and not normalized (bottom).

TPA-BNCDI^{Dip}

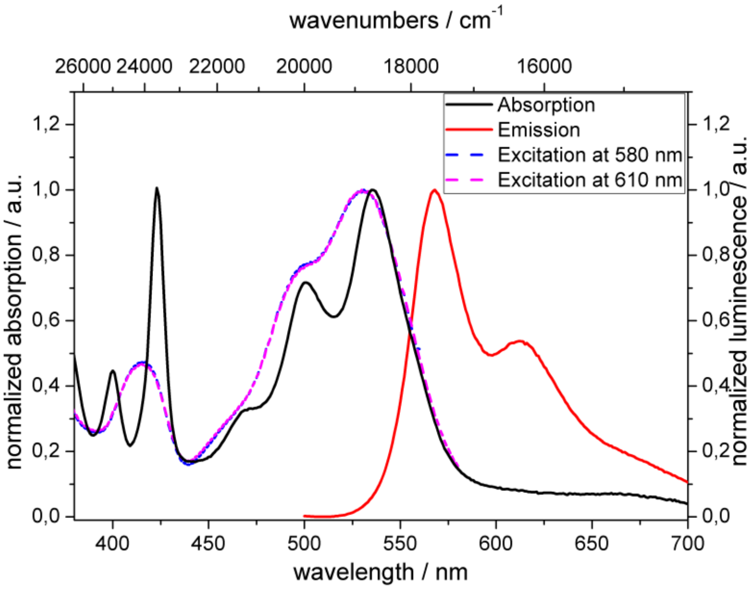

Fig. S62: Absorption/Emission/Excitation spectra of compound **TPA-BNCDI^{Dip}** in cyclohexane.

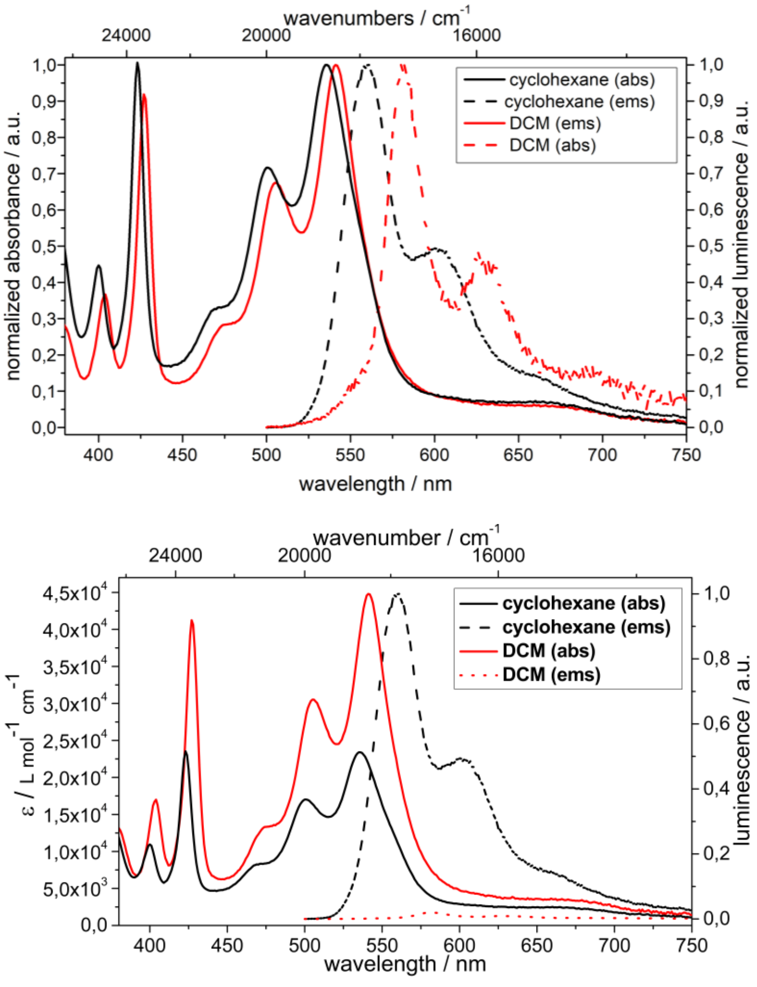

Fig. S63: Absorption/Emission spectra of compound **TPA-BNCDI^{Dip}** in cyclohexane and DCM normalized (top) and not normalized (bottom).

Solvent-dependency for TPA-BNCDIs

Tab. S5: Solvent-dependent luminescence of **TPA-BNCDI**s. The photograph shows **TPA-BNCDI^{Cy}** in DCM (left)/cyclohexane (right) and **TPA-BNCDI^{Dip}** in DCM (left)/cyclohexane(right) under irradiation with UV-lamp at 365 nm.

compound	solvent	λ_{abs} / nm	λ_{ems} / nm	$\Delta\nu_{Stokes}$ /cm^{-1}	Φ_{lum}[a]
TPA-BNCDI^{Cy}	DCM	540	581	1307	<0.01
	cyclohexane	534	545	378	0.81
TPA-BNCDI^{Dip}	DCM	541	574	1158	<0.01
	cyclohexane	535	560	835	0.39

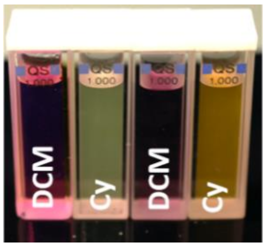

Referenced externally against fluorescein in 0.1 M NaOH.

Electrochemistry

The electrochemical studies were carried out under argon using an Eco Chemie Autolab PGSTAT 30 potentiostat for cyclic voltammetry. A three-electrode configuration was used: the working electrode was a platinum disk, the reference electrode was a saturated calomel electrode and the counter-electrode a platinum wire. All potentials were internally referenced to the ferrocene/ferrocenium couple. For the measurements, concentrations of 10^{-3} M of the electroactive species were used in a 0.2 M solution of tetrabutylammonium hexafluorophosphate in degassed DCM. The scanning rate was 200 mV/s. Non-reversible waves were corrected against Fc/Fc^{+} potential, whereas reversible reduction waves were corrected against $E_{1/2}$p from ferrocene. Absolute HOMO/LUMO levels were calculated according to E_{LUMO}= -4.8 eV- E_{red} and E_{HOMO}= -4.8 eV - E_{ox}.[9]

Overview

Tab. S6: Overview of the redox properties of all **BNCDI**s.

Compound	E_{ox} / V	E_{red1} / V	E_{red2} / V	$E_{ox,onset}$ / V	$E_{red,onset}$ / V	ΔE / V	E_{LUMO}^{b} / eV	E_{HOMO}^{b} / eV
Ph-BNCDI^{Cy}	+0.93	-1.30	-1.50	0.77	-1.09	1.86	-3.71	-5.57
Ph-BNCDI^{Dip}	+1.00	-1.20	-1.49	0.83	-1.05	1.88	-3.75	-5.63
Ph-BNCDI^{Hex}	+0.95	-1.26	-1.48	0.72	-1.07	1.79	-3.73	-5.52
Tph-BNCDI^{Cy}	+0.93	-1.26	-1.48	0.74	-1.10	1.84	-3.66	-5.16
Tph-BNCDI^{Dip}	+0.99	-1.22	-1.49	0.82	-1.05	1.87	-3.71	-5.21
TPA-BNCDI^{Cy}	+0.54	-1.32	-1.63	0.36	-1.15	1.51	-3.69	-5.54
TPA-BNCDI^{Dip}	+0.54	-1.19	-1.50	0.41	-1.09	1.50	-3.75	-5.62

[a] In DCM with Bu_4NPF_6 (0.2 M), a scan rate of 200 mV/s and ferrocene/ferrocenium as reference. [b] Derived from E_{LUMO}= -4.8 eV- E_{red} and E_{HOMO}= -4.8 eV- E_{ox}.[9]

Ph-BNCDI^{Cy} Oxidation

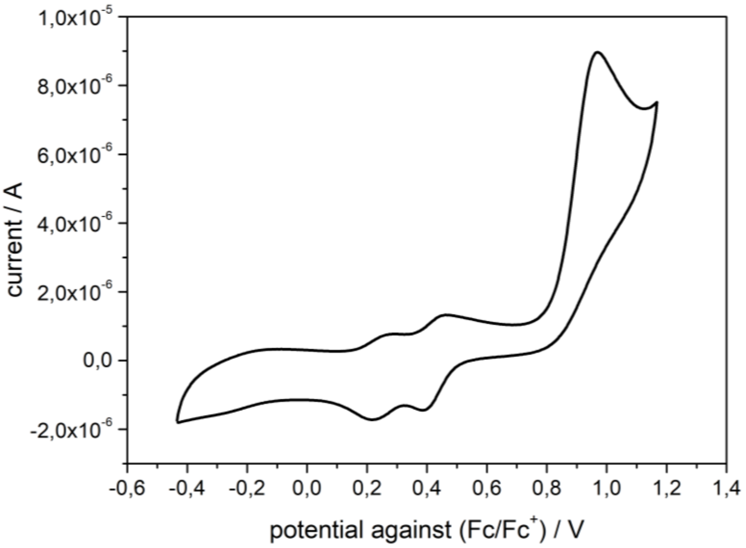

Fig. S64: Oxidation of compound **Ph-BNCDI^{Cy}** corrected against ferrocene/ferrocenium.

Ph-BNCDI^{Cy} Reduction

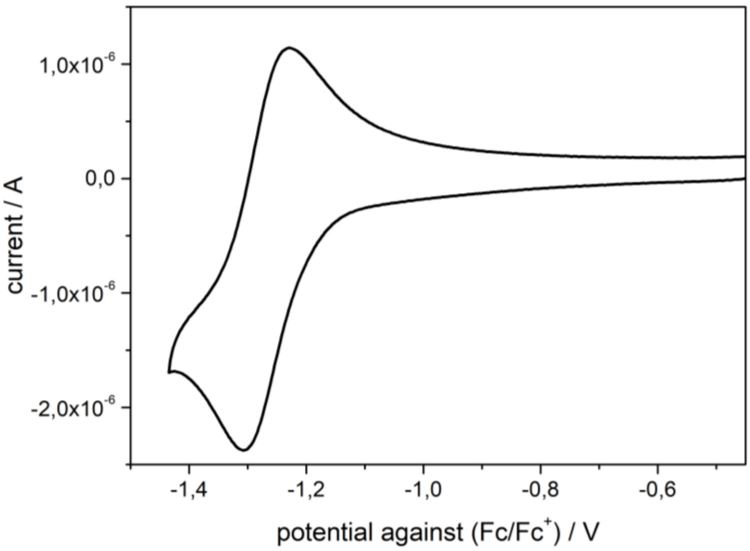

Fig. S65: Oxidation of compound **Ph-BNCDI^{Cy}** corrected against ferrocene/ferrocenium.

Ph-BNCDI^{Cy} Reduction

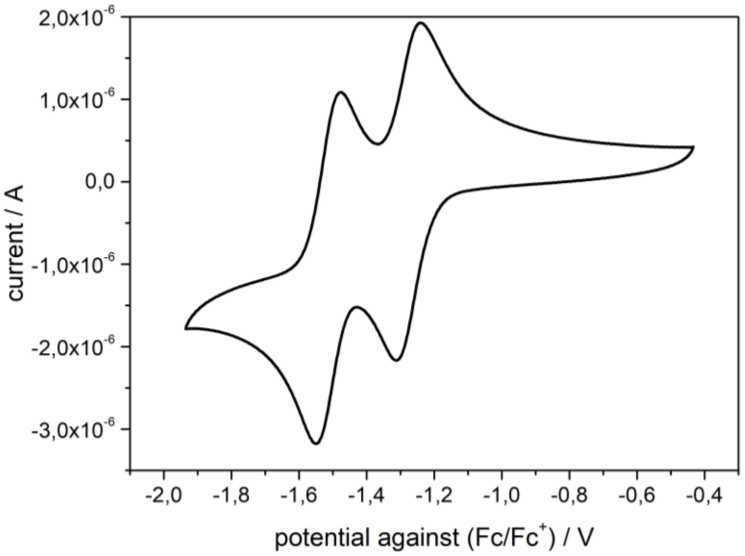

Fig. S66: Oxidation of compound **Ph-BNCDI^{Cy}** corrected against ferrocene/ferrocenium.

Ph-BNCDI^{Dip} Oxidation

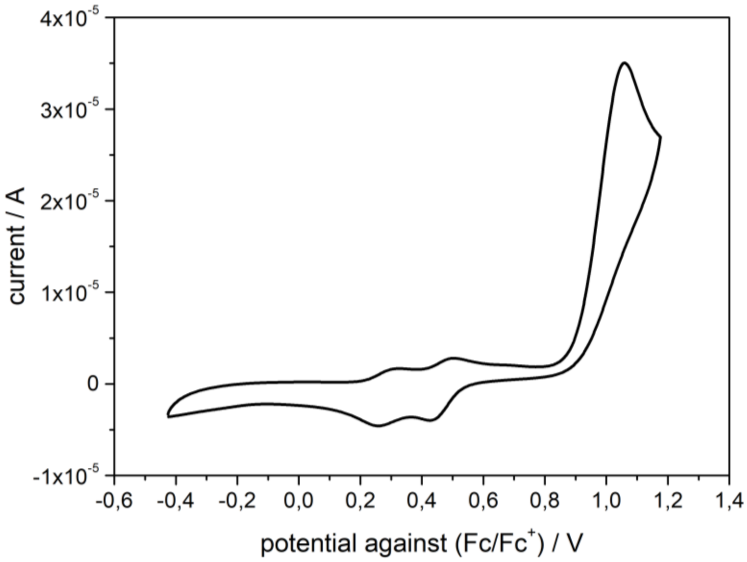

Fig. S67: Oxidation of compound **Ph-BNCDI^{Dip}** corrected against ferrocene/ferrocenium.

Ph-BNCDI^{Dip} Reduction

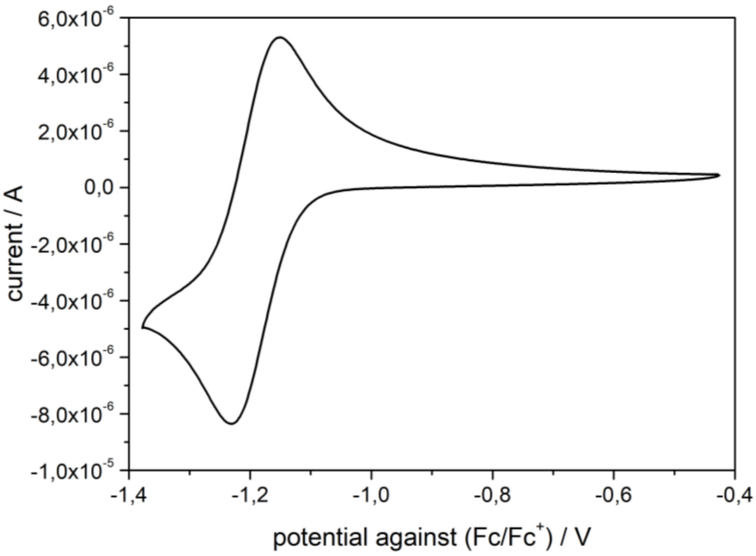

Fig. S68: Reduction of **Ph-BNCDI^{Dip}** corrected against ferrocene/ferrocenium.

Ph-BNCDI^{Dip} Reduction 2

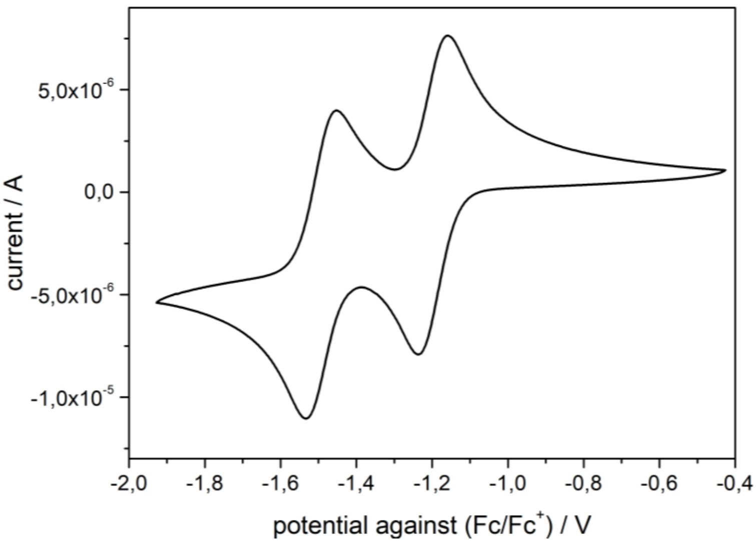

Fig. S69: Reduction of **Ph-BNCDI^{Dip}** corrected against ferrocene/ferrocenium.

Ph-BNCDI^{Hex} Oxidation

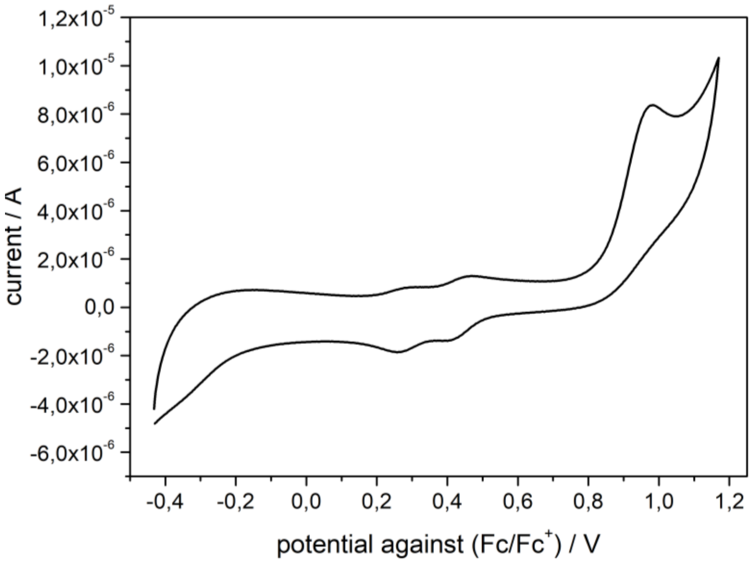

Fig. S70: Oxidation of compound **Ph-BNCDI^{Hex}** corrected against ferrocene/ferrocenium.

Ph-BNCDI^{Hex} Reduction

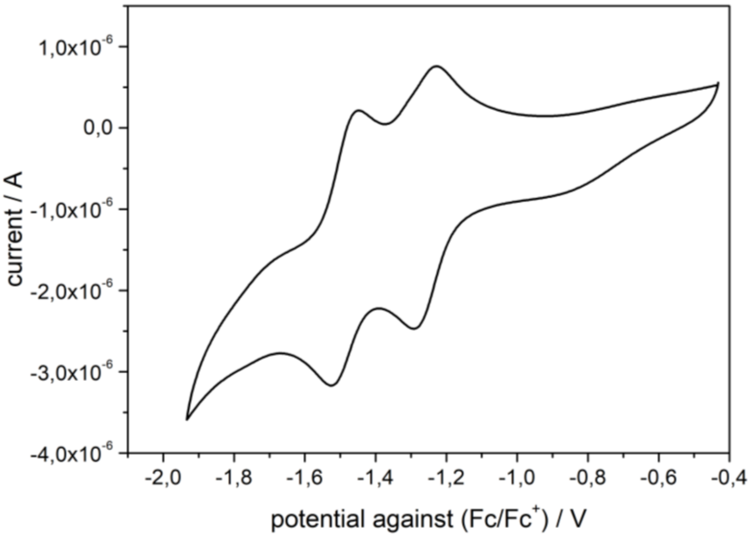

Fig. S71: Oxidation of compound **Ph-BNCDI^{Hex}** corrected against ferrocene/ferrocenium.

Tph-BNCDI^{Cy} Oxidation

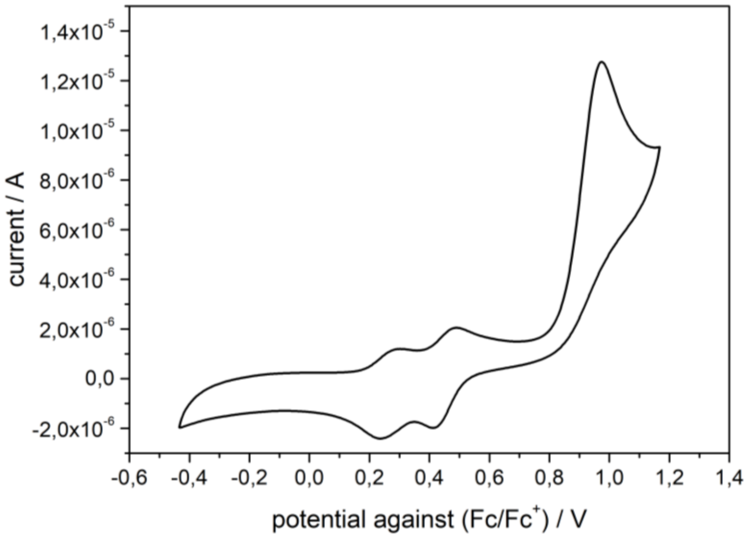

Fig. S72: Oxidation of **Tph-BNCDI^{Cy}** corrected against ferrocene/ferrocenium.

Tph-BNCDI^{Cy} Reduction

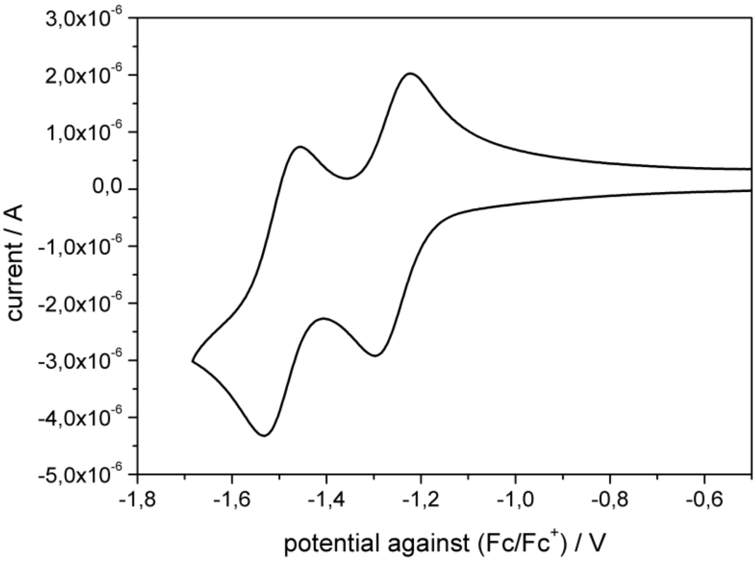

Fig. S73: Reduction of **Tph-BNCDI^{Cy}** corrected against ferrocene/ferrocenium.

Tph-BNCDI^{Dip} Oxidation

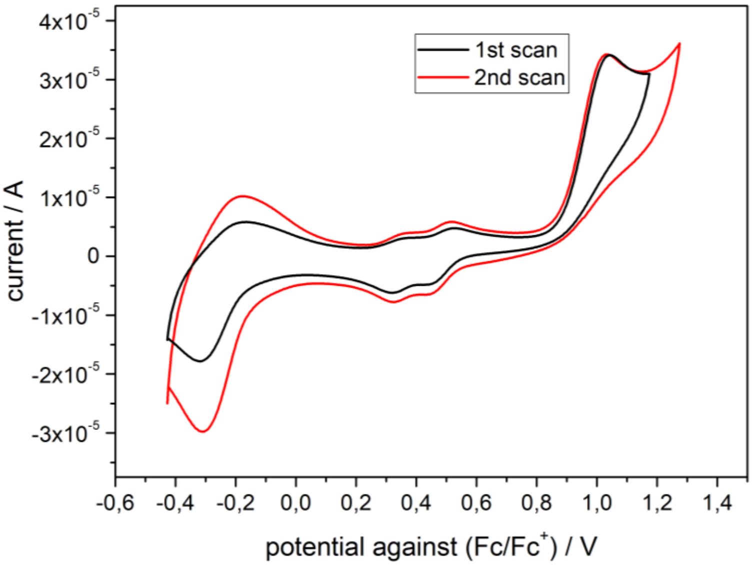

Fig. S74: Oxidation of **Tph-BNCDI^{Dip}** corrected against ferrocene/ferrocenium.

Tph-BNCDI^{Dip} Reduction

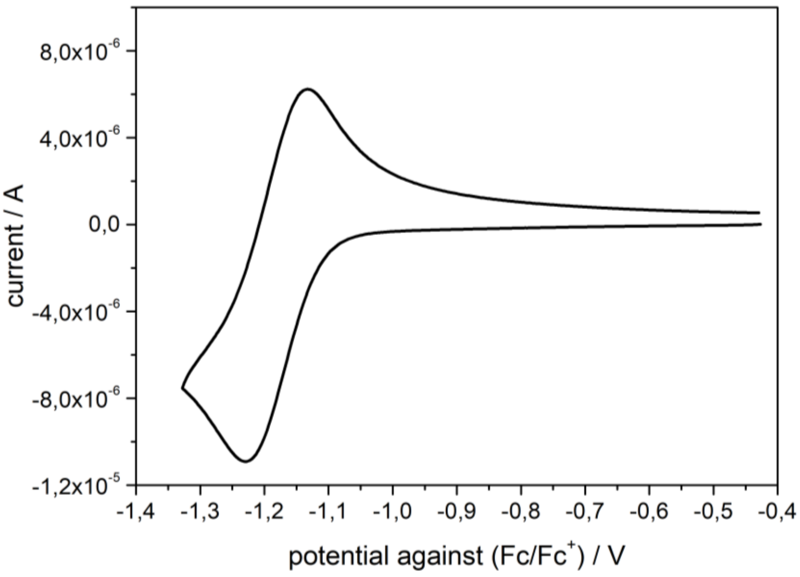

Fig. S75: Reduction of **Tph-BNCDI^{Dip}** corrected against ferrocene/ferrocenium.

Tph-BNCDI^{Dip} Reduction 2

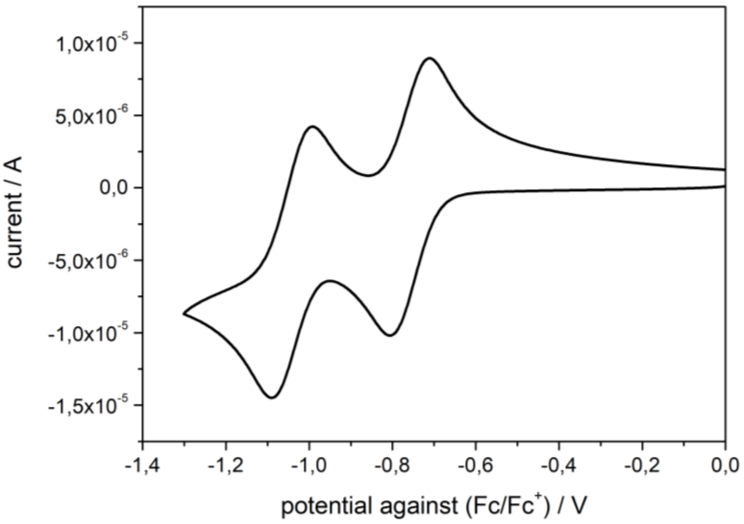

Fig. S76: Reduction of **Tph-BNCDI^{Dip}** corrected against ferrocene/ferrocenium.

TPA-BNCDI^{Cy} Oxidation

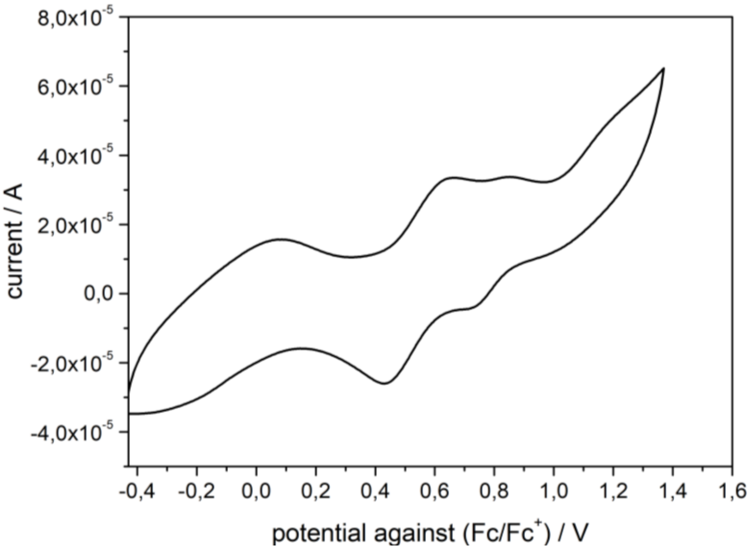

Fig. S77: Oxidation of compound **TPA-BNCDI^{Cy}** corrected against ferrocene/ferrocenium.

TPA-BNCDI^{Cy} Reduction

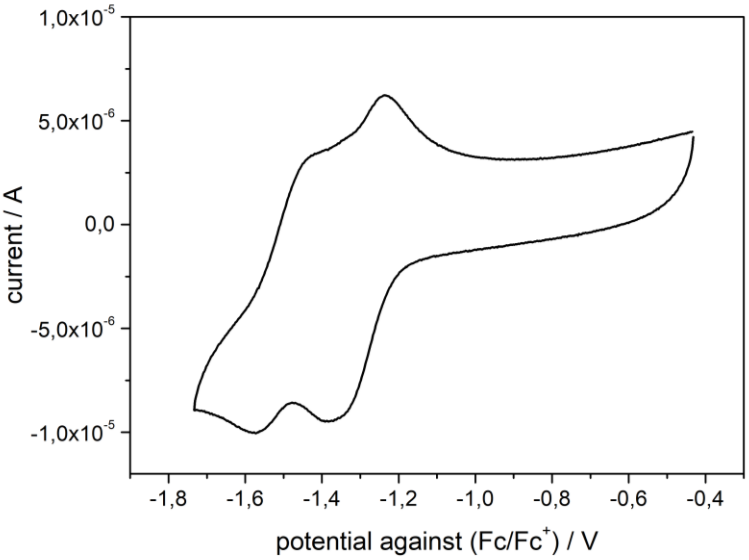

Fig. S78: Oxidation of compound **TPA-BNCDI^{Cy}** corrected against ferrocene/ferrocenium.

TPA-BNCDI^{Cy} Complete Redox

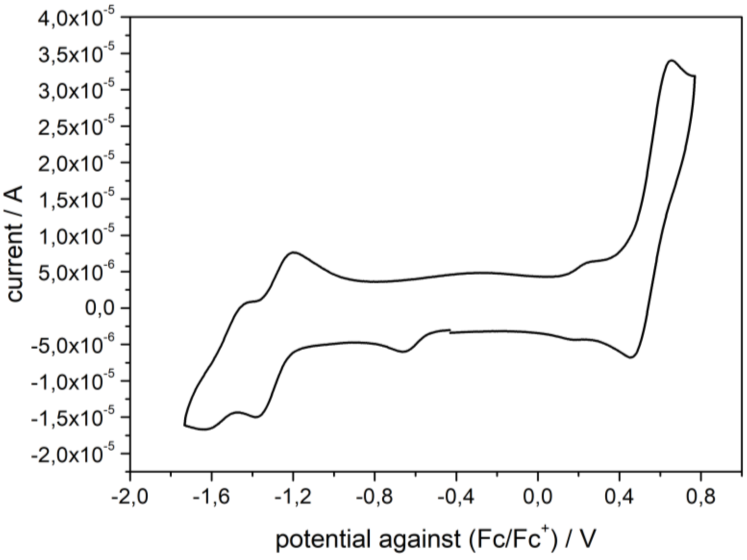

Fig. S79: Oxidation of compound **TPA-BNCDI^{Cy}** corrected against ferrocene/ferrocenium.

TPA-BNCDI^{Dip} Oxidation

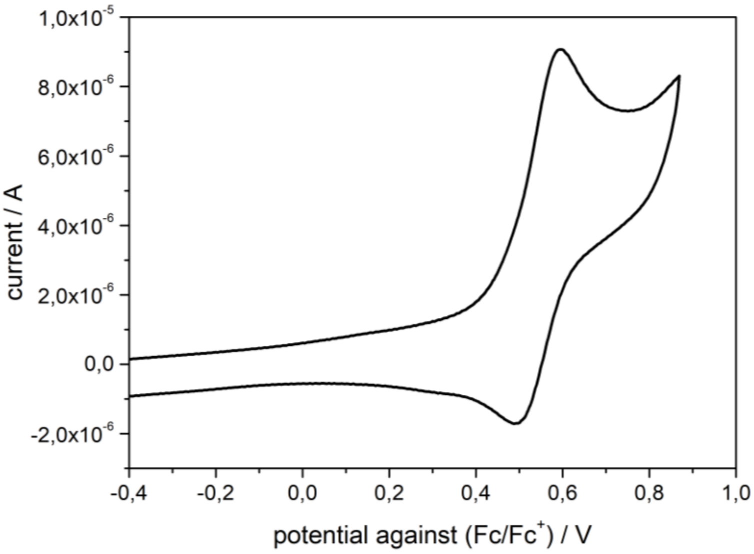

Fig. S80: Oxidation of compound **TPA-BNCDI^{Dip}** corrected against ferrocene/ferrocenium.

TPA-BNCDI^{Dip} Reduction

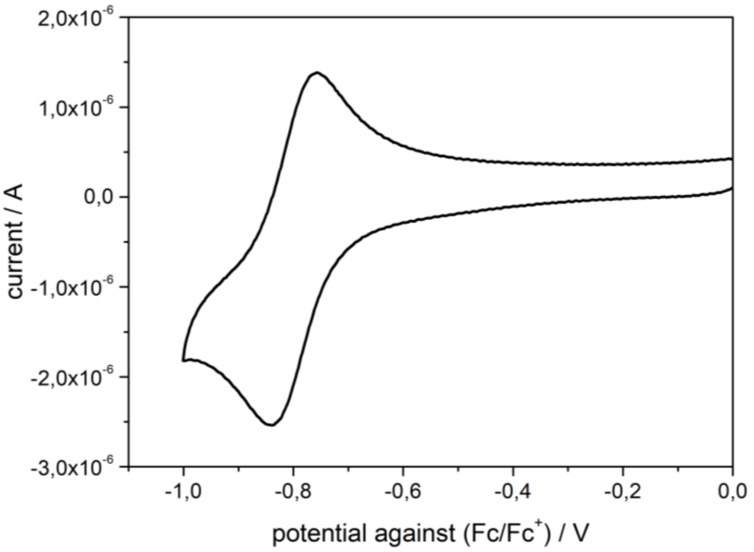

Fig. S81: Oxidation of compound **TPA-BNCDI^{Dip}** corrected against ferrocene/ferrocenium.

TPA-BNCDI^{Dip} Reduction 2

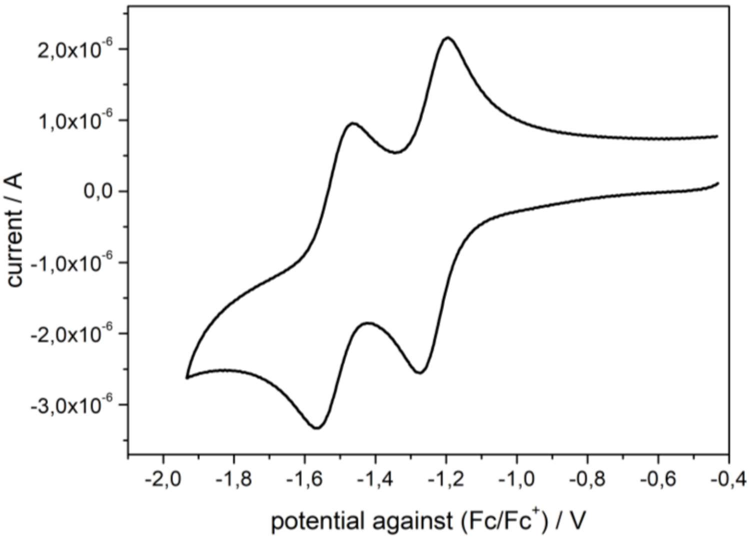

Fig. S82: Oxidation of compound **TPA-BNCDI^{Dip}** corrected against ferrocene/ferrocenium.

TPA-BNCDI^{Dip} Redox

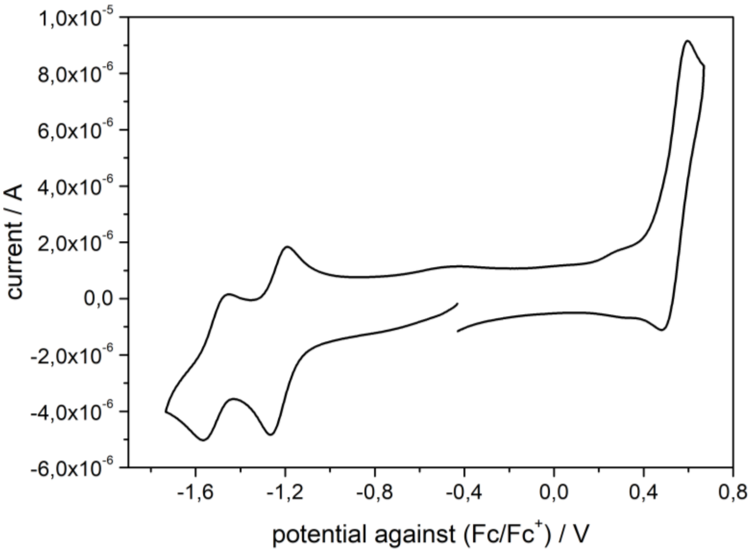

Fig. S83: Oxidation of compound **TPA-BNCDI^{Dip}** corrected against ferrocene/ferrocenium.

Thermogravimetric Analysis (TGA)

For thermal analysis, a Mettler Toledo DSC/TGA 3+ with 40 µL aluminum crucibles was used. Measurements were performed with a gas flow of 20 mL/min nitrogen and a heating rate of 10 °C/min.

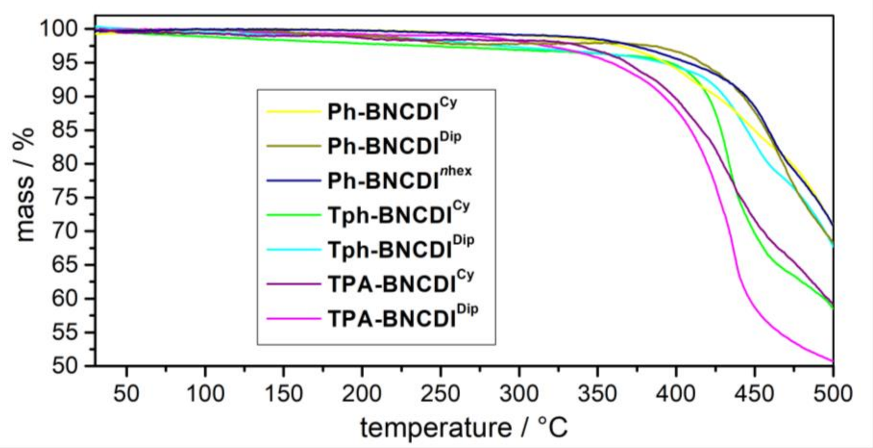

compound	T_{95}^{d} / °C
Ph-BNCDI^{Cy}	390
Ph-BNCDI^{Dip}	411
Ph-BNCDI$^{n\mathrm{Hex}}$	404
TPA-BNCDI^{Cy}	359
TPA-BNCDI^{Dip}	363
Tph-BNCDI^{Cy}	396
Tph-BNCDI^{Dip}	391

Fig. S84: Thermogravimetric analysis of all **BNCDI**s with 10 °C/min with 20 mL/min nitrogen gas flow. **Tab. S7:** Overview of the optical and thermal properties of all **BNCDI**s.

Spectroelectrochemical Experiments

Spectroelectrochemical experiments were performed in DCM with TBAPF$_6$ as electrolyte (0.2 M). The UV/NIR spectrometer was a Jasco V-770 instrument. As cell, an Omni Cell Spec with a platinum grid as the working electrode, a platinum wire as the counter electrode and SCE reference electrode was used. In addition, a Princeton applied Research Model 362 Scanning Potentiostat was used.

Due to the fact that phenyl and thienyl substituted **BNCDI**s showed reliable optoelectronical properties, we subjected **Tph-BNCDI$^{\mathrm{Dip}}$** as model substrate to the experiments. Since these systems exhibited reversible reduction, we were interested in the formation of the **Tph-BNCDI$^{\mathrm{Dip}\bullet-}$** and **Tph-BNCDI$^{\mathrm{Dip}2-}$** species upon reduction (Scheme 3, Fig. S85).

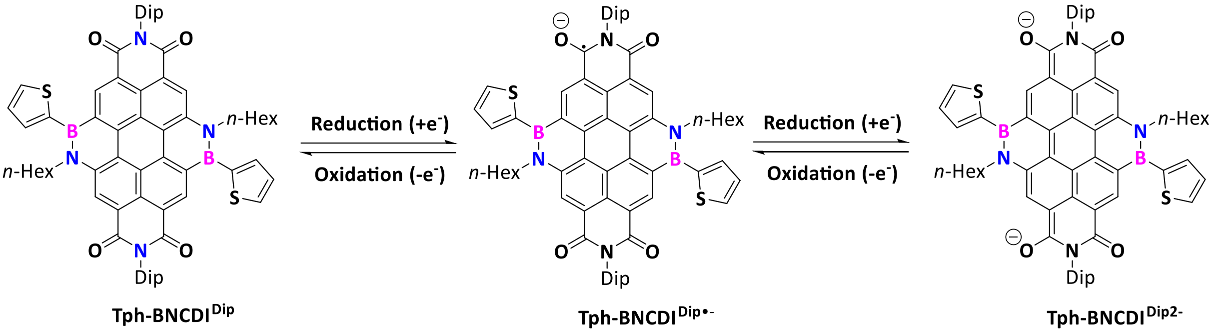

Scheme 3: Proposed formation of **Tph-BNCDI$^{\mathrm{Dip}\bullet-}$** and **Tph-BNCDI$^{\mathrm{Dip}2-}$** upon reduction.

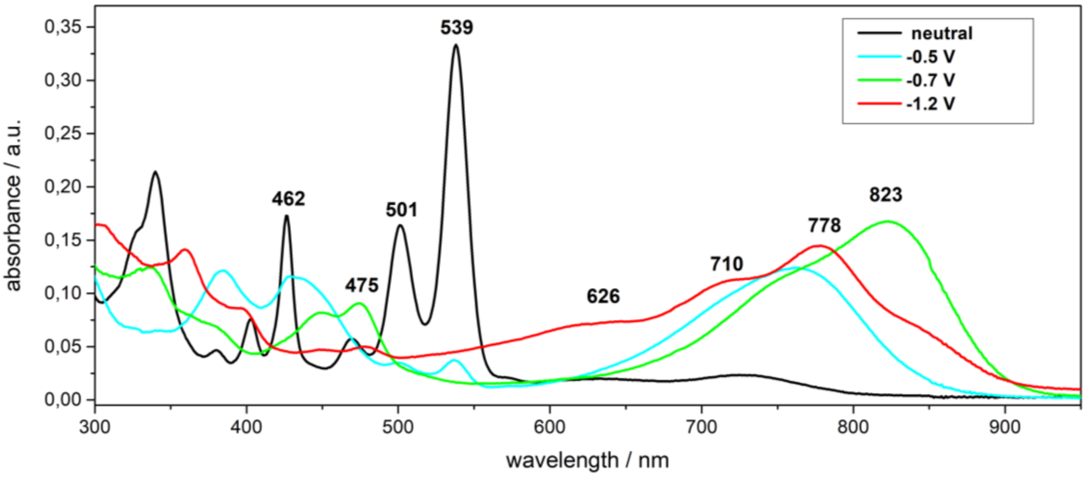

Fig. S85: UV/Vis spectral change during spectroelectrochemical characterization of **Tph-BNCDI$^{\mathrm{Dip}}$** (10^{-4} M) in DCM with 0.2 M TBAPF$_6$ at different potentials: neutral conditions (black), -0.5 V (turquoise). -0.7 V (green) and -1.2 V (red).

The process was irreversible.

After investigation of the **Tph-BNCDI^{Dip}** radical anion and dianion, we were interested in the spectroelectrochemical behavior of the **TPA-BNCDI^{Dip}** since cyclic voltammetric experiments revealed fully reversible oxidation and reduction process. Therefore, the reduction of **TPA-BNCDI^{Dip}** was conducted (Scheme 4, Fig. S86).

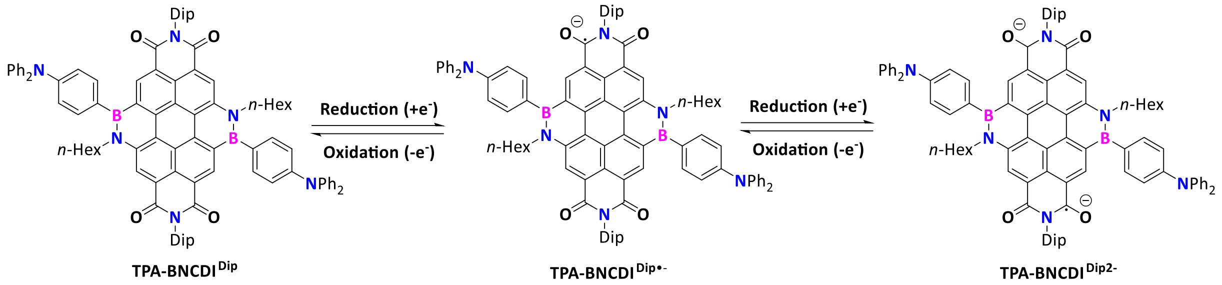

Scheme 4: Formation of **TPA-BNCDI$^{Dip-•}$** and **TPA-BNCDI^{Dip2-}** upon reduction.

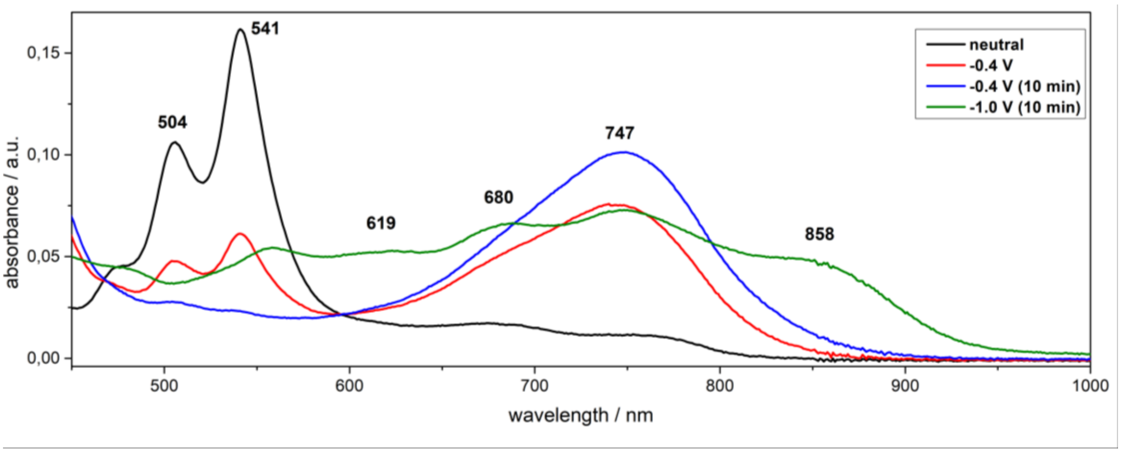

Fig. S86: Spectroelectrochemical characterization of **TPA-BNCDI$^{Dip-•}$** in DCM (10^{-4} M) with 0.2 M TBAPF$_6$ at different potentials.

The observed species differed from the reduced **Tph-BNCDI^{Dip}**. The process was irreversible.

Lewis Behavior

The treatment of **Tph-BNCDI^{Dip}** with boron tribromide and/or TBAF revealed that the fluoride **Tph-BNCDI^{Dip}** complex was less thermodynamically stable than the complex with BBr$_3$, which formed by the addition of boron tribromide; the reverse process was not possible (Fig. S87).

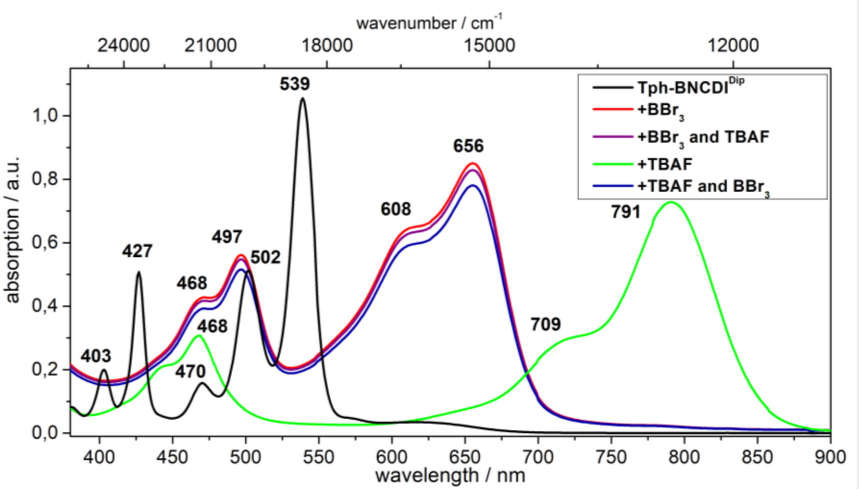

Fig. S87: Absorption spectra of **Tph-BNCDI^{Dip}** with TBAF and boron tribromide measured in DCM.

The interaction of **Tph-BNCDI^{Dip}** and **TPA-BNCDI^{Dip}** with fluoride or boron tribromide resulted in different absorption spectra. (Fig. S88), which were summarized below (Tab. S8).

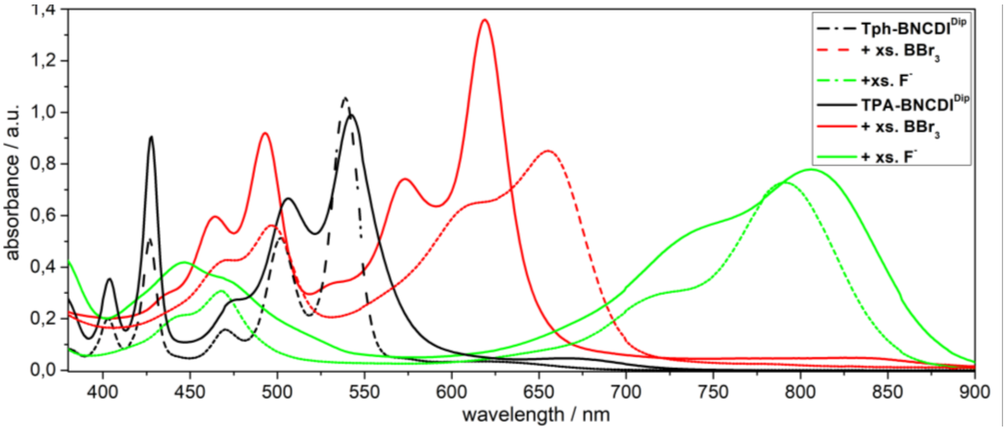

Fig. S88: Absorption and emission spectra of **TPA-BNCDI^{Dip}** and **Tph-BNCDI^{Dip}** their interaction with TBAF measured in DCM.

Tab. S8: Overview of the formed TBAF and BBr$_3$ species with either **TPA-BNCDI^{Dip}** or **Tph-BNCDI^{Dip}**.

	S_0->S_1(0-0)	S_0->S_1(0-1)	S_0->S_1(0-2)	S_0->S_2(0-0)	S_0->S_2(0-1)
Tph-BNCDI^{Dip}	539 nm	502 nm	470 nm	427 nm	403 nm
+BBr$_3$	656 nm	608 nm		497 nm	468 nm
+TBAF	791 nm	709 nm		468 nm	442 nm
TPA-BNCDI^{Dip}	543 nm	506 nm	473 nm	428 nm	404 nm
+BBr$_3$	619 nm	573 nm	531 nm	493 nm	464 nm
+TBAF	805 nm	730 nm		472 nm	444 nm

Moreover, the interaction of the **BNCDI**s with fluoride and boron tribromide was analyzed in detail by titration experiments in combination with absorption spectroscopy.

Titration of the fluoride source with **Tph-BNCDI^{Dip}** and **TPA-BNCDI^{Dip}** revealed two-step processes (Fig. S89).

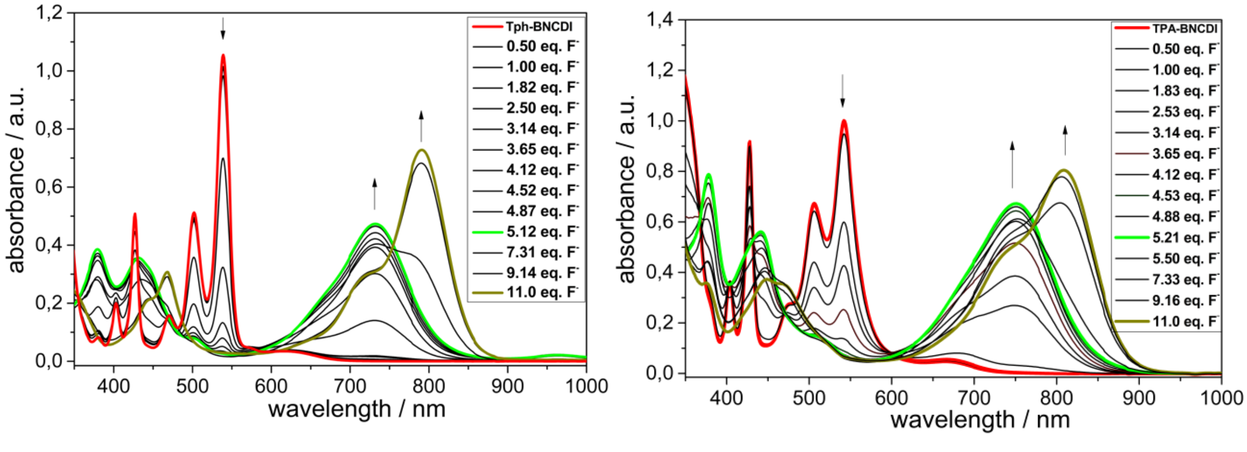

Fig. S89: Absorption and emission spectra of **Tph-BNCDI^{Dip}** (left) and **TPA-BNCDI^{Dip}** (right) their interaction with TBAF measured in DCM.

Upon addition of 0.5 equivalents of TBAF we clearly observed a decrease of the **BNCDI** bands indicating that this experiment is very sensitive towards its analyte and could be useful for sensoring processes. Upon adding more fluoride ions, we noted new absorption bands (600-820 nm) which might arise from the interaction of one fluoride anion with the **BNCDI**s to form the mono fluoride adduct. The limit of interaction was achieved if the system was treated with 11.0 equivalents of fluoride ions indicated by the evolution of another band (600-900 nm) with two peaks (810 nm and 710 nm). There was no auxiliary effect of the triphenylamine moiety noticed in this experiment.

The addition of BBr_3 to **TPA-BNCDI^{Dip}** and **Tph-BNCDI^{Dip}** led to the formation of a blue species with red-shifted absorption maxima (λ_{max} = 619/656 nm) and shoulder peaks (573/608 nm), displaying a vibronic fine structure (Fig. S90).

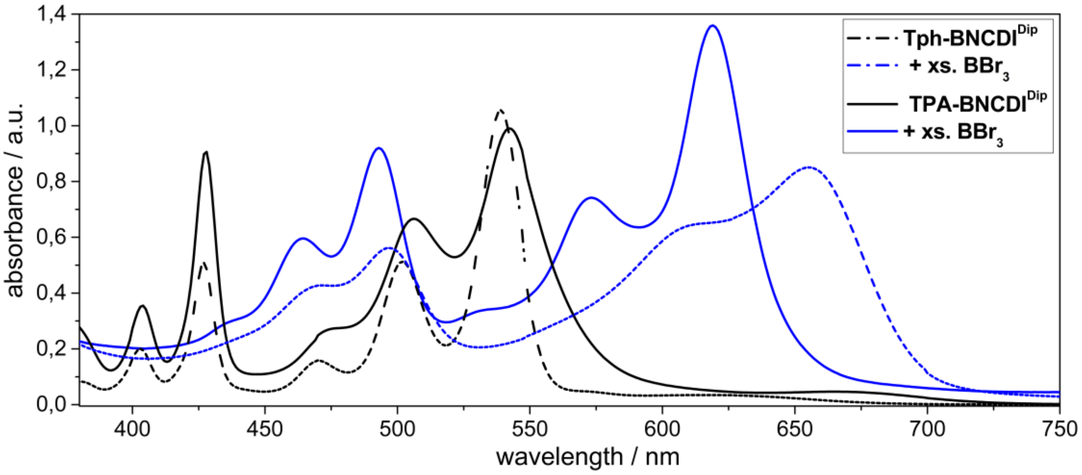

Fig. S90: Absorption spectra of **TPA-BNCDI^{Dip}/Tph-BNCDI^{Dip}** and their interaction with BBr_3.

In the higher energy absorbing region, two new signals (493/497 nm, 464/468 nm) were found with a similar vibronic appearance. Although the small absorption shifts of **TPA-BNCDI^{Dip}** compared to **Tph-BNCDI^{Dip}**, a strong influence of the triphenylamine moiety in this experiment could be excluded. In contrast to the fluoride adducts, the **BBr_3 BNCDI** adducts were not emissive.

Further detailed titrations with boron tribromide were conducted with **Tph-BNCDI^{Dip}** and **TPA-BNCDI^{Dip}** dissolved in DCM (Fig. S91).

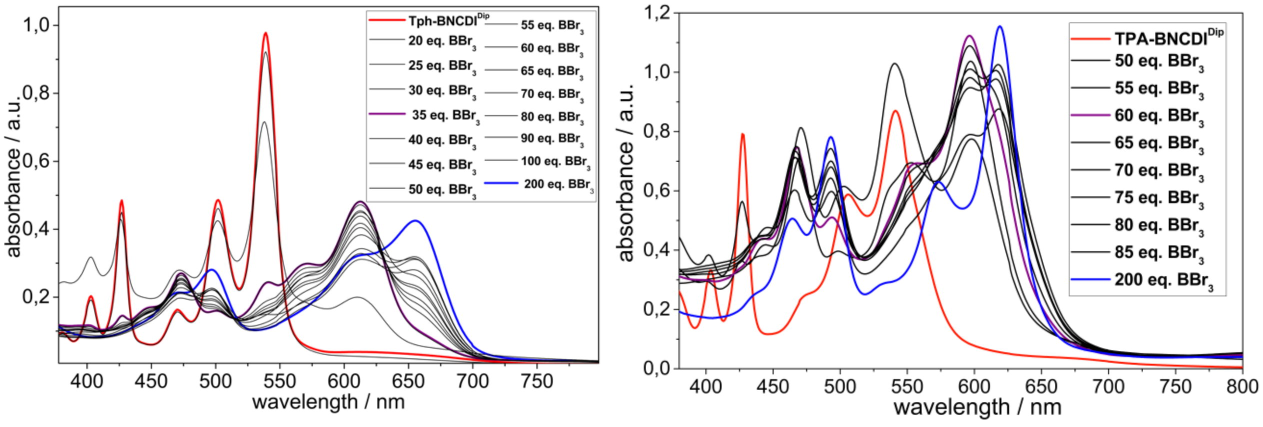

Fig. S91: Absorption and emission spectra of **TPA-BNCDI^{Dip}** and **Tph-BNCDI^{Dip}** interaction with BBr_3. The titration was performed under nitrogen atmosphere and with anhydrous DCM.

The titration of **Tph-BNCDI^{Dip}** with BBr_3 gave similar results as for the **TPA-BNCDI^{Dip}**. Although the final species of the **TPA-BNCDI^{Dip}** was slightly hypsochromically shifted, there was no fundamental difference between the thienyl and triphenylamine derivative. However, the intermediary signal for the **Tph-BNCDI^{Dip}** (620 nm) was formed with fewer equivalents compared to the formation of the **TPA-BNCDI^{Dip}** species (590 nm). In general, this process was completely reversible by dilution or the addition of a protic solvent, e.g. methanol.

Solvent Interactions

Due to the fact that we could obtain dramatic changes in absorption spectra using strong Lewis base or acids we were interested in whether solvatochromism might also arise. Therefore, **Tph-BNCDI^{Cy}** was dissolved in various solvents where cyclohexane, DCM, THF, ethyl acetate, triethylamine and acetonitrile represent the best the high variety of possible interactions. For cyclohexane, DCM and THF slight changes of the absorption spectra were observed that rather could be related to their polarity than to their ability to possess free lone pair. However, we observed strong interactions with coordinating solvents like acetonitrile and TEA (Fig. S92).

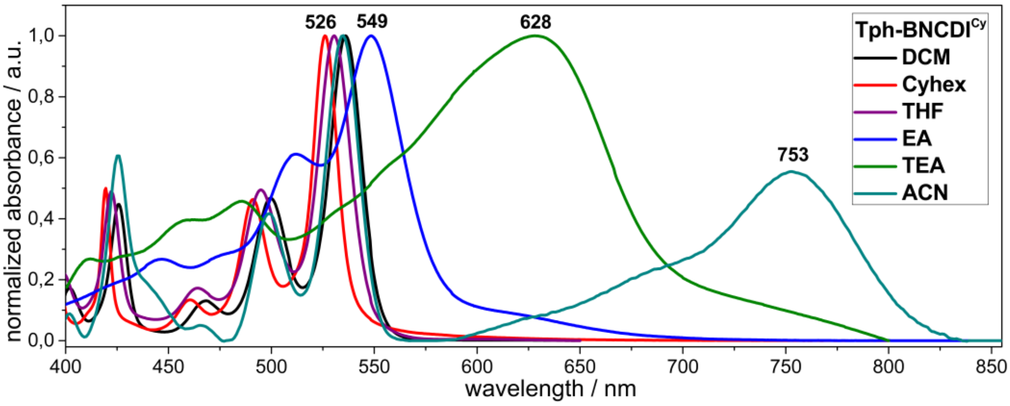

Fig. S92: Interaction of **Tph-BNCDI^{Cy}** with different solvents.

The results of these experiments are summarized below (Tab. 9).

Tab. S9:: Overview of the interaction of **BNCDI**s with common solvents.

Tph-BNCDI^{Cy}	S_{0}->S_1(0-0)	S_{0}->S_1(0-1)	S_{0}->S_1(0-2)	S_{0}->S_2(0-0)	S_{0}->S_2(0-1)
+DCM	539 nm	502 nm	470 nm	427 nm	402 nm
+Cyclohexane	526 nm	491 nm	461 nm	420 nm	397 nm
+THF	531 nm	495 nm	464 nm	423 nm	399 nm
+EA	549 nm	512 nm	475 nm	446 nm	
+TEA	628 nm	555 nm	530 nm	486 nm	456 nm
+ACN[1]	752 nm	686 nm			

[1] Upon dissolving in ANC it appeared that two species were present at the same time (see below)

To further investigate the influence of the triphenylamine substituent on **BNCDI** and its optoelectronic properties upon interaction with different solvents, we repeated the experiments with **TPA-BNCDI^{Cy}** (Fig. S93).

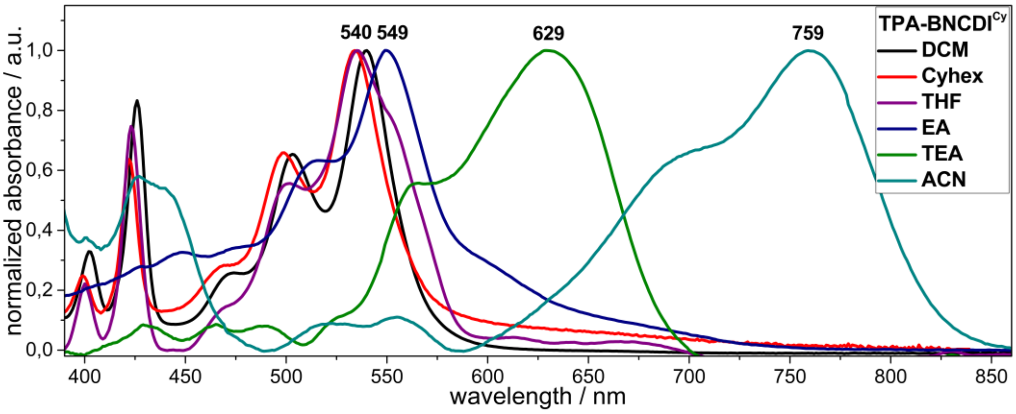

Fig. S93: Interaction of **TPA-BNCDI^{Cy}** with different solvents.

The results of these experiments are summarized below (Tab. S10).

Tab. S10: Overview of the interaction of **BNCDI**s with common solvents.

TPA-BNCDI^{Cy}	$S_{0\text{->}}S_1$(0-0)	$S_{0\text{->}}S_1$(0-1)	$S_{0\text{->}}S_1$(0-2)	$S_{0\text{->}}S_2$(0-0)	$S_{0\text{->}}S_2$(0-1)
+DCM	543 nm	506 nm	473 nm	428 nm	404 nm
+Cyclohexane	540 nm	503 nm	473 nm	426 nm	402 nm
+THF	535 nm	500 nm	467 nm	423 nm	400 nm
+EA	549 nm	514 nm	473 nm	447 nm	427 nm
+TEA	629 nm	563 nm	522 nm	490 nm	465 nm
+ACN	759 nm	690 nm			

[1] Upon dissolving in ACN it appeared that two species were present at the same time (see below)

Since complexation was possible with weak or moderate Lewis bases, e.g. ethyl acetate, THF, tertiary amines or acetonitrile, we concluded that the BN unit showed a weak interaction of the empty boron orbital with the oxygen/nitrogen lone pair of the Lewis base. In most cases, the **BNCDI** species retained the characteristically structured vibronic absorption bands. The observed effect was not limited to TPA-substituted **TPA-BNCDI^{Cy},** as the thienyl-substituted **Tph-BNCDI^{Dip}** exhibited the same behavior. Therefore, an additional effect of the triphenylamine's lone pair was excluded. These findings were especially interesting, since all carbon rylene diimides are only weakly solvatochromic.[10]

Rehm-Weller Equation

To support the intramolecular PeT theory, the energy change for a PeT process was calculated by the Rehm-Weller equation [11] in its simplified version (Eq. 1).[12-15]

$$\Delta G_{PET} \;=\; e(E_{(D+\cdot/\,D)} - E_{(A/\,A-\cdot)}) - E_{00} + \Delta G^0_{solv} \text{ (Eq. 1)}$$

Here, the E_{00} represents the intersection of absorption and emission, and ΔG^0_{solv} is a correction term which includes the coulomb potential for the respective radical ionic species in the given solvent.

Whereas the ΔG^0_{solv} is defined as:

$$\Delta G^0_{solv} = \frac{e^2}{4\pi\varepsilon_0\varepsilon_s r_{DA}} \text{ (Eq. 2)}$$

With the distance of TPA and BNCDI (r_{DA} = 10.5 Å), the following results were obtained.

Tab. S11:: Overview of the parameters used in the Rehm-Weller equation in DCM (ε_s = 8.93).

	$E_{(D+\cdot/\,D)}$ / V	$E_{(A/\,A-\cdot)}$ / V	E_{00} / eV	ΔG^0_{solv} / eV	ΔG_{PET} / eV
TPA-BNCDI^{Cy}	0.54	-1.21	2.21	0.15	-0.31
TPA-BNCDI^{Dip}	0.60	-1.15	2.19	0.15	-0.29

The ΔG_{PET} of **TPA-BNCDI^{Cy}** and for **TPA-BNCDI^{Dip}** in DCM was -0.31/-0.29 eV or -6.69/-7.15 kcal/mol. Therefore, the process was exergonic and feasible. This was in accordance with literature where ΔG_{PET}= -0.2 eV to -0.3 eV is described as barrier for PeT processes.[16]

In cyclohexane the redox potentials require additionally the Born correction:

$$\Delta G_{PeT} \;= e\big(E_{(D+\,/\cdot D)} - E_{(A\,/\,A-\cdot)}\big) + \Delta G_{redox} - E_{00} + \Delta G^0_{solv} \text{ (Eq. 3)}$$

with

$$\Delta G_{redox} = \frac{e^2}{8\pi\varepsilon_0 r_{DA}} * \left(\frac{1}{\varepsilon_{ref}} - \frac{1}{\varepsilon_s}\right) \text{ (Eq. 4)}$$

Tab. S12:: Overview of the parameters used in the Rehm-Weller equation in cyclohexane (ε_s = 2.02).

	$E_{(D+\cdot/D)}$ / eV	$E_{(A/A-\cdot)}$	ΔG_{redox}	E_{00} / eV	ΔG^0_{solv}	ΔG_{PeT}
TPA-BNCDI^{Cy}	0.54	-1.21	-0.260	2.30	0.68	0.39
TPA-BNCDI^{Dip}	0.60	-1.15	-0.262	2.26	0.68	0.43

The ΔG_{PeT} of **TPA-BNCDI^{Cy}** and for **TPA-BNCDI^{Dip}** in cyclohexane was 0.39/0.43 eV or 8.99/9.92 kcal/mol. The process was endergonic and therefore not feasible.

Computational Details and TICT search

To perform the calculations, we used simplified structures, in which the long hexyl chains as well as the R group were replaced by methyl groups for the sake of computational efficiency. This is justified by the remarkably similar experimental properties of dyes in which cyclohexyl or diisopropylphenyl groups are used. To model the spectral features, we used a computational method relying on a hybrid protocol, in which the total and transition energies are determined with second-order Coupled-Cluster calculations (CC2),[17] whereas the geometries, and vibrations are computed at the Time-Dependent Density Functional Theory (TD-DFT) level,[18] and environmental effects accounted for by using the well-known Polarizable Continuum Model (PCM).[19] All CC2 calculations were achieved with Turbomole[20] applying the resolution-of-identity approach and selecting the *def2*-SVPD atomic basis set. All (TD-)DFT calculations but the constrained ones (see below) were performed using the Gaussian16.A03 program.[21] For the Gaussian calculations, we used tightened self-consistent field (10^{-10} a.u.) and geometry optimization (10^{-5} a.u.) convergence thresholds, and a large DFT integration grid (so-called *sperfine* grid,). These (TD-)DFT calculations relied on the CAM-B3LYP range-separated hybrid functional.[22] Following the basis set combination approach proposed elsewhere,[23] we selected the 6-31G(d) atomic basis set for determining the geometrical and vibrational parameters whereas the transition energies were computed with 6-31+G(d). The nature of the ground-state stationary points was confirmed by analytical Hessian calculations that returned 0 (minima) imaginary vibrational modes. Environmental effects on the transition energies were accounted for using a LR+cLR[24] model in its *non-equilibrium* limit for both absorption and emission. Excited-states were represented using density difference plots, in which the excited-state density was determined at the TD-DFT level. In these plots blue and red regions respectively indicate decrease and increase of electron density upon photon absorption. For evaluation the possibility of PeT, we used constrained DFT,[25] as implemented in Q-Chem 5.3.[26] These calculations were performed with the CAM-B3LYP functional and the 6-31G(d) basis set. The CPCM solvent model was used in combination with UFF radii to model solvent effects. For comparison, the energy of the lowest bright excited-state was optimized at the same level of theory with the same code using "standard" TD-DFT.

To exclude a TICT-like transition, we have scanned the dihedral angle between the CDI core and the Ph (the Ph and the TPA moiety) ring from 15° to 90° (0° to 90°) and computed the excited-state energies at the LR+cLR-PCM/TD-CAM-B3LYP/6-31+G(d) level in both solvents. As can be seen in Fig. S94, both graphs show only one minimum in both solvents, indicative that TICT likely does not play a role here. This conclusion is well in line with their limited role in the EDD plot (Fig. 6 in the manuscript).

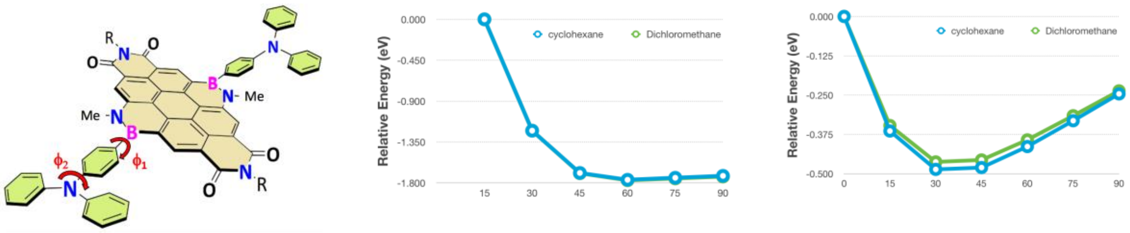

Fig. S94: Scans of the total energies of **TPA-BNDCI** when performing rotation around two selected dihedral angles.

Literature

1. J. Buchenska, *J. Appl. Polym. Sci.*, **2001**, *80*, 1914-1919.
2. X. Mo, H.-Z. Chen, M.-M. Shi, M. Wang, *Chem. Phys. Lett.*, **2006**, *417*, 457-460.
3. R. K. Gupta, A. S. Achalkumar, *J. Org. Chem.*, **2018**, *83*, 6290-6300.
4. S. Sengupta, R. K. Dubey, R. W. Hoek, S. P. van Eeden, D. D. Gunbas, F. C. Grozema, E. J. Sudholter, W. F. Jager, *J. Org. Chem.*, **2014**, *79*, 6655-6662.
5. F. Wurthner, V. Stepanenko, Z. Chen, C. R. Saha-Moller, N. Kocher, D. Stalke, *J. Org. Chem.*, **2004**, *69*, 7933-7939.
6. A. Lik, L. Fritze, L. Muller, H. Helten, *J. Am. Chem. Soc.*, **2017**, *139*, 5692-5695.
7. B. Wrackmeyer, *Z. Naturforsch. B.*, **2015**, *70*, 421-424.
8. Z. Zhang, R. M. Edkins, J. Nitsch, K. Fucke, A. Steffen, L. E. Longobardi, D. W. Stephan, C. Lambert, T. B. Marder, *Chem. Sci.*, **2015**, *6*, 308-321.
9. J. L. Bredas, R. Silbey, D. S. Boudreaux, R. R. Chance, *J. Am. Chem. Soc.*, **1983**, *105*, 6555-6559.
10. H. Langhals, *Description of properties of binary solvent mixtures*, in *Similarity models in organic chemistry, biochemistry and related fields*, eds. R. I. Zalewski, T. M. Krygowski and J. Shorter, Elsevier, Amsterdam u.a., **1991**, vol. 42, 283-342.
11. D. Rehm, A. Weller, *Z. Phys. Chem.*, **1970**, *69*, 183-200.
12. J. R. Lakowicz, *Principles of Fluorescence Spectroscopy*, Springer US, Boston, 3rd edn., **2006**.
13. G. J. Kavarnos, *Fundamental concepts of photoinduced electron transfer*, Springer Berlin Heidelberg, Berlin, Heidelberg, **1990**.
14. D. Rehm, A. Weller, *Ber. Bunsenges. Phys. Chem.*, **1969**, *73*, 834-839.
15. D. Rehm, A. Weller, *Isr. J. Chem.*, **1970**, *8*, 259-271.
16. L. Eberson, *Electron Transfer Reactions in Organic Chemistry*, Springer-Verlag Berlin Heidelberg, **1987**.
17. O. Christiansen, H. Koch, P. Jørgensen, *Chem. Phys. Lett.*, **1995**, *243*, 409-418.
18. C. Adamo, D. Jacquemin, *Chem. Soc. Rev.*, **2013**, *42*, 845-856.
19. J. Tomasi, B. Mennucci, R. Cammi, *Chem. Rev.*, **2005**, *105*, 2999-3093.
20. TURBOMOLE V6.2 2010, a development of University of Karlsruhe and Forschungszentrum Karlsruhe GmbH, 1989-2007, TURBOMOLE GmbH, since 2007; available from http://www.turbomole.com.,
21. M. J. Frisch, G. W. Trucks, H. B. Schlegel, G. E. Scuseria, M. A. Robb, J. R. Cheeseman, G. Scalmani, V. Barone, G. A. Petersson, H. Nakatsuji, X. Li, M. Caricato, A. V. Marenich, J. Bloino, B. G. Janesko, R. Gomperts, B. Mennucci, H. P. Hratchian, J. V. Ortiz, A. F. Izmaylov, J. L. Sonnenberg, Williams, F. Ding, F. Lipparini, F. Egidi, J. Goings, B. Peng, A. Petrone, T. Henderson, D. Ranasinghe, V. G. Zakrzewski, J. Gao, N. Rega, G. Zheng, W. Liang, M. Hada, M. Ehara, K. Toyota, R. Fukuda, J. Hasegawa, M. Ishida, T. Nakajima, Y. Honda, O. Kitao, H. Nakai, T. Vreven, K. Throssell, J. A. Montgomery Jr., J. E. Peralta, F. Ogliaro, M. J. Bearpark, J. J. Heyd, E. N. Brothers, K. N. Kudin, V. N. Staroverov, T. A. Keith, R. Kobayashi, J. Normand, K. Raghavachari, A. P. Rendell, J. C. Burant, S. S. Iyengar, J. Tomasi, M. Cossi, J. M. Millam, M. Klene, C. Adamo, R. Cammi, J. W. Ochterski, R. L. Martin, K. Morokuma, O. Farkas, J. B. Foresman, D. J. Fox, Gaussian 16 Rev. B.01, **2016**.
22. T. Yanai, D. P. Tew, N. C. Handy, *Chem. Phys. Lett.*, **2004**, *393*, 51-57.
23. D. Jacquemin, A. Planchat, C. Adamo, B. Mennucci, *J. Chem. Theory Comput.*, **2012**, *8*, 2359-2372.
24. P. M. Verite, C. A. Guido, D. Jacquemin, *Phys. Chem. Chem. Phys.*, **2019**, *21*, 2307-2317.
25. Q. Wu, T. Van Voorhis, *Phys. Rev. A*, **2005**, *72*.
26. A. I. Krylov, P. M. W. Gill, *Wiley Interdiscip. Rev. Comput. Mol. Sci.*, **2013**, *3*, 317-326.